جمهورية العراق
وزارة التعليم العالي والبحث العلمي
جامعة بابل
كلية العلوم للبنات
قسم فيزياء الليزر

توظيف تقنية الانبعاثات المستحثة بالليزر (LIF) لتشخيص خلايا سرطان القولون المعاملة ب TiO_2 النانوي

اطروحة قدمتها
الى مجلس كلية العلوم للبنات في جامعة بابل
وهي جزء من متطلبات نيل درجة الدكتوراه فلسفه
في العلوم / فيزياء الليزر وتطبيقاته

من قبل الطالبة
تمارة علي ناصر
بكالوريوس في علوم فيزياء الليزر جامعة بابل (2015)
ماجستير علوم فيزياء الليزر ، جامعة بابل (2018)
بإشراف

ا.م.د لازم حسن عبود
كلية العلوم للبنات / قسم فيزياء الليزر

ا.د محمد عبدالله حميد
كلية العلوم / قسم الفيزياء

2022م 1443هـ

Republic of Iraq
Ministry of Higher Education and Scientific Research
University of Babylon
College of Science for women
Department of laser Physics

Implementation Laser Induced Fluorescence (LIF) Technique to Diagnose Colon Cancers Cell Treating with TiO_2 Nanoparticles

A Thesis

Submitted to the Council of the College of Sciences for Women,

University of Babylon

In partial Fulfillment of the Requirements for the Degree of Doctor of Philosophy in Laser Physics and its Applications

By:

Tamara Ali Nasser Diwan

B.Sc., Laser Physics and its Applications, University of Babylon (2015)

M.Sc., Laser Physics and its Applications, University of Babylon (2018)

Supervised by:

Assis. Prof. Dr. Lazem Hassan Aboud

University of Babylon

College of Sciences for Women

Department of laser Physics

Prof .Dr. Mohammed Abdullah Hameed

Baghdad University

College of Science

physics department

2022 A.D

1443 A.H

﴿وَيسألُونَكَ عَنِ الرّوحِ قُل الرُّوحُ مِن أَمرِ رَبّى وَمَآ أوتيتُم مِّنَ العِلمِ إلا قَلِيلاً ﴾

صدق الله العلي العظيم

(سورة الإسراء / الآية 85)

dedications

This Dissertation is dedicated to

My father… .. the shortest way to gain God's approval

My mother….. for her patience with me in all circumstances

Brother….the source of my strength

My sisters…… the hope of my life and those

CKNOWLEDGMENTS

At the beginning, I praise Allah for giving me health and determination to complete this thesis and shape its present form. I thank Allah for his kindness.

I would like to express my deep gratitude and appreciation to the supervisor the Assistant Professor Dr. lazim hassan abbode for his guidance, suggestions, support and encouragement throughout the research work.

I am also thankful to the Assistant Professor Dr. Mohammed Abdullah Hameed for his support and advice, and to all professors, lecturers, teachers and physics students Laser and Molecular Physics Group for their help, to all my friends and to all those who helped me directly or indirectly to complete this work.

I own earnest thanks to all members of my family my parents, sisters, and brothers for their support and encouragement and to everyone who helped me prepare this letter.

God bless you all.

Tamara

2022

Abstract:

Cancer is a major health problem in which control cancer cells divide resulting in abnormal growth and metastasis. Laser fluorescence spectroscopy (LIF) has been used as a potential tool for cancer diagnosis. The influence of two very important parameters of sensor design aspects, excitation-collecting geometry and excitation wavelength on cell spontaneous fluorescence response and malignancy resolution, was investigated. An attempt was made to determine the optimal sensor configuration to develop a diagnostic procedure to enhance a small spectral difference to significantly improve the accuracy of fluorescence cancer diagnosis. Also, in this work, a nano-material was prepared for the purpose of killing cancer cells. Thin films with titanium dioxide nanostructures were prepared on glass substrates using a DC magnetron sputtering technique. The operating parameters of the plasma spray system were optimal, while the sedimentation time was changed in order to determine the optimal conditions for obtaining high-quality samples. Monophase (Anatase) TiO_2 using an $Ar:O_2$ gas mixture at a ratio of 50:50 The characterization results showed that the average crystal size of titanium dioxide samples was 17.74 nm while the minimum size of nanoparticles was 60. Cell culture means cells are removed from living tissue and then made. Grow them in an artificial environment until they are ready for nanoparticle testing, that is, direct irradiation in the laboratory. Nanoparticles have the ability to target tumor tissues that are explored by tumor vascular defects, enhancing the permeability and retention effect that occurs in tumor tissues allowing passive targeting of cancers in contrast to normal tissues which are usually impermeable to infiltration of tio2 nanoparticles. Nanoparticles can be directly injected into a colon cancer cell with minimal effects on its normal tissue

surroundings. The fluorescence spectra of colon cancer cells after adding several concentrations of the nanomaterial (1000, 500, 250, 125, 62.50, 31.25) μg/ml, where the best results were obtained, which correspond to the statistical analysis of the cells .At high concentrations, it was observed that the fluorescence spectrum was very low, and this indicates the destruction of cancer cells, due to the small size of the nanomaterial that can penetrate into the cell and spread into the cytoplasm of the cell. The desire of this thesis was to determine the best concentration of nanoparticles, which results in the optimal solution for treating cancer. The results showed the best concentration 250μg/ml that gives the maximum number of destroyed cancer cells The MTT scale is used to evaluate human colon cancer in vitro proliferation in vitro cancer cells in response when exposed to serial double-dilutions of a concentration of Tio2NPs present in cell line culture that clearly showed reduced cell viability compared to the normal (0 μg/ml) cell. Using an additional assay with the MTT assay, cell toxicity shows a significant ($p < 0.01$) increase (1000 μg/ml).

الخلاصة :

يعد السرطان مشكلة صحية كبرى تنقسم فيها الخلايا السرطانية السيطرة مما يؤدي إلى نمو غير طبيعي وانتشار ورم خبيث تم استخدام الفلورة المحتثة بالليزر (LIF) كأداة محتملة لتشخيص السرطان. تم التحقيق في تأثير معلمتين مهمتين للغاية من جوانب تصميم المتحسس ، وهما تصميم المنظومة والطول الموجي المستخدم في الفلورة للخلية ودقة الورم الخبيث. بُذلت محاولة لتحديد تكوين الاستشعار الأمثل لتطوير إجراء تشخيصي لتعزيز اختلاف طيفي صغير لتحسين دقة تشخيص الإصابة بسرطان الفلورة بشكل كبير. ايضا في هذا العمل تم تحضير مادة نانوية الهدف منها قتل الخلايا السرطانية . تم تحضير أغشية رقيقة ذات بنية نانوية من ثاني أكسيد التيتانيوم على ركائز زجاجية باستخدام مغنطرون متفاعل مع التيار المستمر تقنية الترذيذ. كانت معلمات تشغيل نظام الترذيذ بالبلازما الأمثل ، في حين تم تغيير وقت الترسيب من أجل تحديد الأمثل شروط الحصول على عينات عالية الجودة. أحادي الطور (أناتاز) TiO_2 باستخدام خليط غاز $Ar: O_2$ بنسبة 50:50 أظهرت نتائج التوصيف أن متوسط حجم البلورات لثاني أكسيد التيتانيوم 17.74 نانومتر بينما كان الحد الأدنى كان حجم الجسيمات النانوية 60 .تعني زراعة الخلايا إزالة الخلايا من الأنسجة الحية ثم صنعها نموهم في بيئة اصطناعية حتى أصبحوا جاهزين للاختبار النانوية ، وهذا هو التشعيع المباشر في المختبر. تمتلك الجسيمات النانوية القدرة على استهداف أنسجة الورم التي تستكشفها عيوب الأوعية الدموية الورمية ، وتعزيز النفاذية وتأثير الاحتفاظ التي تحدث في الأنسجة السرطانية تسمح بالاستهداف السلبي للسرطانات على عكس الأنسجة الطبيعية التي عادة ما تكون غير منفذة لتسلل الجسيمات النانويةTiO_2 . يمكن للجسيمات النانوية عن طريق الحقن المباشر لخلية سرطان القولون مع تأثيرات قليلة على محيطها نسيج طبيعي. تم حساب أطياف الفلورة لخلايا سرطان القولون بعد إضافة عدة تراكيز من المادة النانوية (1000 ، 500 ، 250 ، 125 ، 62.50 ، 31.25) ميكروغرام / مل ، حيث تم الحصول على أفضل النتائج ، والتي تتوافق مع التحليل الإحصائي للخلايا ،عند التراكيز العالية لوحظ أن طيف الفلورة كان منخفضاً جداً ، وهذا يدل على تدمير الخلايا السرطانية ، بسبب صغر حجم المادة النانوية التي يمكن أن تخترق الخلية وتنتشر في سيتوبلازم الخلية. كانت الرغبة في هذه الرسالة هي تحديد أفضل تركيز للجسيمات النانوية مما ينتج عنه الحل الأمثل لعلاج السرطان. أظهرت النتائج أفضل تركيز 250 ميكروغرام / مل والذي يعطي أكبر عدد من الخلايا السرطانية المدمرة يتم استخدام مقياس (MTT) للتقييم سرطان القولون البشري في الخلايا السرطانية المختبرية لمعرفة الاستجابةً عند تعرضه للتخفيفات المضاعفة التسلسلية لـ

تركيز TiO_2NPs الموجود في زراعة خط الخلية والذي أظهر بشكل واضح انخفاض في بقاء الخلية مقارنةً بالخلية الاعتيادية (0 ميكروغرام / مل) يتم استخدام اختبار إضافي مع اختبار MTT ، تظهر سمية الخلية زيادة معنوية (1000) ($P <0.01$ ميكروغرام / مل) .

List of figures

List of tables

Abbreviations

Symbol	Description
LIF	Laser induced fluorescence
PLIF	Planar laser induced fluorescence
CCD	Charge-coupled device
CFP	Cyan fluorescence protein
FRET	Fluorescence resonance energy transfer
RET	Process of resonance energy transfer
DsRFP	Red fluorescence protein from Re coral Disco soma strata
TCOs	Transparent conducting oxides
CE/LIF	capillary electrophoresis with laser-induced fluorescence
TR-LIFS	Time-resolved laser-induced fluorescence spectroscopy
ECM	extracellular matrix
SS-DNA	single-strand DNA
UV-LIF	Ultra violet-Laser Induced Fluorescence
LIDAR	Light Detection and Ranging
NPS	Nano pulse stimulation
LIBS-LIF	Laser-induced breakdown spectroscopy–laser-induced fluorescence
μCE	Micro capillary electrophoresis
MS_2	Escherichia virus
CW	Continuous wave
LED	Light-emitting diode
ICCD	Linear Charge-coupled device
SNR	signal-to-noise ratio
FLIM	Florescence life time imaging microscopy
CARS	Coherent anti-Stokes Raman scattering
SHG	Second harmonic generation
THG	Third harmonic generation
PVD	physical vapor deposition
DC	Direct current
TiO_2	Titanium Dioxide
CHO	Chinese hamster ovary
XRD	X-ray diffraction
AFM	Atomic force microscopy
SEM	scanning electron microscopy
FTIR	Fourier-transform infrared spectroscopy

EDX	Energy Dispersive X-ray Diffraction
PBS	Phosphate Buffer Saline
DDW	Deionized distilled water

CONTANTS

Chapter Four Results and Discussion

1-1 introduction

Laser-induced fluorescence (LIF) is (spontaneous) emission from atoms or molecules that have been excited by (laser) radiation. The phenomenon of induced fluorescence was first seen and discussed back in 1905 by Robert Williams Wood [1], many decades before the invention of the laser. If a particle resonantly absorbs a photon from the laser beam, the particle is left in an excited energy state. Such a state is unstable and will decay spontaneously, emitting a photon again. The excited state of finite lifetime emits its photon on return to a lower energy level in random directions. It is this fact that allows one to measure an absorption signal directly. Conveniently, the fluorescence is observed at 90 ^{o} to a collimated laser beam. In principle, a very small focal volume V_c may be defined in the imaging set-up, resulting in spatial resolution of the laser–particle interaction volume; note that spatial resolution cannot normally be realized in an experiment, which measures the absorption directly. In a sense, the method of LIF may be seen as a fancy way of measuring the absorption of species, but with a bonus. Absorption spectroscopy, which detects the transmitted light, has a limited sensitivity [2]. The problem is that one has to detect a minute amount of missing light in the transmitted beam, i.e. one encounters the problem of the difference of large near-equal numbers. The use of pulsed lasers aggravates the problem due to their normally substantial pulse-to-pulse intensity fluctuations, which limit the signal-to-noise ratio. With fluorescence detection the signal can be detected above a background, which is (at least in favorable cases) nearly equal to zero, and detection at a single photon level is relatively easy to achieve[3].

1-2 Laser Induced Fluorescence (LIF)Spectroscopy

LIF is a powerful technique more and more commonly used by the chemical physicist for probing gas-phase atomic or molecular species, even in minute amounts, and determining their internal states distribution. The principle is quite simple: by absorption of one or several photons from the laser beam the probed species are pumped from an initial state (i) to an excited state from which radiation is subsequently emitted as transitions take place to final states (f).

All or part of the emitted radiation is detected. Usually, each time it is possible, the light is detected at a wavelength different from the laser wavelength (the states i and f are different) to eliminate any spurious signal due to scattered laser light [4]. Since lasers have narrow bandwidths and are easily tunable over large wavelength domains the technique is very well adapted to determine ro-vibrational populations of reaction products. Indeed, the laser being swept, whenever it coincides with a molecular absorption line, the reaction product makes a transition to an excited electronic state from which it fluoresces. The fluorescence intensity recorded as a function of the laser wavelength is usually called an excitation spectrum. The intensities of the different lines thus observed are converted to relative populations of the various product internal states with the help of Franck -Condon factors and rotational line strengths. In these excitation spectra the spectral resolution is given by the bandwidth of the laser [5], as in figure (1-1) :

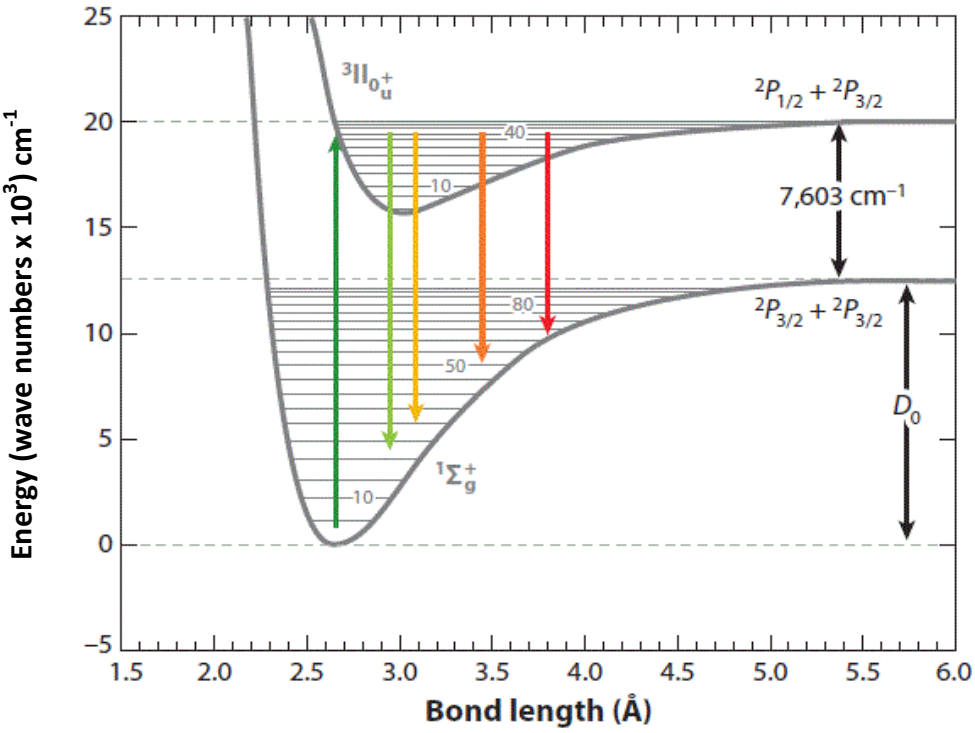

Fig. (1-1): fluorescence process, a particular vibrational-rotational level [6]

In the LIF technique, a laser is tuned so that its frequency matches that of an absorption line of some atom or molecule of interest. The absorption of the laser photons by this species produces an electronically excited state which then radiates. The fluorescent emission is detected using a filter or a monochromatic followed by a photomultiplier. Because a particular absorption line is selected, the excited state has definite and identifiable vibrational, rotational, and fine structure quantum numbers [7].

This clean state preparation has significant advantages for spectroscopic and collision studies, in contrast to the congestion often found in ordinary emission spectra from, for example, a discharge. Since the lower state responsible for the absorption is also definite, considerable selectivity is provided by LIF when used as a diagnostic tool. In addition, its high degree of sensitivity, the spatial and temporal resolution available, and its non-intrusive nature are important attributes for this purpose. Finally,

special LIF methods not possible in non-laser spectroscopy, such as two photon excitation, yield new information and make possible new diagnostic probes. LIF as a whole has had a tremendous impact on the study of the electronic spectra of small molecules[8]. As in figure (1-2):

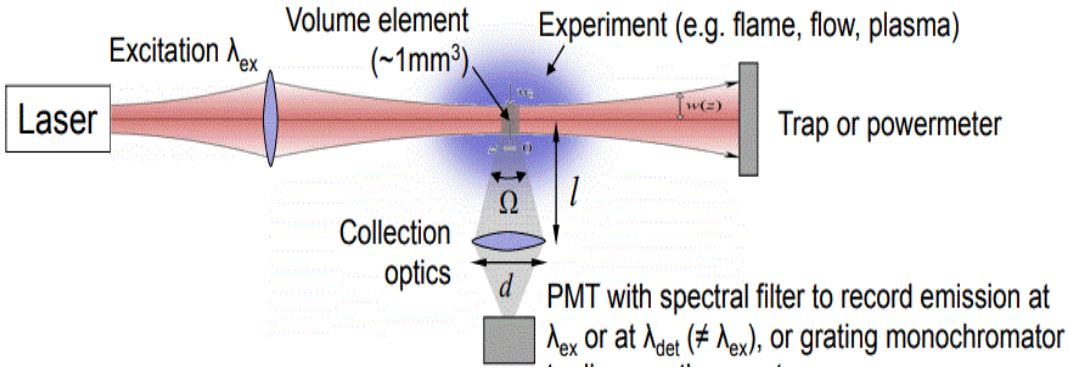

Fig. (1-2): Typical experimental setup for LIF systems[8]

a- Recording modes:

1. Emission intensity at a fixed detection wavelength
2. Fluorescence spectrum (spectrometer)
3. Excitation spectrum (scanned laser)
4. Can be extended to 2-d with CCD array detector (PLIF)
5. Can also measure temporal behavior.as figure (1-3) :

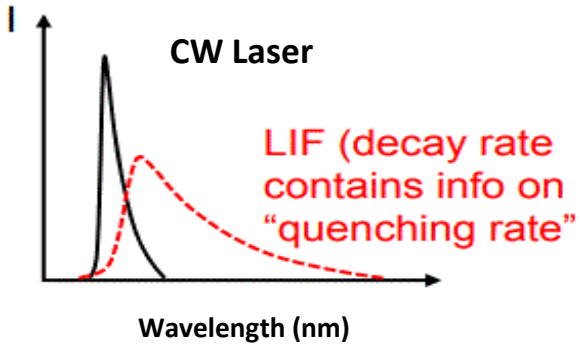

Fig. (1-3): LIF quenching rate [9]

LIF signal and fluorescence quantum yield depend on collisional transfer rates among upper levels and the number of these monitored by the detection system.as figure (1-4):

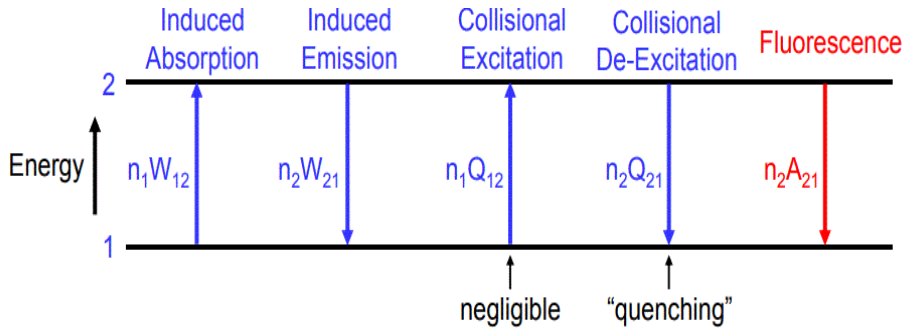

Fig. (1-4): Entry-level model for LIF (two levels)[10].

1-2-1 Two-photon excitation in proteins

In order to largely increase the signal-to-background ratio for single-molecule detection of auto fluorescent proteins in live cells, one could envisage to further shift the wavelength of the excitation light to the red by using two photon excitation. The basic advantage for using two photon excitation is resting on the earlier observation that the two-photon absorption cross-section of a variety of fluorescent molecules scales super-linearly with the one-photon absorption cross-section [11] . Hence,

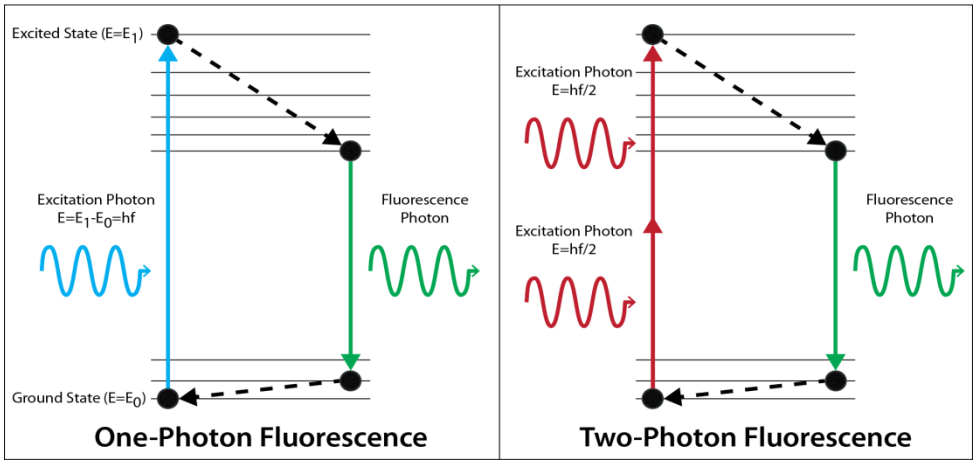

Fig. (1-5): Two-photon excitation [11].

The ratio of the effective excitation rate of a fluorophore with high one-photon absorption cross-section, like the fluorescent proteins, and a fluorophore with a low one-photon absorption cross-section, like flavines, will be largely increased for two-photon excitation. The second advantage of two-photon excitation is that it constitutes a good method to scan a

three-dimensional tissue space with laser excitation configured to excite two (or more) photons at discrete locations in the tissue. This particular applicability for depth discrimination in thick tissues results from the fact that fluorescence signal intensity is highly dependent on the degree of photon flux, which decreases rapidly as a function of distance from the. focal plane[12].

Two-photon microscopy has been involved with numerous fields including: physiology, neurobiology, embryology and tissue engineering. Even thin, nearly transparent tissues (such as skin cells) have been visualized with clear detail due to this technique [13]. Two-photon microscopy's high speed imaging capabilities may also be utilized in noninvasive optical biopsy. In cell biology, two-photon microscopy has been aptly used for producing localized chemical reactions [14]. Using two-photon fluorescence and second-harmonic generation–based microscopy, it was shown that organic porphyrin-type molecules can have different transition dipole moments for two-photon fluorescence and second harmonic generation[15] , which are otherwise thought to occur from the same transition dipole moment. Non-degenerative two-photon excitation, or using two photons of unequal wavelengths, was shown to increase the fluorescence of all tested small molecules and fluorescent proteins [16].

1-2-2 Fluorescence Resonance Energy Transfer in proteins

Many areas of biological research are interested in the precise position and nature of interactions between specific molecular species in living cells, but investigations are typically hampered by the poor resolution of the equipment used to investigate these phenomena. Traditional wide field fluorescence microscopy allows for the localisation of fluorescently tagged molecules within the Rayleigh criterion's optical

spatial resolution limits of around 200 nanometers (0.2 micrometer). However, in order to fully comprehend the physical interactions between protein partners in a typical bimolecular process, the relative proximity of the molecules must be calculated with greater accuracy than allows classic diffraction-limited optical imaging methods [17].

The technique of fluorescence resonance energy transfer (more commonly referred to by the acronym FRET), when applied to optical microscopy, permits determination of the approach between two molecules within several nanometers, a distance sufficiently close for molecular interactions to occur [18]. Typical fluorescence microscopy techniques rely upon the absorption by a fluorophore of light at one wavelength (excitation), followed by the subsequent emission of secondary fluorescence at a longer wavelength. The wavelengths of excitation and emission are often tens to hundreds of nanometers apart. The use of certain fluorophores to label cellular components such nuclei, mitochondria, cytoskeleton, Golgi apparatus, and membranes allows them to be located in both fixed and live samples [19].

Specialized fluorescence filter combinations can be used to analyze the proximity of labeled molecules within a single cell or tissue section by simultaneously labeling various sub-cellular structures with individual fluorophores that have separated excitation and emission spectra. Molecules that are close together than the optical resolution limit appear to be coincident using this approach, and this apparent spatial proximity suggests the possibility of a chemical link. In most cases, however, the normal diffraction is insufficient to determine whether an interaction between biomolecules actually takes place [20]. Fluorescence resonance energy transfer is a process by which radiation less transfer of energy occurs from an excited state fluorophore to a second chromophore in

close proximity. Because the range over which the energy transfer can take place is limited to approximately 10 nanometers (100 angstroms), and the efficiency of transfer is extremely sensitive to the separation distance between fluorophores, resonance energy transfer measurements can be a valuable tool for probing molecular interactions [21].

The mechanism of fluorescence resonance energy transfer involves a donor fluorophore in an excited electronic state, which may transfer its excitation energy to a nearby acceptor chromophore in a non-radiative fashion through long-range dipole-dipole interactions. The theory supporting energy transfer is based on the concept of treating an excited fluorophore as an oscillating dipole that can undergo an energy exchange with a second dipole having a similar resonance frequency [22]. In this regard, resonance energy transfer is analogous to the behavior of coupled oscillators, such as a pair of tuning forks vibrating at the same frequency. In contrast, radiative energy transfer requires emission and reabsorption of a photon and depends on the physical dimensions and optical properties of the specimen, as well as the geometry of the container and the wave front pathways. Unlike radiative mechanisms, resonance energy transfer can yield a significant amount of structural information concerning the donor-acceptor pair[23].

Resonance energy transfer is not sensitive to the surrounding solvent shell of a fluorophore, and thus, produces molecular information unique to that revealed by solvent-dependent events, such as fluorescence quenching, excited-state reactions, solvent relaxation, or anisotropic measurements. [24] The major solvent impact on fluorophores involved in resonance energy transfer is the effect on spectral properties of the donor and acceptor. Non-radiative energy transfer occurs over much longer distances than short-range solvent effects, and the dielectric nature

of constituents (solvent and host macromolecule) positioned between the involved fluorophores has very little influence on the efficacy of resonance energy transfer, which depends primarily on the distance between the donor and acceptor fluorophore. [25]

1-2-3 Principles of Fluorescence Resonance Energy Transfer

The process of resonance energy transfer (RET) can take place when a donor fluorophore in an electronically excited state transfers its excitation energy to a nearby chromophore, the acceptor. In principle, if the fluorescence emission spectrum of the donor molecule overlaps the absorption spectrum of the acceptor molecule, and the two are within a minimal spatial radius, the donor can directly transfer its excitation energy to the acceptor through long-range dipole-dipole intermolecular coupling [26]. A theory proposed by Theodor Förster in the late 1940s initially described the molecular interactions involved in resonance energy transfer, and Förster also developed a formal equation defining the relationship between the transfer rate, interchromophore distance, and spectral properties of the involved chromophores [27]. Resonance energy transfer is a non-radiative quantum mechanical process that does not require a collision or generate heat. When energy is transferred, the fluorescence of the donor molecule is quenched by the acceptor molecule, and if the acceptor is a fluorochrome, enhanced or sensitized fluorescence emission is detected [28]. Exciting a specimen containing both donor and acceptor molecules with light of maximum and detecting light released at wavelengths centered on the acceptor's emission maximum will reveal the phenomena. [29].

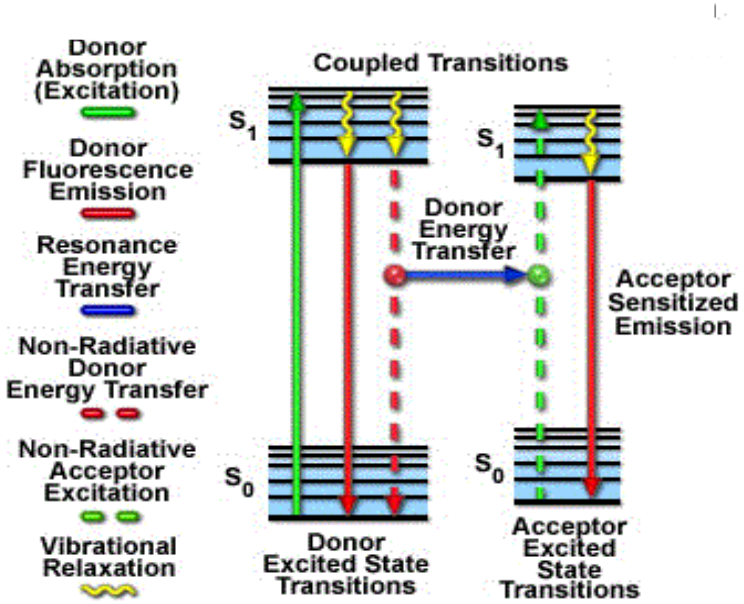

Fig. (1-6): resonance energy transfers jablonski diagram.[29]

Presented in Figure (1-6) is a Jablonski diagram illustrating the coupled transitions involved between the donor emission and acceptor absorbance in fluorescence resonance energy transfer. Absorption and emission transitions are represented by straight vertical arrows (green and red, respectively), while vibrational relaxation is indicated by wavy yellow arrows [30]. The coupled transitions are drawn with dashed lines that suggest their correct placement in the Jablonski diagram should they have arisen from photon-mediated electronic transitions. In the presence of a suitable acceptor, the donor fluorophore can transfer excited state energy directly to the acceptor without emitting a photon. The resulting sensitized fluorescence emission has characteristics similar to the emission spectrum of the acceptor[31].

In summary, the rate of energy transfer depends upon the extent of spectral overlap between the donor emission and acceptor absorption spectra, the quantum yield of the donor, the relative orientation of the donor and acceptor transition dipole moments, and the distance separating the donor and acceptor molecules[32].

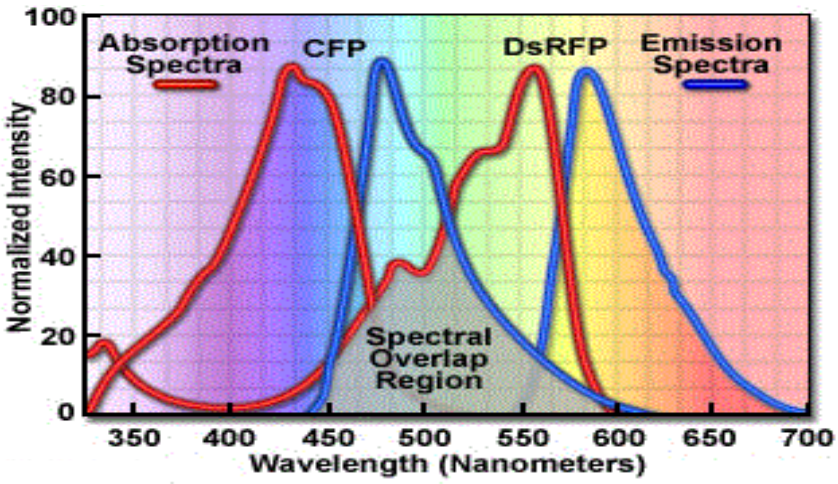

Fig. (1-7): donor- acceptor spectral overlap region[32]

Presented in Figure (1-7) are the absorption and emission spectra of cyan fluorescent protein (the donor) and red fluorescent protein (the acceptor) when compared for their potential application as a fluorescence resonance energy transfer pair. Absorption spectra for both biological peptides are illustrated as red curves, while the emission spectra are presented as blue curves [33]. The region of overlap between the donor emission and acceptor absorption spectra is represented by a gray area near the base of the curves. Whenever the spectral overlap of the molecules is increased too far, a phenomenon known as spectral bleed-through or crossover occurs in which signal from the excited acceptor [34].

If macromolecules are labeled with a single donor and acceptor, and the distance between the two fluorochromes is not altered during the donor excited state lifetime, then the distance between the probes can be determined from the efficiency of energy transfer through steady state measurements [35]. In cases where the distance between the donor and acceptor fluctuates around a distribution curve, such as protein assemblies, membranes, single-stranded nucleic acids, or unfolded proteins, FRET can still be employed to study the phenomena, but time-

resolved lifetime measurements are preferred. Several biological applications that fall into both cases, including conformational changes, dissociation or hydrolysis, fusion of membrane-like lipid vesicles, and ligand-receptor interactions [36]. Although various methods are available for the measurement of fluorescence resonance energy transfer in the optical microscope, none are completely without disadvantages.

Some techniques require more elaborate and expensive instrumentation, while others are based on assumptions that must be carefully validated. Certain approaches are appropriate for fixed specimens, but cannot be applied to living cell systems, while other methods must incorporate significant corrective calculations or data analysis algorithms. It is certain, however, that FRET analysis shows great promise for further development in the utility and scope of biological applications. Dramatic improvements in instrumentation have occurred in recent years, particularly with respect to time-resolved techniques [37].

Fluorescence lifetime measurements that were only accomplished with extreme difficultly in the past are now aided by picosecond and nanosecond technologies. Advances in fluorescent probe development have produced smaller and more stable molecules with new mechanisms of attachment to biological targets. Fluorophores have also been developed with a wide range of intrinsic excited state lifetimes, and a significant effort is being placed on development of a greater diversity in genetic variations of fluorescent proteins. Entirely new classes of fluorescent materials, many of which are smaller than previous fluorophores and allow evaluation of molecular interactions at lower separation distances, promise to improve the versatility of labeling and lead to new applications of the FRET technique [38].

1-3 Nano photonics and Nano devices

Nano is a Greek word meaning dwarf and used as a measure of about (10^{-9} m).Modern electronic devices highly depend on the nanoscale. Nano photonic technology also refers to devices that restrict light wavelength within Nano size [39].Thin films are sensitive to surface properties [40], which includes transparent conducting oxides (TCOs) used in various practical applications because of their unique physical and chemical properties with nanostructures, the sizes, shapes, and different structures that have contributed to developments in Nano science. Methods and Techniques of deposition thin film has been explained and described the importance of thin film multi-layer systems used in critical applications such as photo-detectors, solar cells, photo catalysts, optical windows and filters, and gas sensors [41].

1-3-1 Definition Nano photonics and Nano devices

Nano photonics can be defined as the science and engineering of light-matter interactions [42]. Photonics this term initially used to describe the connection between light technologies and electronics in the field of communication. After that, the light was determined to be of a high intensity up to 10^{18} and sufficient for it to occur nonlinear interactions, its divided into nonresonant (without absorption) and resonant(with absorption). Nano photonics aims to regulate optical energy and convert it on a nanoscale scale by merging the properties of metals, organics, semiconductors, organometallics, polymers, and dielectric materials to generate new, combined states of light and matter known as meta-materials. Nano photonics is thought to have the ability to provide ultra-small optoelectronic components, as well as higher speeds and bandwidth [43] .

1-4 Literature survey

In 2003, Fu-Hua Wang1 and Takashi Yoshitake1 they studied The method based on capillary electrophoresis with laser-induced fluorescence detection (CE/LIF) was developed for determination of magnetic iron oxide nanoparticles (hydrodynamic diameters of 100 nm) functionalized with molecules containing primary amino groups. The present method provides an efficient and fast tool for sensitive determination of the efficacy of bimolecular functionalization of magnetic nanoparticles. The CE/LIF technique requires only negligible sample volumes for analysis, which is especially suitable for controlling the process of preparation of functionalized nanoparticles with unique properties aimed to be used for diagnostic or therapeutic [44].

In 2003, Moon S. Kim, Alan M. Lefcourt, and Yud-Ren Chen they explained A LIF imaging system developed to capture multispectral fluorescence emission images simultaneously from a relatively large target object is described. With an expanded, 355-nm Nd: YAG laser as the excitation source, the system captures fluorescence emission images in the blue, green, red, and far-red regions of the spectrum centered at 450, 550, 678, and 730 nm, respectively, from a 30-cm-diameter target area in ambient light. Images of apples and of pork meat artificially contaminated with diluted animal feces have demonstrated the versatility of fluorescence imaging techniques for potential applications in food safety inspection [45].

In 2004, Peter Ashjian and Amir Elbarbary they explained Time-resolved laser-induced fluorescence spectroscopy (TR-LIFS) is demonstrated here to noninvasively monitor the formation of osteogenic extracellular matrix (ECM) produced by putative stem cells derived from human adipose tissue. The results are consistent with those obtained by

conventional histochemical techniques (immunofluorescence and Western blot) and demonstrate that TR-LIFS is a potential tool for monitoring the expression of distinct collagen types and the formation of collagen cross-links in intact tissue constructs [46].

In 2006, Chan Kyu Kim and Rajamohan R Kalluru they studied A compact, highly specific, inexpensive and user friendly optical fiber LIF sensor based on fluorescence quenching by nanoparticles has been developed to detect single-strand (ss-) DNA hybridization at femtomolar level. The fluorescence of fluorophore-tagged ss-DNA increases by a factor of 80 when it binds to a complimentary DNA, while the addition of single-base mismatch DNA had no effect on the fluorescence efficiency [47].

In 2013 Joshi-Deepak and KumarAnil K.MainiRamesh they explained Standoff detection of biological warfare agents in aerosol form using Ultra violet-Laser Induced Fluorescence (UV-LIF) spectroscopy method . Range-resolved detection and identification of biological aerosols by both Nano-second and non-linear femto-second LIDAR is also discussed. Calculated received fluorescence signal for a cloud of typical biological agent Bacillus globigii (Simulants of B. anthracis) at a location of ~5.0 km at different concentrations in presence of solar background radiation has been described [48].

In 2014 Jagdish P Singh and Sunil K. Kiwanian they explained Laser induced fluorescence (LIF) spectroscopy has emerged as a potential tool for the cancer diagnosis. A comprehensive analytical study of a compact optical fiber LIF based sensor for in-vitro point monitoring of tissue auto-fluorescence as a non-invasive tool for cancer diagnosis is presented. An attempt has been made to determine an optimum sensing configuration to develop a diagnostics procedure to enhance small but

consistent spectral difference between the normal and malignant tissue from various parts of animal body to greatly improve the accuracy of the auto-fluorescence cancer diagnosis [49] .

In 2018, Jorge Marques da Silva and Andrei Borissovitch Utkin they studied use of fluorescence techniques, namely, pulse-amplitude-modulated fluorometry, was crucial to understanding the photo physiology of these microbial communities, since they made it possible to measure biofilms' photosynthetic activity without disturbing their delicate spatial organization within sediments or soils. The use of LIF added further technical advantages, enabling measurements to be made at a considerable distance from the samples, and under daylight. and in biotechnological applications of photosynthetic biofilms [50] .

In 2018, Siqi Guo, Yu Jing, Incline. Berkus they explained Nano pulse stimulation (NPS) as a developing technology has been studied for minimally invasive, nonthermal local cancer elimination for more than a decade. Here we show that a single NPS treatment results in complete regression of the poorly immunogenic, metastatic 4T1-Luc mouse mammary carcinoma. Impressively, spontaneous distant organ metastases were largely prevented, even in those animals with incomplete tumor regression. All tumor-free mice were protected from secondary tumor cell challenge, demonstrating a vaccine-like effect [51].

In 2019, Valentina Gabbarini and Riccardo Rossi they explained applicability of LIF to the classification of viruses, Experimental tests were performed in which different viruses were irradiated with a UV laser emitting at 266 nm and the emitted spectra were recorded by a spectrometer. The classification techniques show the possibility of discriminating viruses. Although the application of the LIF technique to biological agents has been thoroughly this work aims at validating for the

first time its applicability to virological analyses. allowing fast responses to epidemiologic reducing their risks [52].

In 2019 Fatemeh Ghasemi, Parviz Parvin and Maryam Lotfi shown that formaldehyde, a tissue preserver, demonstrates fluorescence properties. Here, laser-induced fluorescence spectroscopy is carried out in order to differentiate between normal and cancerous tissues of interest, namely human breast, larynx and colon. Although no spectral shift appears with changes in formaldehyde concentration, the fluorescence emission of impregnated tissues undergo a notable red shift versus fluorophore concentration and the cancerous tissues exhibit a definite blue shift with respect to normal tissues. This emphasizes that endogenous fluorophores in molecules of interest within the scaffold show some spectral shift properties, mainly due to the high propensity for formation of covalent chemical bonds between proteins in tissues [53].

In 2019 D.S. Arabia, Z.A. Abdel-Salama, H.A. Godabc, M.A. Haritha they studied LIF is a spectrochemical analytical technique that was used to obtain bacteria spectral fingerprints in the liquid phase. Two laser wavelengths, 266 nm (UV) and 405 nm (violet), have been used as excitation light sources delivering output power 5 mW and 100 mW, respectively. The results of LIF analysis showed that the differences in fluorescence bands intensity can be used as a fingerprint for each bacterial species. In addition, the fluorescence emission intensities of the two strains were exponentially related to the concentration of the bacteria [54].

In 2019, Yinhua Jiang, Juan Kang and Yarui Wang they studied laser-induced breakdown spectroscopy–laser-induced fluorescence (LIBS-LIF) spectroscopy was first applied to carry out rapid and sensitive trace lead analysis in medicinal herb samples. To overcome the problem

of diversity on the sample size, shape, and density for different samples, original samples were pulverized to powder and then pressed into pellets for spectral analysis [55].

In 2019, Ahmed L.Abdel Gawad and Yasser El-Sharkawy they studied Early diagnosis of tooth enamel demineralization, and dentin caries lesions, present a valuable solution to avoid or decrease their deleterious effect. The aim of this study was to design a simple, effective, and non-invasive technique, employing a novel laser wavelength to classify and differentiate between various tooth abnormalities in-vitro, by estimating wavelengths, showing distinctive appearance for each tooth class [56].

In 2020 Zachary A. Duca and Nicholas C. Speller they explained Micro capillary electrophoresis (μCE) enables high-resolution separations in miniaturized, automated microfluidic devices. Pairing this powerful separation technique with laser-induced fluorescence (LIF) enables a highly sensitive, quantitative, and compositional analysis of organic molecule monomers and short polymers, which are essential, ubiquitous components of life on Earth. Improving methods for their detection has applications to multiple scientific fields, particularly those related to medicine, industry, and space science. Here, a modular benchtop system using μCE with LIF detection was constructed and tested by analyzing standard amino acid samples of valine, serine, alanine, glycine, glutamic acid, and aspartic acid in multiple borate buffered solutions of increasing concentrations from 10 mM to 50 mM, all (pH 9.5) [57].

In 2021, Oloche Owoicho, Charles Ochieng' Olwal and Osbourne Quaye they studied laser-induced fluorescence-light detection and ranging (LIF-LiDAR) has been used to identify MS_2 bacteriophage on artificially contaminated surgical equipment or released amidst other

primary biological aerosol particles in laboratory-like close chamber. It has also been shown to distinguish between different picornaviruses [58].

1-5 Aim of Work

The aim of this research is:

1- Synthesis of TiO_2 Nanoparticles by using DC Sputtering Technique.

2- Use the laser induced fluorescence (LIF) technique in Diagnosing Colon Cancer Cells treated with TiO_2 Nanoparticles.

3- Analysis and study of some optical properties of colon cancer cells before and after treatment with TiO_2 nanoparticles according to certain concentrations, depending in particular on fluorescence spectra.

2-1 Introduction

In this chapter, the principle of LIF is introduced to give an overview of the main parameters of this technique, its basic tools and applications, in addition to knowing the advantages of this technique, as well as learning about the process of tissue transplantation of cancer cells as a bio-chemical application of a technique LIF.

2-2 Laser Induced Fluorescence (LIF) Principle

LIF is a two-step process: absorption of a laser photon followed by emission of a fluorescence photon from the excited state. For absorption the laser wavelength (λ_{Laser}) must match an allowed energy transition of the LIF-active molecule (atom). Only a fraction Φ_{LIF} of these excited molecules fluoresces, the rest relaxes without light emission. An optical filter selects the usually red-shifted fluorescence light at the emission wavelength (λ_{LIF}). Only the fraction η of all emitted LIF-photons is detected and converted to the camera signal.

Upon relaxation back into the ground state they sometimes emit fluorescence quanta at longer wavelengths than the exciting laser wavelength and with a characteristic average stay in the excited higher state, the fluorescence lifetime. When a good separation between laser and fluorescence wavelength is given by using high-quality optical filters or spectrographs, highest detection sensitivities can be reached. When using femto-, pico-,nano or microsecond lasers, the fluorescence lifetime of a sample can be determined [59]. Typically they are found in the range of pico- or nanoseconds. In the case of “forbidden” electronic transitions excited-state-lifetimes of micro- or milliseconds occur. Such long-lasting luminescence lifetimes are especially interesting for bio-analytical applications. Fluorescence spectroscopy is primarily concerned with

electronic and vibrational states. Generally, the species (molecule of the substance) being examined has a ground electronic state (a low energy state) of interest, and an excited electronic state of higher energy. Within each of these electronic states there are various vibrational states. In fluorescence, the species is first excited, by absorbing a photon, from its ground electronic level to one of the various vibration states in the excited electronic level.

Collisions with other molecules cause the excited molecule to lose vibration energy until it reaches the lowest vibrational state of the excited electronic level. The molecule then drops down very fast (10^{-9} s range) to one of the various vibrational levels of the ground electronic state again, emitting a photon in that process. As molecules may drop down into any of several vibrational levels in the ground state, the emitted photons will have different energies, and thus frequencies [60].

It is also possible to classify Laser Induced Fluorescence into continuous wave or time-resolved LIF. Continuous wave (CW) LIF utilises a continuous laser for excitation and is employed when only spectral information is required. In time-resolved LIF, a pulsed laser is used to excite the sample and its emission (either a single wavelength or the full spectrum) is detected as a function of time. This provides valuable time-resolved information such as the lifetimes of chemical intermediates and their associated time-gated spectral evolution [61] . As shown in the figure (2-1):

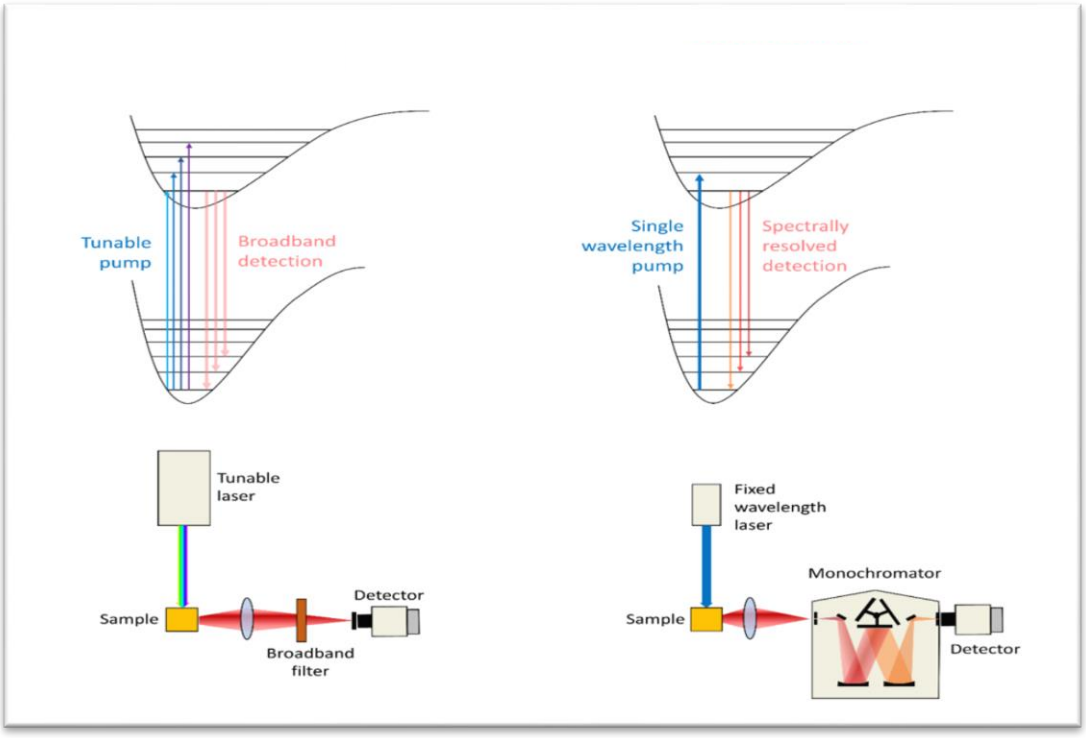

Fig.(2-1): Schematic representation of excitation LIF spectroscopy [60] .

2-3 LIF Technology System

The attached devices used in LIF technology are shown in the figure (2-2):

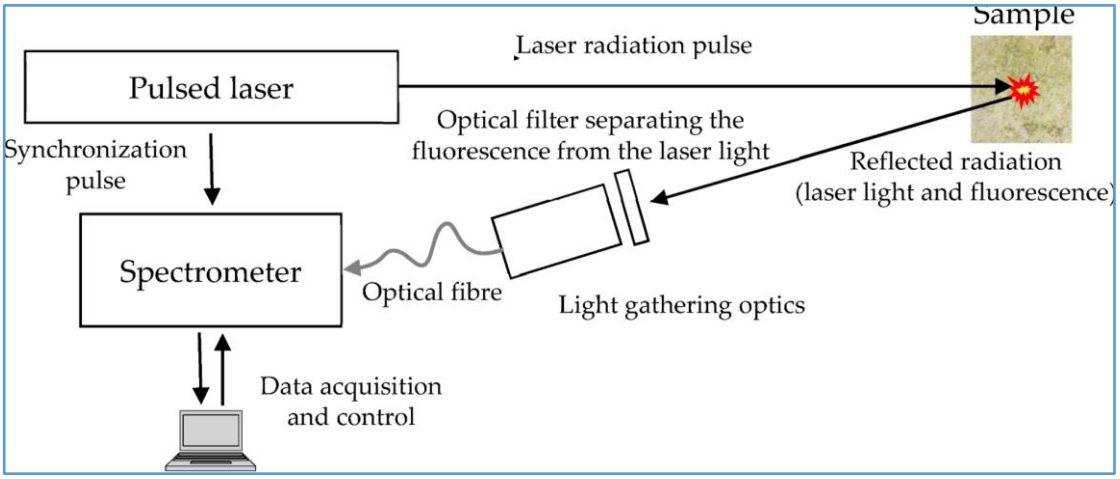

Fig.(2-2): Optical devices used in LIF technology [62].

2-3-1 Laser Source

The most widely used laser in LIF technology is the green diode laser with a wavelength of 532 nm The diode laser is basically just a combination of a LED and a laser. It means that the original photons are generated in a same fashion than in LEDs and then these photons are used to generate more photons by stimulated emission. In a diode laser all this is done inside the same device [63] .One of the main requirements in a laser is to have and excess amount of excited electrons. This is called populated inversion and in diode lasers it is achieved by injecting a large amount of electrons to the junction with a relatively high current. The amount of current that is needed to achieve the sufficient amount of excited electrons is called lasing threshold. This lasing enables the device to produce really high optical power and because the emitted light is coherent it also enables various ways to control the light beam [64]. As shown in Figure (2-3):

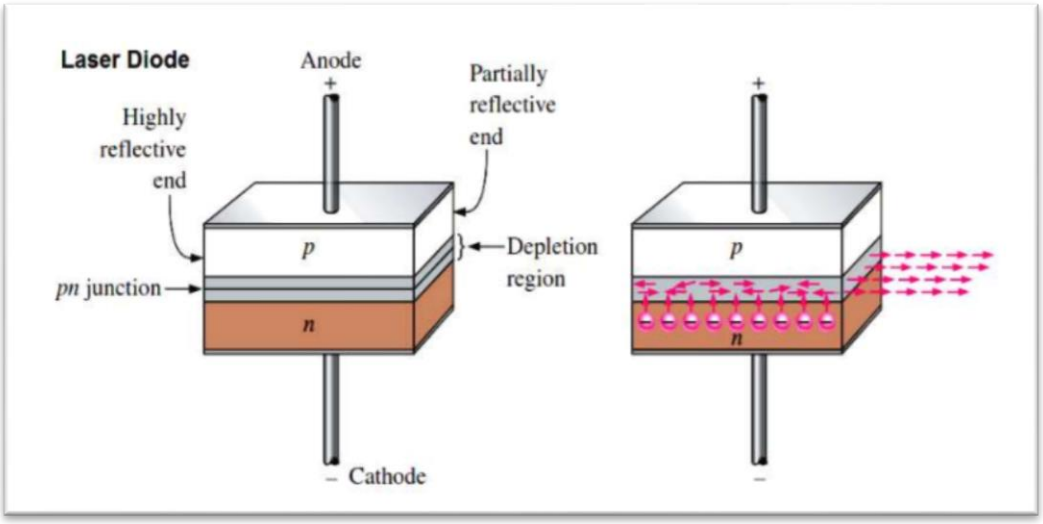

Fig.(2-3). Structure of diode laser [65] .

2-3-2 Optical Fiber

The recent use of optical fibers is a good result for transmitting light over long distances. It is important to improve fiber-optic materials, now

possible to concentrate the energy density of the order of megawatts per square centimeter at the end of the fiber, without damage, by Putting a lens at the end of the optical fiber. Placing the optical fiber close to the sample at a distance of a few millimeters is an important way to collect emissions from samples, as the collecting angle of the end of the fiber allows light to be collected. It has been proposed to use optical fiber beams to simultaneously obtain spectral emission from different regions of the spectral emission of some elements. The use of a single optical fiber collect the emission from the sample makes the LIF system suitable for studying a sample located at a great distance, providing a unique advantage for its industrial applications. Optical fibers transmit laser pulses over distances of up to 100 meters. Thus the emitted light can be collected and sent back to the detector using the same fiber or a second fiber optic cable [66].

2-3-3 Detector and Spectrometer

A spectrometer is a device that neutralizes the light emitted by a sample. It is made from the entrance aperture, two mirrors and a diffraction grating. The light enters through the hole and reaches the first mirror that meets the light and directs it towards the groove. Also, light is reflected at different angles depending on the wavelength. The second mirror focuses the light towards the position of the detector. Different types of reagents are used in LIF technology depending on the practical application. If the required information is 2D, the most commonly used devices are CCD and ICCD devices. CCD detectors provide a lower signal in the background, while ICCD detectors provide improved signal-to-noise ratio (SNR), fast response time of a few nanoseconds, and wide detection ranges from the visible to the infrared region of the

electromagnetic spectrum, but their cost is much higher than CCD detectors [67].

2-4 Fluorescence

Fluorescence describes a phenomenon where light is emitted by an atom or molecule that has absorbed light or electromagnetic radiation from a source. In absorption, high energy light excites the system, promoting electrons within the molecule to transition from the ground state, to an excited state. Here, the electrons quickly relax to the lowest available energy state. Once this state is achieved and after a fluorescence lifetime, the electrons will relax back to ground state, releasing their stored energy as an emitted photon. Usually, the emitted light has lower energy than the absorbed radiation. Methods regarding this subject are mostly used in the biochemical and biophysical field [68]. Fluorescence requires a fluorophore (molecule with a rigid conjugated structure) In absorption, high energy light excites the system, promoting the electron within the molecule to transition from the ground state, to the excited state. The entire fluorescence process is cyclical. Unless the fluorophore is irreversibly destroyed in the excited state, the same fluorophore can be repeatedly excited and detected. So, a single fluorophore can create thousands of photons, due to the high sensitivity of detection techniques [69].

Fluorescence plays an important role in clinical medicine, especially a diagnostic and research tool. The useful properties of fluorescence are applied in techniques such as fluorescence microscopy and fluorescence spectrometry. Here fluorescence has many aims, such as to detect viruses and to identify hormones. Another area where it is used, is in immunochemistry, to identify the distribution of a specific protein within a tissue, for example, a fluorochrome can be used to mark the protein via

an antibody. FRET and FLIM are also two techniques related to fluorescence Furthermore, fluorescence also used in surgery as a medical imaging technique that is used to detect structures during surgery. As we can see, there are many advantages of using fluorescence in medicine.

The techniques associated with it, are very simple and specific. It is fairly sensitive and thus can detect low quantitates of a compound. Unfortunately, not all substances are able to emit light, and therefore techniques using fluorescence cannot always be applied. fluorescence plays a key role in oncology. Through flourescending-protein-markers that attach only to cancer cells, it will be possible to differentiate precisely between healthy and mutated cells. Thus, these cancer cells can be specifically targeted and attacked, whilst, the healthy cells remain unharmed. This will result in a very effective new form of chemotherapy for the benefit of the patients [70].

2-4-1 Photo Physics of Fluorescence Proteins

Fluorescence-based assays are crucial experimental tools which allow the detailed dissection of molecular mechanisms. The assays can be performed in real-time, in solution, with high-time resolution and sensitivity down to single molecules. This has allowed the measurement of protein interactions, enzymatic activity, conformation changes, localization of proteins, and the ability to see individual proteins moving in real time.[71] Proteins have intrinsic fluorescence due to residues such as tryptophan. A fluorophore reports upon the protein it is attached to and its environment. In the simplest case, this allows proteins to be visualized or counted through photo bleaching. More advanced assays can measure protein–protein interactions or conformation changes, by measuring intensity changes and fluorescence. With all of these approaches,

ensemble bulk or single-molecule measurements are possible. Bulk measurements offer the greater flexibility with the least requirements in terms of fluorescence properties. Single-molecule measurements provide a greater sensitivity because the ensemble averaging can mask rare, or short-lived, states [72].

2-4-1-1 Fluorescence in Sensing Imaging & Microscopy

The great advantage of fluorescence as a tool is that, being an optical phenomenon in most cases it involves non-ionizing radiation is nondestructive and mirmally invasive, and can therefore be applied to living cells and tissues. This is a feature it shares with nonfluorescence-based, optical microscopy techniques such as, for example, coherent anti-Stokes Raman scattering (CARS) and second harmonic generation (SHG) and third harmonic generation (THG) imaging. Compared to bioluminescence or chemiluminescence techniques, an advantage of using fluorescence is that a single fluorophore can be excited repeatedly, unlike bioluminescence or chemiluminescence, which irreversibly produces only a single photon per chemical reaction of interacting molecules. Compared to radioactive labeling techniques, fluorescence methods are easier to manage, and the samples are less cumbersome to dispose of than those involving radioactive methods. Indeed, improving the spatial resolution in optical microscopy has recently become a field of great activity, which has spawned several promising methods, some of which have already been commercialized [73].

Conventional fluorescence microscopy relies on contrast according to the fluorescence intensity, with the fluorescence detection sensitivity extending down to the single molecule level . Due to the Stokes shift of fluorescence emission, the exciting light can be eliminated from the image so that only fluorescence on a dark background is detected, leading

to a high contrast . Two- and three-dimensional fluorescence imager, to locate, for example, labeled proteins can be recorded using wide-field or one- or two-photon confocal scanning techniques. Confocal microscopy, the basic principle of which is a 1955 invention by Minsky (1988), is based on a of focused light scanned across the sample and detecting the fluorescence through a pinhole [74].

This spot allows out-of-focus fluorescence emanating from above and below the focal plane to be eliminated from the image. This optical sectioning feature is also achieved by the more recent technique of multiphoton excitation microscopy . The invention of laser and computers with image processing capacity and the demonstration of the advantages of this microscopy for cell biology have led to a widespread use of confocal and multiphoton excitation microscopy over the last decade or so Time-lapse imaging allows the temporal evolution of the system to be studied, and fluorescence bleaching techniques can provide information about the diffusion of the fluorescent probe [75]. Imaging of FRET between a fluorescent donor and acceptor enables the determination of protein interaction and conformational changes well below the optical diffraction limit [76]. The key purpose of fluorescence microscopy is the localization of fluorescent dyes, nanoparticles, or proteins in the specimen, which can be achieved by mapping the fluorescence intensity [77].

2-4-4 Absorbance

Absorbance is defined as "the logarithm of the ratio of incident to transmitted radiant power through a sample (excluding the effects on cell walls)". Alternatively, for samples which scatter light, absorbance may be defined as "the negative logarithm of one minus absorptance, as measured on a uniform sample [78]. The term is used in many technical areas to

quantify the results of an experimental measurement. While the term has its origin in quantifying the absorption of light, it is often entangled with quantification of light which is "lost" to a detector system through other mechanisms. What these uses of the term tend to have in common is that they refer to a logarithm of the ratio of a quantity of light incident on a sample or material to that which is detected after the light has interacted with the sample. The term absorption refers to the physical process of absorbing light, while absorbance does not always measure only absorption: it may measure attenuation (of transmitted radiant power), caused by absorption, but also reflection, scattering, and other physical processes [79].

The roots of the term absorbance are in the law of (Lambert law). As light moves through a media, it will become dimmer as it is being "extinguished". Bouguer recognized that this extinction (now often called attenuation) was not linear with distance traveled through the medium, but related by what we now refer to as an exponential function. If I_o is the intensity of the light at the beginning of the travel and I_s the intensity of the light detected after travel of a distance T, is given by:

$$T = \frac{I_s}{I_0} = exp(-\mu d) \qquad \text{----------(2-1)}$$

where μ is called an attenuation constant (a term used in various fields where a signal is transmitted through a medium) or coefficient. The amount of light transmitted is falling off exponentially with distance. Taking the Napierian (natural) logarithm in the above equation, we get:

$$-ln(T) = ln\frac{I_0}{I_s} = \mu d \qquad \text{----------(2-2)}$$

For scattering media, the constant is often divided into two parts

$$\mu = \mu_s + \mu_a \qquad \text{----------(2-3)}$$

separating it into a scattering coefficient μ_s , and an absorption coefficient μ_a , obtaining:

$$-ln(T) = ln\frac{I_0}{I_s} = (\mu_s + \mu_a)d \qquad \text{----------(2-4)}$$

If a size of a detector is very small compared to the distance traveled by the light, any light that is scattered by a particle, either in the forward or backward direction, will not strike the detector. In such case, a plot of -ln(T) as a function of wavelength will yield a superposition of the effects of absorption and scatter. Because the absorption portion is more distinct and tends to ride on a background of the scatter portion, it is often used to identify and quantify the absorbing species. Consequently this is often referred to as absorption spectroscopy, and the plotted quantity is called "absorbance", symbolized A[80]:

$$\mathrm{A}_{10} = \mu_{10} d \qquad \text{----------(2-5)}$$

2-5 Advantages of Using LIF Technology

LIF technology has the following advantages over some other analysis methods:

1- LIF technology can detect and analyze multiple items simultaneously, i.e. a simple and straightforward method To analyze multi-element materials.

2- Quick (or instant) elemental analysis. Extraction and stir are done in one step.

3- Different materials can be analyzed using avoid sample contamination and obtain accurate results.

4-The equipment is inexpensive, and the cost of analyzing samples with LIF is low compared to traditional analytical techniques others provide good sensitivity to some elements. It can be applied to detect all elements in the periodic table.

5- Telemetry can be carried out from distances of up to 50 meter. [81,82]

2-6 Sputtering Technique

Sputtering is a physical process in which atoms in a solid-state (Target) are bombarded by energetic ions, causing them to be freed and flow into the gas phase (mainly noble gas ions). Sputtering is commonly confused with sputter deposition, a high-vacuum-based coating technology that belongs to the PVD (physical vapor deposition) process family. Sputtering is also employed in surface physics as a cleaning procedure for high-purity surface preparation and as a way for assessing the chemical composition of surfaces [83]. As shown in figure (2-4):

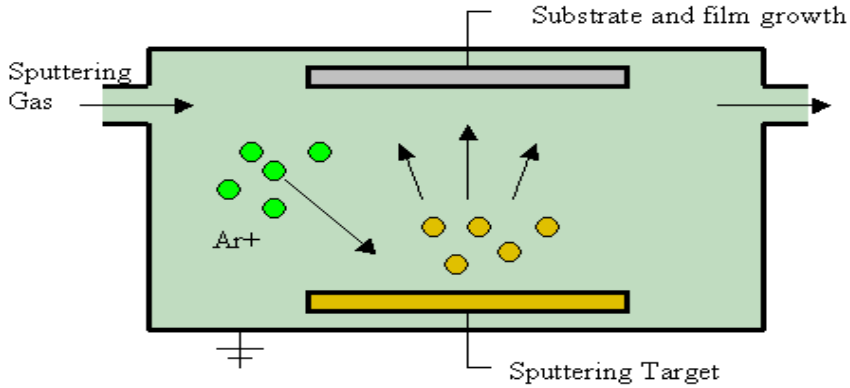

Fig. (2-4): Sputtering Technique[83].

2-6-1 Sputtering theory

Three steps make up a sputtering deposition:

1.Particles are emitted from a solid target as a result of momentum transfer from the ions blasting the target. Due to many collisions and dispersions of sputtered particles by sputtering gas molecules such as Ar atoms,

2 - The moving process is the most typical of sputter deposition and has a significant impact on the formed films.

3-The main portion of the deposition process includes nucleation and growth processes, which is something that most vapor deposition technologies have in common [84]. As shown in Figure (2-5):

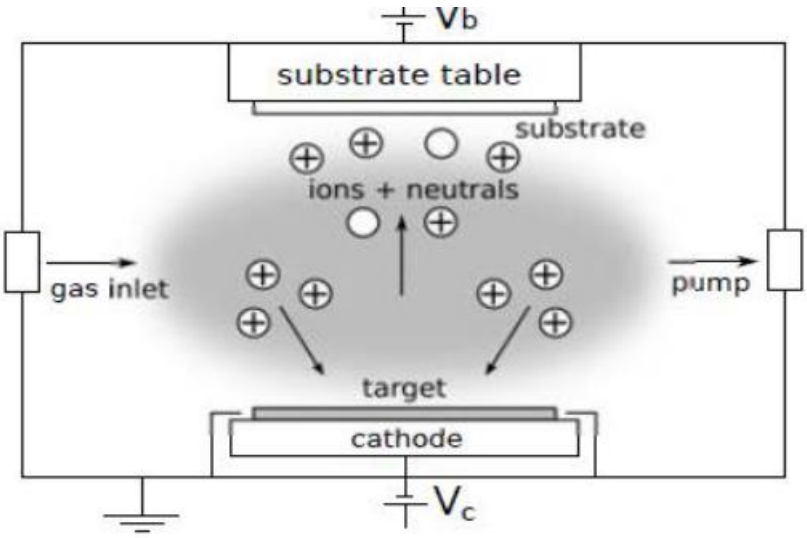

Fig. (2-5): The schematic drawing of sputtering setup [84] **.**

Sputtering is a vital and popular method in the PVD process. Atoms are ejected off the surface of the target material during the sputtering process by the transfer of sustained momentum from an atomic-sized energetic bombardment particle, commonly a gaseous ion accelerated from a plasma [85]. That is, depending on the kinetic energy of the bombing particles, multiple phenomena may occur when charged particles are bombarded on a solid surface. When bombing energy are

less than 5 kV, reactions are restricted to the surface's outer layer, with arriving particles being reflected, or entering into a thermal equilibrium with the surface. The potential energy of the bombed species is responsible for removing the secondary electrons, or in the case of the installed surface, responsible for breaking and rearranging the bonds. In the kinetic energy that exceeds the binding energy of the surface atoms, the lattice atoms are pushed to new locations, that cause the atoms to move from the surface and damage the surface. Its energy is around four times that of the target material's sublimation heat. Physical sputtering, which is the basis of the deposition technique used in this study [86], is characterized by the expulsion and dislodging of atoms into the gas phase. The basic principle of sputtering is simple momentum transfer as a result of collisions. As shown in Figure (2-6):

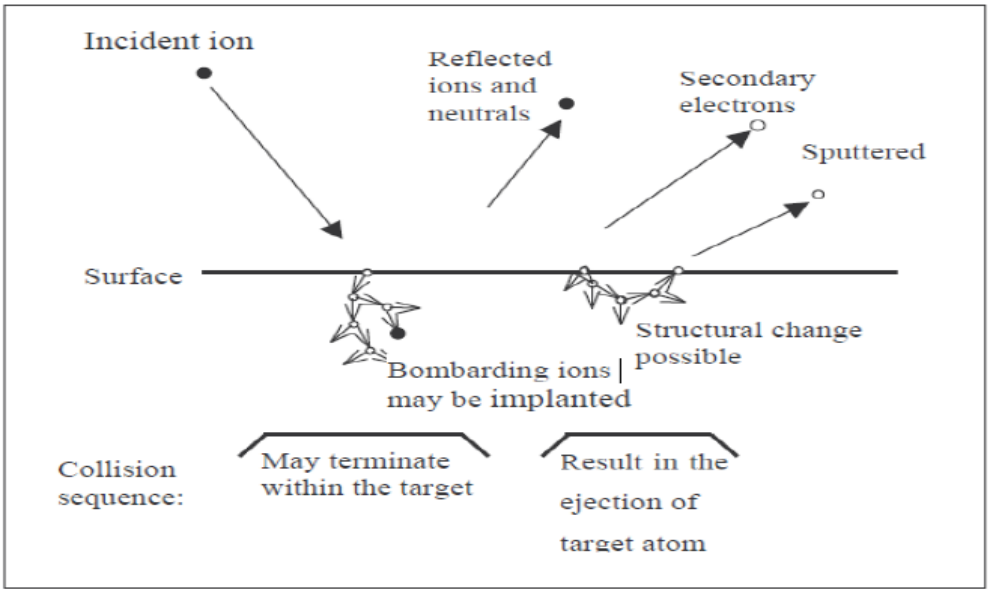

Fig. (2-6):The processes generated by the impact of very energetic particle on a target surface [87].

There are several characteristics that distinguish the sputtering process from the rest of the deposition processes:

1-Metals, semiconductors and insulators can be deposited using direct current or radiofrequency sputtering, both reactively (to form oxidizing films, nitrides or carbides), and non-reactively. In addition, materials of complex composition such as stainless steel and Pyrex glass can be deposited on condition that the cathode is cooled. Vacuum evaporation of these materials is almost impossible.

2-Sputtering produces films that have same stoichiometry as materials of target.

3-The relative simplicity of controlling film thickness once the process parameters are defined to obtain a measurable thickness, any desired thickness can be achieved by keeping the parameters and changing the deposition time only.

4-The values of sputtering yields compared to the vapor pressure values of different materials are closer to each other. This makes the deposition of the multi-layer films more controllable by sputtering.

5-Possible formation of new phase structure from target material .

6-Lifetime of target material is long .

7-DC Sputtering systems can be constructed readily from primitive materials.

The following points summarize the drawbacks of this technique:

1-It requires provide vacuum.

2-To produce high-quality films, this technique requires many variables to optimize, complexity.

3-Dedicated equipment for sputtering process are highly costs and require clean room facilities.

4-It produces pollution such as increased porosity, pinholes, gas incorporation into film.

5- This technique often slower than other techniques [88].

2-6-2 Sputtering configurations

Sputtering is classified as diode sputtering (cathode or radio frequency), reactive sputtering, bias sputtering, magnetron sputtering, and ion beam sputtering based on the source and process orientation. The sputtering deposition technique employs several energy sources, and the operating pressure varies depending on the power arrangement. DC A pair of planar electrodes, the cathode and anode, are used to create sputtering. The negative electrode is used to deposit the target material, and the anode is used to deposit the substrate [85]. The maximum energy (E_{max}) of the atoms which removed from the target in DC sputtering systems is determined by the applied voltage, by acceleration a single charged ion through a voltage difference of (1V) and transmit kinetic energy of (1 eV) to the ion, and for the applied voltage, the atoms are sputtered from the target with a wide distribution of energies [88].A parameter called the sputter yield (S), which is the removal rate of surface atoms due to ion bombardment, is defined as the mean number of atoms removed from the surface of a solid per incident ion and is given by [86]:

$$S=\frac{\text{Atoms removed}}{\text{Incident ions}} \qquad \ldots\ldots\ldots\ldots\ldots\ldots \text{(2-6)}$$

The sputter yield is large when m ions ≈ m atoms, it depends on mass, ions, and direction of incident ions.

For sputter deposition of thin films in DC systems, applied voltages between 100 and 1000V are commonly utilized. The density of sputter current has a big impact on the sputtering rate. 0.1-10 mA/cm^2 is a typical range. The rate of deposition accelerates as the current density rises. However, because materials arrive reach the substrate surface at a faster rate, processes including surface diffusion and agglomeration at present

growth sites, as well as nucleation with other growth sites, take less time. The type of sputter gas and pressure have a significant impact on the sputtering rate and qualities of the deposited layer. Because it is not desirable for the sputter gas to interact with the target in most instances, noble gases with large masses are utilized. Because xenon and krypton have bigger atomic masses than argon, they provide higher sputter yields. However, argon is more typically employed since it is less expensive and more readily available. The average distance traveled by the sputter atoms before they contact with the gas atoms is determined by the gas pressure, and this is known as the mean free path (m), which is inversely proportional to the gas pressure. The short mean free path means before the sputtered atoms are deposited on the substrate they that will undergo many collisions with the gas atoms. It can influence the porosity of the deposited film as well as its crystallization and surface morphology [88]. DC systems cannot be used to sputter targets because the target will be charged as a result of the electrical discharge.

The fundamental advantage of DC diode sputtering systems is that they are very simple and can be built with commonly accessible materials at a minimal cost. The quality of the films deposited for these systems, on the other hand, is relatively low, owing to the considerable working pressure required to maintain the electrical discharge. The use of magnetic fields to confine the electrical discharge in the area around the target is a fantastic way to lower the pressure of sputter gas. Sputtering systems that use magnet groups around the target are referred to as direct DC magnetrons. With these systems, the sputter gas pressure can be as low as (10 Torr) and high-quality films can be produced at deposition rates that are identical to those obtained with evaporation deposition techniques. Unfortunately, the usage of DC systems and DC magnetron systems is difficult to sputter magnetic materials and insulators [87].

In this work, the films were formed using the DC reactive magnetron sputtering process, which allows the deposition of composite materials of different compositions, and high deposition rate, excellent uniformity of coating and control of deposition parameters are the main advantage of using this technology [89].

2-6-3 Magnetron Sputtering

Magnetron sputtering can be used to create thin films and coatings on a variety of substrates. The technology was first used in industry at the end of the 1970s. The magnetron sputtering process is useful not just in industry, but also in science and technology research.

This approach has a high productivity, is environmentally friendly, and produces particles of the desired size. Using a static magnetic field, this approach confines electrons in the area of the cathode target of an essentially DC discharge. The Lorentz force is the force acting on a charged particle in the presence of a magnetic field. [90].

$$\vec{F} = q(\vec{E} + \vec{V} \times \vec{B}) \qquad \text{……..……(2-7)}$$

where q is the charge of particle, is electric field, is the velocity of charged particle and is the magnetic field .

The electron confinement leads to dense plasma adjacent to the cathode target and abundance of ions to perform sputtering as they are accelerated across the cathode sheath. The sputter process releases the film forming material from the cathode target and these species are either ionized or not before they fall onto a substrate to form a film or coating [91]. In general, there are two standard types of magnetic field configuration used in deposition by magnetron sputtering .

Balanced magnetron: The inner and outer magnets are of equal strength, allowing electrons to be confined close to the target surface. This

indicates that the plasma does not reach the substrate, resulting in low ion bombardment of the substrate during film growth, resulting in reduced atom mobility on the substrate.

Unbalanced magnetron: The magnetic field arrangement is unbalanced if the inner magnet has a stronger pole than the outer magnet (type I unbalanced magnetron). The magnetic field lines open up and extend towards the substrate in the type II arrangement because the inner pole is weaker than the outer pole. The electrons follow the field lines and, therefore, the plasma is also extended to the substrate. Ion bombardment during growth can beneficially influence the film properties, such as increase coatings density and improve adhesion to the substrate [90].

Despite the benefits offered by unbalanced magnetrons, it is still difficult to uniformly coat complex components at acceptable rates from a single source. As a result, numerous magnetron systems have been introduced in try to commercialize this technology. The magnetic arrays of nearby magnetrons in a multiple magnetron system can be designed with either identical or opposite magnetic polarity. In the first situation, the arrangement is described as mirrored, while in the second case, it is described as closed field. The field lines in the mirrored casing are directed towards the chamber walls.

Following these lines, secondary electrons are lost, resulting in a low plasma density in the substrate region. In the closed field configuration, on the other hand, the field lines are connected between the magnetrons. The substrate is in a high-density plasma area, therefore there are few losses to the chamber walls. The effectiveness of the closed field configuration . As can be seen, operating in the closed field mode results in an ion-to-atom ratio incident at the substrate some 2-3 times greater

than that obtained under the same conditions in the mirrored, or single unbalanced magnetron configurations [83]. As shown in Figure (2-7):

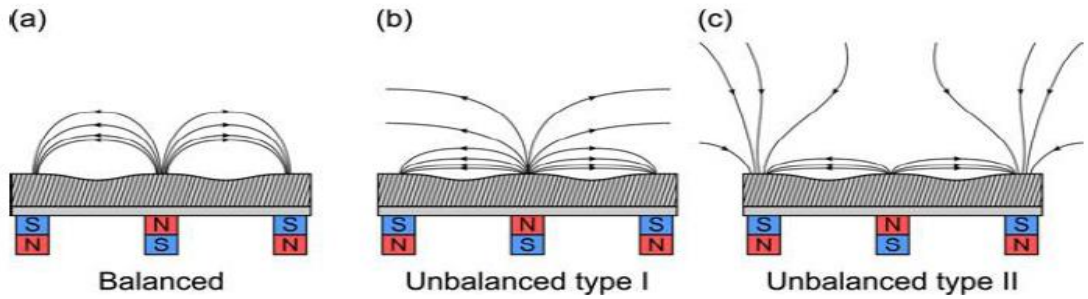

Fig. (2-7): The schematic of the magnet configuration.(a) all the field lines that originate from the central magnet enter the annular magnet (b) all the field lines originate from the central magnet, while some do not enter the annular magnet (unbalanced type I), and (c) all the field lines originate from the annular magnet, and some do not enter the cylindrical central magnet (unbalanced type II) [91] .

2-7 Titanium Dioxide TiO_2NPs

TiO_2 has a molecular weight: 79.866 and other names as titanic oxide, titanic acid anhydride, titanium anhydride, titanium, titanium white. Titanium dioxide is mined from natural deposits. It also is produced from other titanium minerals or prepared in the laboratory, Titanium dioxide also can be prepared by heating Ti metal in air or oxygen at elevated temperatures [92]. Nanoscale titanium dioxide (TiO_2) attracts considerable attention due to its unique physicochemical and catalytic properties, which found application in various fields, where it is defined as an inexpensive material, earth abundant, chemically stable, nontoxic, and environment friendly.

2-7-1 Physical and Chemical Properties of Titanium Dioxide

Titanium dioxide is an n-type semiconductor with a large energy band gap, with rutile and anatase optical band gaps of 3.0 and 3.2 eV, respectively, and brookite optical band gaps ranging from 3.13 to 3.40 eV. However, the band gap of nanostructured materials can be narrowed by adding structural flaws or doping with non-metal and metal components. TiO_2 thin films have a high dielectric constant of 40 to 86 and a high resistivity of up to $10^8\Omega$.cm. Titanium dioxide is made up of two elements, Ti: 59.95% and O: 40.05% ,Its density 4.23g/cm3 , Mohs hardness 5.8 (anatase and brookite) and 6.2 (rutile),with index of refraction 2.488 (anatase), 2.583 (brookite) and 2.609 (rutile),melts at 1843C°, insoluble in water and dilute acids, soluble in concentrated acids but it does not dissolve completely [92].

2-7-2 Crystal Structure

Titanium dioxide usually appearing in an amorphous phase or as three crystalline phases: anatase and rutile tetragonal phases, , and an orthorhombic phase brookite. Rutile is the most stable phase, in which both anatase and brookite are metastable, transforming to rutile when heated . It has been claimed that phase transformation of the amorphous state to anatase takes place between 300 and 500 degrees Celsius, with further transformation to rutile taking place between 600 and 1000 degrees Celsius. The tetragonal structures of rutile and anatase have six and twelve atoms per unit cell, respectively. Each Ti atom is coordinated to six O atoms in both phases, and each O atom is linked to three Ti atoms. The TiO6 octahedron is slightly distorted, with two Ti-O bonds slightly larger than the other four and some O-Ti-O bond angles shifted

from 90 degrees (greater distortion in anatase than rutile). Rutile and anatase crystal structures are made up of TiO_6 octahedral chains, with four edges in anatase and two in rutile.In the case of brookite, it has distorted TiO6 octahedral sharing three edges. Moreover, brookite has eight formula units in the orthorhombic cell, in which the interatomic distances and O-Ti-O bond angles are similar to those of rutile and anatase, nevertheless it has six different Ti-O bonds .Rutile, anatase and brookite unit cells. The lattice parameters for rutile are a= 0.4594 nm and c= 0.2958 nm, while anatase has lattice parameters of a= 0.3785 nm and c= 0.9515 nm, and brookite has lattice parameters of a= 0.9184 nm, b= 0.5447 nm, and c= 0.5145 nm [93]. As shown in Figure (2-8):

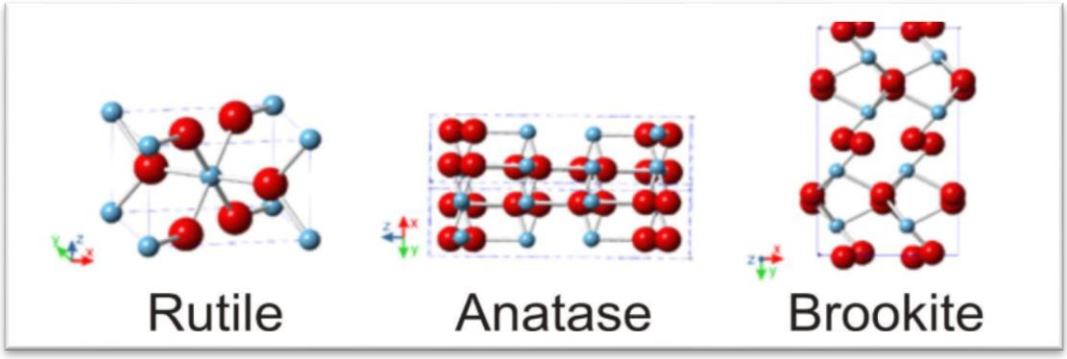

Fig.(2-8) : Unit cells of TiO_2 Rutile, Anatase and Brookite [93].

2-8 Cancer Therapeutic Effects of TiO_2 NPs

Cancer is a group of diseases which cause an abnormal and uncontrolled cell division coupled with malignant behavior such as invasion and metastasis. Despite remarkable advances in modern medical sciences, cancer remains a disease difficult to treat and becomes a leading cause of death worldwide (around 13% of all deaths). During the past 70 years, the number of cancer death has continued to rise, as compared to the slight increase in the number of people died of other diseases such as

heart diseases, cerebrovascular diseases, and pneumonia [94]. In these days, radiotherapy and chemotherapy are the principal treatment modalities aimed at eradicate solid tumors that are located deep inside the body. However, [95] these methods have suffered from their non-specific mode of action, which not only kills cancer cells but also harms normal cells at the same time. [96]. Since the current chemotherapy is mainly based on a whole-body treatment with the chemotherapeutic agents, it is inevitable to cause many dangerous side effects associated with the non-selective cytotoxic effect of the medications [97].

2-8-1 Earlier Detection and Diagnosis by Nano Technology

In the fight against cancer, half of the battle is won based on its early detection. Nanotechnology provides new molecular contrast agents and materials to enable earlier and more accurate initial diagnosis as well as in continual monitoring of cancer patient treatment [98]. For cancer, Nano devices are being investigated for the capture of blood borne biomarkers, including cancer-associated proteins circulating tumor cell Already clinically established as contrast agents for anatomical structure, nanoparticles are being developed to act as molecular imaging agents, reporting on the presence of cancer-relevant genetic mutations or the functional characteristics of tumor cells. This information can be used to choose a treatment course or alter a therapeutic plan [99].

2-8-2 Treatment and Therapy

Cancer therapies are currently limited to surgery, radiation, and chemotherapy. All three methods risk damage to normal tissues or incomplete eradication of the cancer [100]. Nanotechnology offers the means to target chemotherapies directly and selectively to cancerous cells and neoplasms, guide in surgical resection of tumors, and enhance the

therapeutic efficacy of radiation-based and other current treatment modalities. All of this can add up to a decreased risk to the patient and an increased probability of survival [101].

Research on nanotechnology cancer therapy extends beyond drug delivery into the creation of new therapeutics available only through use of nanomaterial properties. Although small compared to cells, nanoparticles are large enough to encapsulate many small molecule compounds, which can be of multiple types. At the same time, the relatively large surface area of nanoparticle can be functionalized with ligands, including small molecules, DNA or RNA strands, peptides, aptamers or antibodies. These ligands can be used for therapeutic effect or to direct nanoparticle fate in vivo [102]. These properties enable combination drug delivery, multi-modality treatment and combined therapeutic and diagnostic, known as “theranostic,” action. The physical properties of nanoparticles, such as energy absorption and re-radiation, can also be used to disrupt diseased tissue, as in laser ablation and hyperthermia applications [103].

Integrated development of innovative nanoparticle packages and active pharmaceutical ingredients will also enable exploration of a wider repertoire of active ingredients, In addition, immunogenic cargo and surface coatings are being investigated as both adjuvants to nanoparticle-mediated and traditional radio- and chemotherapy as well as stand-alone therapies. Innovative strategies include the design of nanoparticles as artificial antigen presenting cells and in vivo depots of immunostimulatory factors that exploit nanostructured architecture for sustained anti-tumor activity [103].

2-8-3 Safety of Nanotechnology Cancer Treatment

Nanotechnology is a powerful tool for combating cancer and is being put to use in other applications that may reduce pollution, energy consumption, greenhouse gas emissions, and help prevent diseases. There is nothing inherently dangerous about being Nano sized [104] . There are so many ambient incidental nanoparticles, in fact, that one of the challenges of nanoparticle exposure studies is that background incidental nanoparticles are often at order-of-magnitude higher levels than the engineered particles being evaluated [105].

As with any new technology, the safety of nanotechnology is continuously being tested. The small size, high reactivity, and unique tensile and magnetic properties of nanomaterials—the same properties that drive interest in their biomedical and industrial applications However, the majority of available data indicate that there is nothing uniquely toxic about nanoparticles as a class of materials. In fact, most engineered nanoparticles are far less toxic that household cleaning products, insecticides used on family pets, and over-the-counter dandruff remedies [106]. Certainly, the nanoparticles used as drug carriers for chemotherapeutics are much less toxic than the drugs they carry and are designed to carry drugs safely to tumors without harming organs and healthy tissue [107] .

2-9 Cell Culture

cell culture is a type of biotechnological technique where cells are artificially grown in a favorable environment. cell culture is a common and widely used technique for the isolation of cells and their culture under artificial conditions. This technique was developed as a laboratory technique for particular studies; however, it has since been developed to

maintain live cell lines as a separate entity from the original source. The development of cell culture techniques is due to the development of basic tissue culture media, which enables the working of a wide variety of cells under different conditions [108] .

In vitro culture of isolated cells from different animals has helped in the discovery of different functions and mechanisms of operations of different cells. Some of the areas where cell culture has found most applications include cancer research, vaccine production, and gene therapy. The growth of cells on artificial media is difficult than growing microorganisms on artificial media and thus, require more nutrients and growth factors. However, advances in the culture media have made it possible to culture both undifferentiated and differentiated cells on artificial media. Depending on the purpose and application of the technique, cells, tissues, or organs can be used for the culture process [109] .

2-9-1 applications of cell culture

The following are some of the applications of animal cell culture:

a. Production of vaccines

1. cell culture is an important technique used for the development of viral vaccine production.
2. The technique has been used for the development of a recombinant vaccine against hepatitis B and poliovirus.
3. Immortalized cell lines are used for the large-scale or industrial production of viral vaccines [110].

b. Recombinant proteins

1. cell cultures can also be used for the production of recombinant therapeutic proteins like cytokines, hematopoietic growth factors, growth factors, hormones, blood products, and enzymes.
2. Some of the common cell lines used for the production of these proteins are baby hamster kidney and CHO cells [110].

d. Model systems

Cells obtained from cell culture can be studied as a model system for studies related to cell biology, host-pathogen interactions, effects of drugs, and effects due to changes in the cell composition [110].

e. Cancer Research

1. Animal cell culture can be used to study the differences in cancer cells and normal cells as cancer cells can also be cultured.
2. The differences allow more detailed studies on the potential causes and effects of different carcinogenic substances.
3. Normal cells can be culture to form cancer cells by the use of certain chemicals, viruses, and radiation.
4. Cancer cells can also be used as test systems for studies related to the efficiencies of drugs and techniques used in cancer treatment [110] .

2-9-2 Advantages of Cell Culture

The following are some of the advantages of animal cell culture;

1. Cell culture is superior to other similar biotechnological approaches as it allows the alteration of different physiological and physiobiological conditions like temperature, pH, and osmotic pressure.

2. cell culture enables studies related to cell metabolism and understand the biochemistry of cells.
3. It also allows observation of the effects of various compounds like proteins and drugs on different cell types.
4. The results from cell cultures are consistent if a single cell type is used [111] .
5. The technique also enables the identification of different cell types on the basis of the presence of markers like molecules or by karyotyping.
6. The use of cell culture for testing and other processes prevents the use of animals in experiments.
7. cell culture can be used for the production of large quantities of proteins and antibodies, [111].

2-9-3 Disadvantages of Cell Culture

Even though cell culture has been used as a technologically advanced method, there are some disadvantages associated with this approach

1. It is a specialized technique that requires trained personnel and aseptic conditions. The technique is an expensive process as it requires costly equipment.
2. The subsequent subculture of the cell culture might results in differentiated properties as compared to the original strain.
3. The method produces a minuscule amount of recombinant proteins, which further increases the expenses of the process.
4. Contamination with mycoplasma and viral infection occur frequently and are difficult to detect and treat.
5. The cells produced by this technique lead to instability due to the occurrence of aneuploidy chromosomal constitution [112] .

2-9-4 Cancer Cell Culture

The continual development of tumor cell culture techniques is vital. Traditional cell culture methods use a two-dimensional monolayer. With continuous improvements being made, this method has become a standard technology in life sciences at present. However, due to the inherent flaws of traditional culture, it fails to correctly imitate the architecture and microenvironments of in vivo, which makes 2D-cultured cells different from cells growing in vivo in terms of morphology, proliferation, cell-cell and cell-matrix inter-connections, signal transduction, differentiation and other aspects [113,114]. In order to improve these simulations of cell microenvironments in vivo, culture has become the next frontier of cell biology research.

As the intersection between tumor cell biology and tissue engineering, in vitro tumor models simulate the in vivo physiological microenvironment, and may be useful at the pre-clinical development stage to identify potentially successful prototypes and eliminate failures at an early stage. This means that it has potential to bridge the gap between traditional monolayer cell culture and tumor cytology experiments in vivo. Therefore, an increasing number of tumor biologists have begun to emphasize the importance of tumor cell culture. [115,116], including preclinical drug screening, cancer stem cell maintenance and differentiation, signal abnormal transduction and other aspects [117,118]. For example, compared with monolayer cultures, cells in culture generally exhibit a reduced sensitivity to certain chemotherapeutic agents [119]. These results and the exponentially increasing number of studies surrounding this topic convey the importance of tumor cell culture [120].

As shown in Figure (2-9):

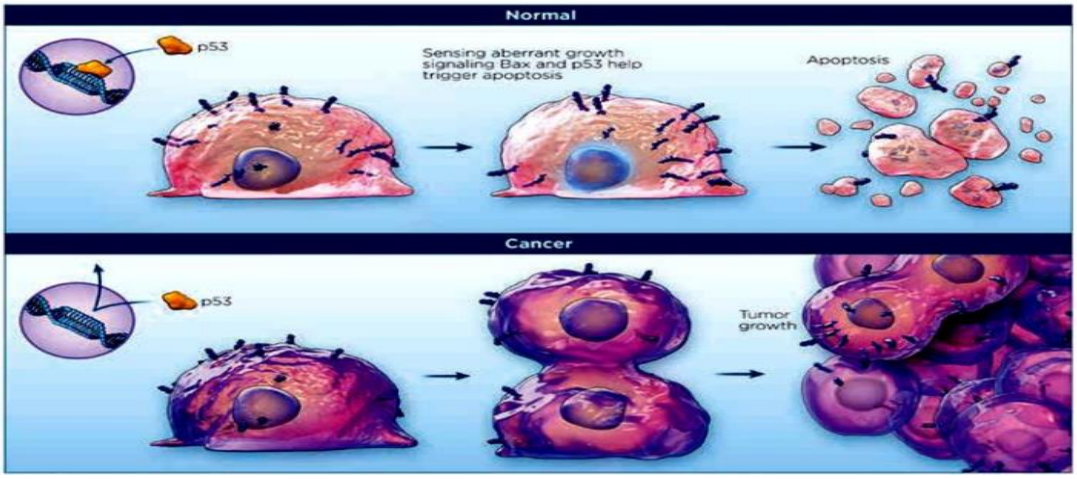

Fig. (2-9): Cancer Cell culture [120].

2-9-5 Colon Cancer

Colon cancer is the world's second most common cause of cancer-related death in both men and women, and the second most fatal cause of cancer-related death in both men and women. It affects more than 35,000 patients worldwide each year, with a 9.4% incidence rate, and kills more than 55,000 people [121]. Colon cancer accounts for 8.5 percent of all cancers and is linked to lifestyle variables such as obesity, drinking, smoking, and other factors [122]. Depending on the site of the metastatic growth, typical treatment for colon cancer comprises assisting (application or administration) chemotherapeutic drugs and surgery. The present chemotherapeutic drugs, on the other hand, cause substantial side effects and high toxicity. which also increase the risk of death. Chemotherapy is one of the most important treatments for cancer patients. However, the efficacy of the chemotherapeutic drugs is still limited in most solid tumors [123].

2-9-6 Main Interaction of Photon with Matter

The energy transfer from photon beams to the substance differs from the energy transfer from other rays. There are five different types of photon interactions with atoms. Photoelectric effect, Compton scattering, pair creation, photonuclear interactions, and Rayleigh scattering are some

of the methods used. The photoelectric effect, Compton scattering, and pair creation are all important interactions in radiotherapy, in which all or part of the photon energy is transmitted to atom electrons via the Coulomb contact. Rayleigh scattering is a simple deviation in the course of an incident photon caused by a Colombian contact between the photon and an electron atom that occurs without a change in the photon's energy [124]. When a photon reaches the nucleus and subsequently liberates a proton or neutron, this is known as a photonuclear interaction. However, this type of photon contact occurs seldom (less than 5% of the time), thus it is not common. The photoelectric effect is prevalent when the photon energy is less than 0.1 MeV, while Compton scattering is typical when the photon energy is between 0.1 and 1.022 MeV. Pair formation interactions are common at energies over 1.022 MeV. Compton scattering is frequent for materials with low atomic numbers, such as carbon, water, and human tissue, throughout a large range of energy (0.02 – 30) MeV, but this effect diminishes as the atomic number of the substance increases [125].

2-9-7 Mechanisms of Radiation Damage to DNA

Within the cell, radiation interacts with molecules at random. Although deoxyribonucleic acid (DNA) is the primary target for cell death, cellular and nuclear membrane damage is also a factor. Healthy cells that have been irradiated but have not been rendered fatal may be able to repair DNA damage. Ionizing radiation causes DNA damage, which is generated either directly by ionization within the DNA molecule or indirectly by the action of chemical radicals formed as a result of local ionizations in cell water [126]. Free radicals play a role in indirect DNA damage. A pair of ions is created when photon radiation (electrons and positrons from pair formation) interacts with water (H_2O). The electron

will combine with H_2O to form H_2O- and the positron will combine with H_2O to form H_2O+ . These H_2O+ and H_2O- are called ion radicals (not free radicals). Ion radicals are very unstable and rapidly dissociate: H_2O+ becomes H+ and OH• , and H_2O- becomes H• and OH− , OH• and H• are free radicals figure (2-11),[126]:

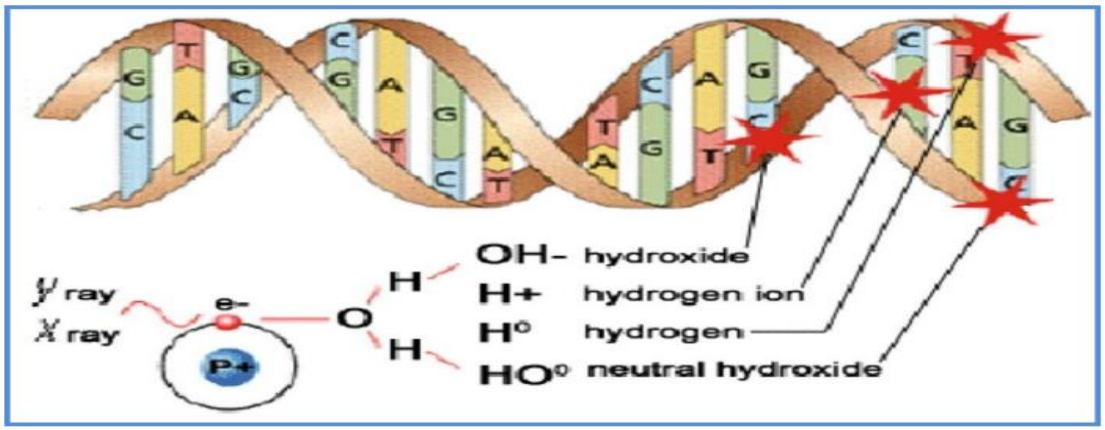

Fig. (2-10): Mechanisms of Radiation Damage to DNA [126].

3-1 Introduction

In this chapter, the experimental parts of the work includes synthesizing of Titanium dioxide nanostructures by a lab closed-field unbalanced dual magnetron DC reactive sputtering system. Also, the laser induced fluorescence technology (LIF) and its main parts were prepared, such as the laser source used and the rest of the optical parts used to collect the spectrum emitted from the prepared samples. With a description and how to prepare colon cancer cell samples. Figure (3-1) presents a flow chart of the experimental part of the work in which the main sections are explained:

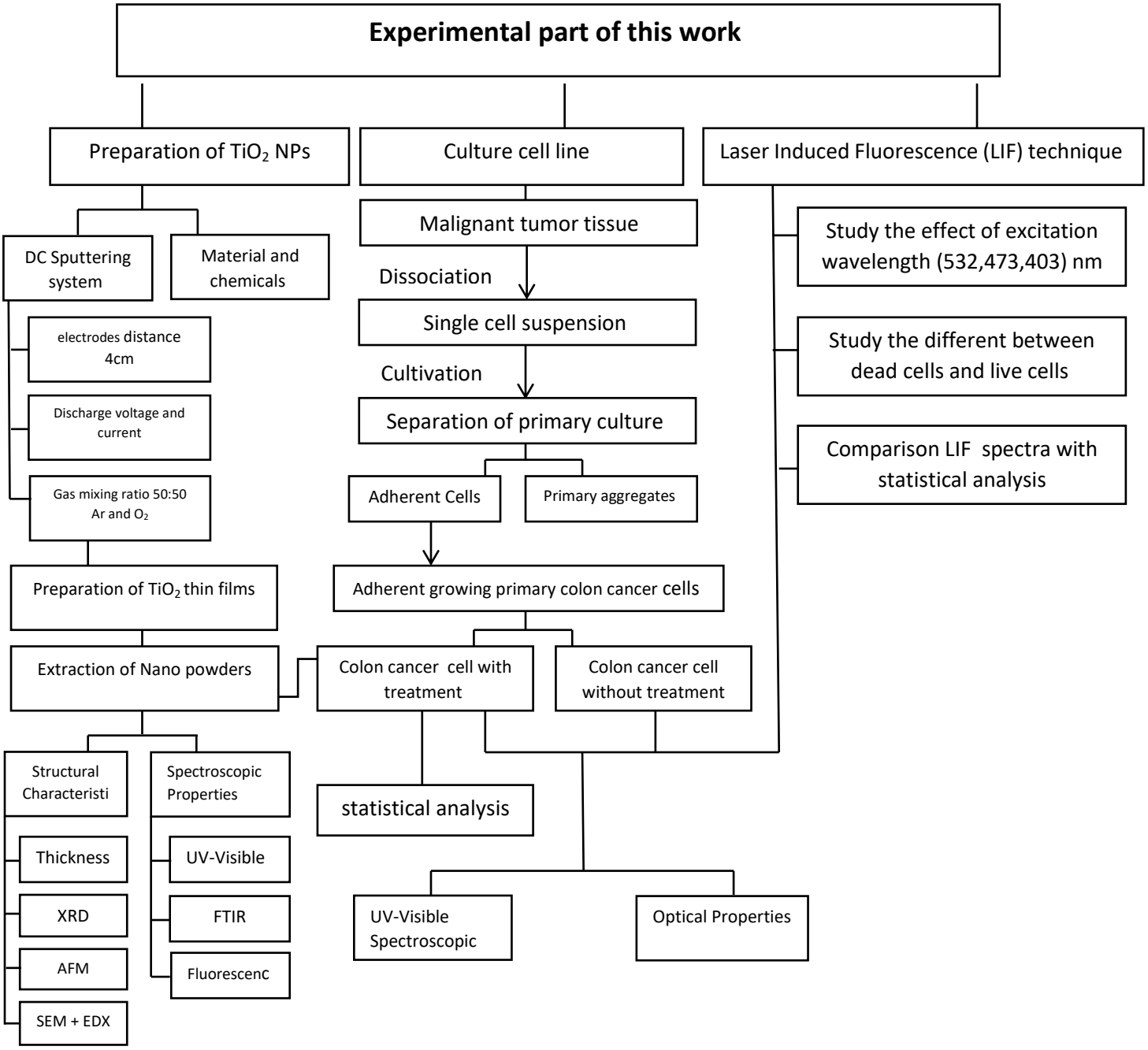

Fig. (3-1): The flow chart of the experimental part of the present work.

3-2 Sputtering System

The DC reactive magnetron sputtering system used in this work done in physics laboratory in the College of Science / University of Baghdad, includes vacuum chamber, discharge electrodes and magnetron assembly, vacuum unit, dc power supplies, gas supply system, gas mixing unit, cooling system and measuring tools, as shown in figure (3-2):

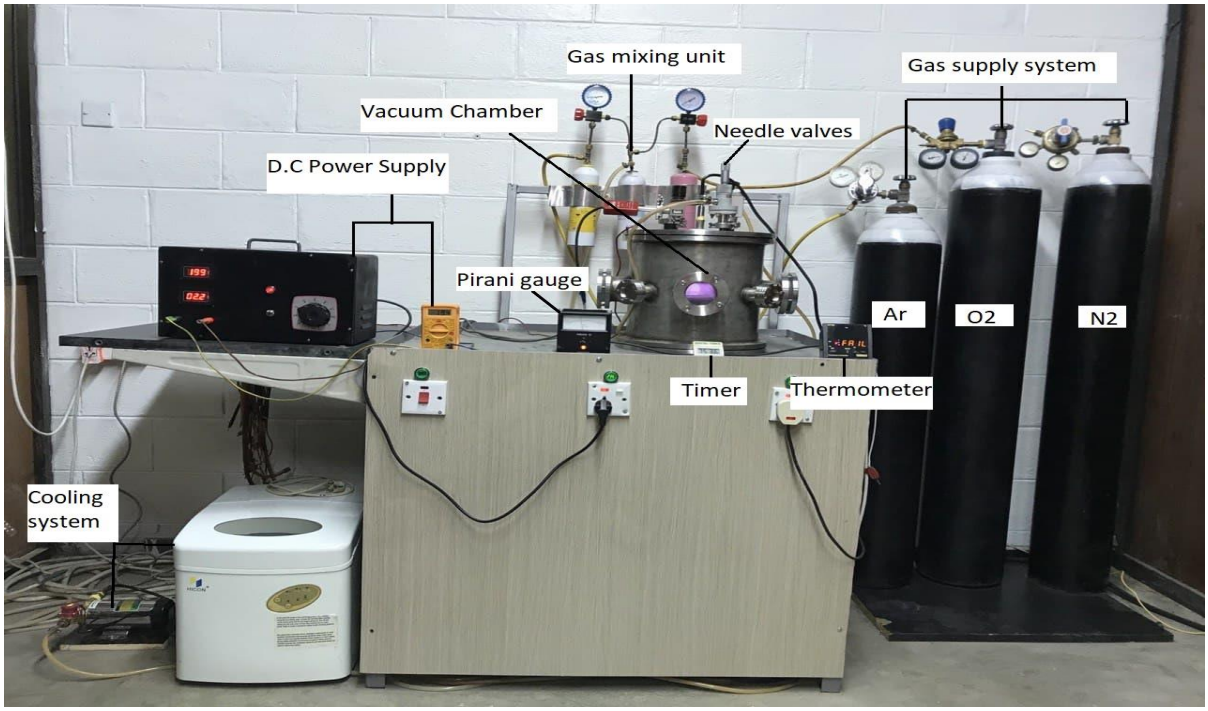

Fig. (3-2): The magnetron sputtering system used in the present work.

Table (3-1) :Properties of magnetron sputtering system

The height of champer	37.5 cm
Cathode diameter	80 mm
Anode diameter	90 mm
Cathode thickness	8.5 mm
Anode thickness	6.5 mm
The distance between the electrodes	4cm
Pumping speed	24 cm^3/h
Pressure	10^{-1} mbar
Power source	2kv
Gas mixing ratio	50:50

3-2-1 Deposition Chamber

They are used to monitor the discharge that occurs inside the chamber, as shown in the figure ,as shown in figure (3-3):.

Fig. (3-3): The deposition chamber in sputtering system.

3-2-2 Discharge Electrodes and Magnetron Assembly

Stainless steel was used to construct two discharge electrodes (anode and cathode), as shown in figure (3-4):

Fig. (3-4) : The magnetron assembly on electrodes.

3-2-3 Gas Mixing Unit

The stainless steel gas mixer in this system includes three cylinders for mixing oxygen and argon, as well as oxygen cylinders, flowmeters, gas flow regulators, needle valves, and connections and connectors. Initially, several gas mixtures were used to determine the optimum gas mixture but the final results were presented for the samples prepared using the optimum mixture [127] ,as shown in figure (3-5):

.

Figure (3-5): The gas mixing unit

3-2-4 Vacuum Unit

A two-stage rotary pump (Leybold-Heraeus) .The vacuum pressure inside the chamber is measured using an Edward Pirani gauge, as shown in figure (3-6):

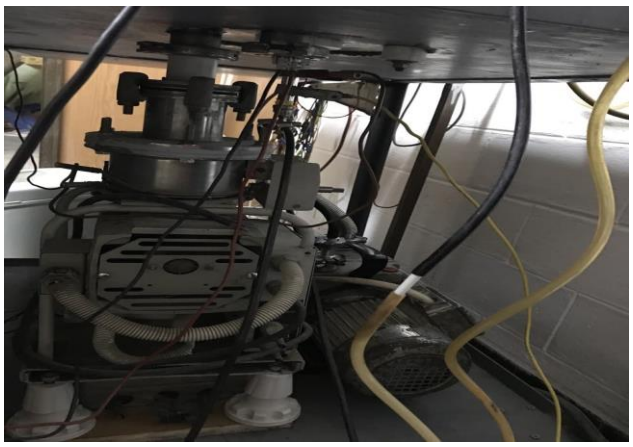

Fig. (3-6): The vacuum unit.

3-2-5 DC Power Supply

DC power source (Edwards 2A) was used to deliver the electrical power required for generating discharge inside the vacuum chamber via high tension cables. [108] As shown in figure (3-7):

Fig. (3-7): The DC power supply

3-2-6 Cooling System and Thermometer

The room-temperature water was cooled and circulated via a channel in discharge electrodes, with a maximum flow rate of 30 l/min, this machine can cool the water to around 4°C and disperse it, as shown in figure (3-8):

Fig. (3-8):The cooling system.

3-2-7 Titanium Dioxide

Titanium dioxide, also known as Titanium(IV) oxide is the inorganic compound with the chemical formula TiO_2 When used as a pigment, The table (3-2) shows the Properties of Titanium:

Table (3-2) :Properties of Titanium [129].

Titanium (Ti)	
Atomic number	22
Appearance	Silvery grey-white metallic
Classification	Titanium is a transition metal
Atomic weight	47.867 g/mol
Crystal structure	close-packed hexagonal
Density	4.54 g/cm^3
Melting point	1941K (1668 °C)
Molar heat capacity	25.060 J/(mol. K)
Oxidation states	+2,+3,+4
Electronegativity	1.54
Ionization energies	1^{st}: 658.8 kJ/mol 2^{nd}: 1309.8 kJ/mol, 3^{rd}: 2652.5 kJ/mol
Atomic radius	147 pm
Thermal conductivity	21.9 W/(m. K)
Electrical resistivity	420 Ω. m (at 20°C)
Surface binding energy	4.90 eV

3-2-8 Preparation of Thin Film Samples

For the deposition process, the targets were cleaned and dried. Before the experiments, the glass substrates on which the thin films were deposited were cleaned. On the cathode, the target was carefully maintained. The system's operating conditions were split into two categories: constant and variable. Vacuum pressure, current limiting resistance, discharge voltage, discharge current, flow velocity, deposition temperature, inter-electrode spacing, and gas mixing ratio are all constant operating conditions. The variable operating conditions were 1, 1:30, 2, 2:30, and 3 hours of deposition time. Many experiments were performed to determine the optimum working pressure as well as the optimum mixing ratio of Ar and O_2 gases. Also, it was determined the optimum inter-electrode distance between 1 to 8 cm, from the experiments results,4cm has been specified as the optimum inter-electrode distance. The optimum discharge current was determined according to the stability of the discharge plasma. The cathode was cooled by circulating water through the cooling channel while the anode was left to be heated in order to enhance the adhesion between the deposited film and the substrate.

3-2-9 Extraction of Nano powders from prepared thin films

The experimental part of this work in Department of Physics, College of Education, Al-Iraqia University، Baghdad, Iraqis schematically shown in Figure 1(a). The vacuum chamber is made of galvanized steel and can be

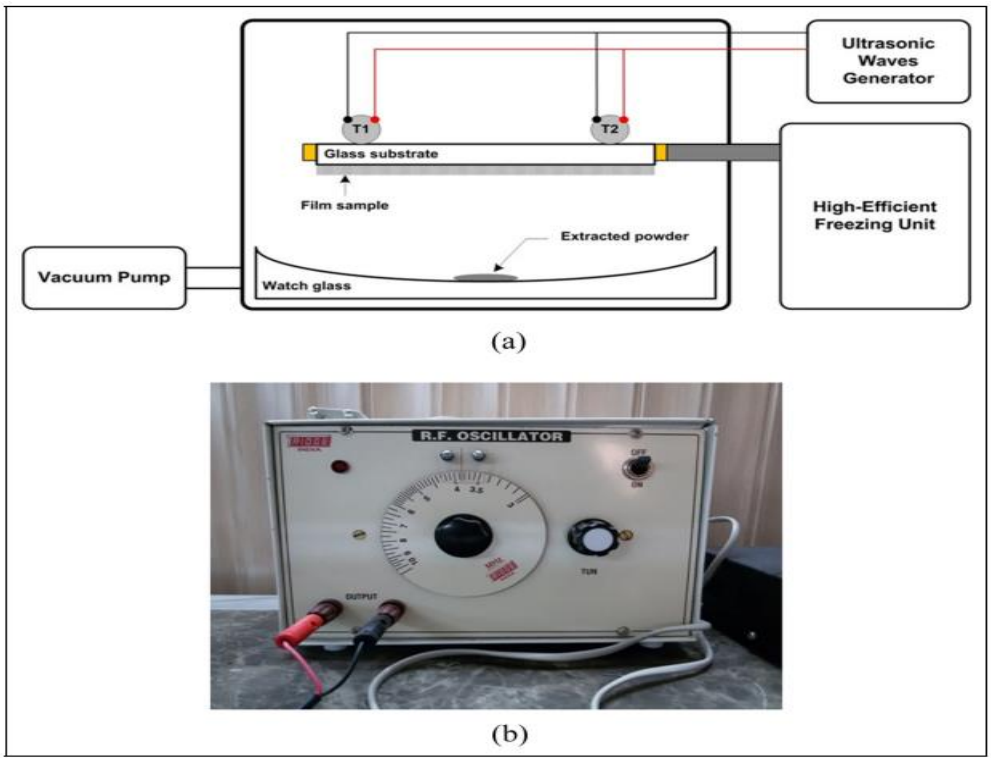

Fig. (3-9) : Experimental setup of the powder extraction method (a) and ultrasonic generator used in this work (b).[130]

Evacuated down to 10^{-5} mbar using rotary and diffusion pumps. The film sample can be maintained on a copper plate and cooled down to -20 C using a high-efficiency freezing unit. The ultrasonic waves were generated by a Triode R.F. Oscillator (Figure (b)) and two transducers (T_1 and T_2) operating in the frequency range of 3–50MHz. The extracted powder was collected on a clean watch glass. The procedure is started by evacuating the chamber down to 10^{-4} mbar and then closing the valve between the chamber and the vacuum pump to isolate the chamber. Freezing unit is then operated to cool the holder and substrate down to -20 C. Now, the thin film on the nonmetallic substrate starts to shrink. After 1 h, the freezing unit is turned off and the temperature of the holder and substrate starts to increase. It was found that the temperatures of the holder and substrate are very close to each other during the work period. Room temperature can be reached after 6–10 h depending on the

temperature of surrounding environment. The film now is expanded over the substrate surface. Turning the ultrasonic source on is the next step. The time period of exposing the sample to the ultrasonic waves depends on several parameters such as film thickness, type of material, freezing and final temperatures. The final step involves stirring the copper plate holding the sample, slowly for 1 h, to remove as much of the film material as possible [130], as shown in figure (3-10):

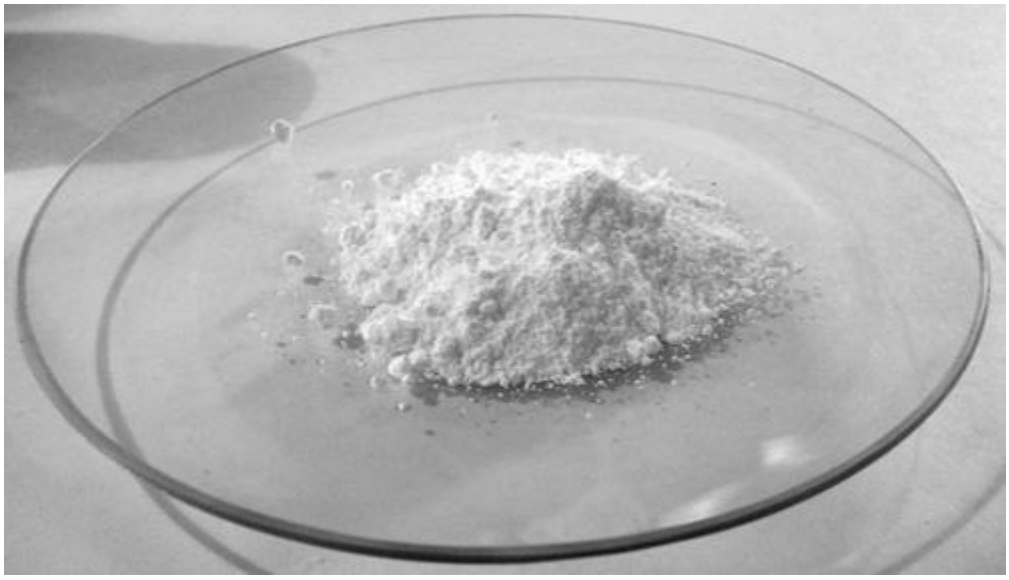

Fig. (3-10):Titanium dioxide powder

3-3 The structural and spectral characteristics of Nano-powders

The samples were prepared in this work characterized in order to determine their structural and spectral characteristics. The measurements and characterization tests include X-ray diffraction (XRD) patterns, atomic force microscopy (AFM), scanning electron microscopy (SEM), Fourier-transform infrared spectroscopy (FTIR)pensive, X- Energy-Dis, Ray (EDX) Spectroscopy, UV-Visible spectroscopy .

3-3-1 X-Ray Diffraction (XRD)Analysis

In order to study the structural properties of the prepared samples, the x-ray diffraction patterns were recorded by a Shimadzu 6000 X-Ray diffract meter system. this work done in physics laboratory in College of Applied Sciences/ University of Technology, This system measures the diffraction intensity as a function of Bragg's angle. The radiation source is Cu (kα) with wavelength of 1.5406Å, current of 30mA and voltage of 40 kV. The scanning angle (2θ) could be varied in the range of 20-60 degree with a speed of 4 deg /min.

The inter-planer distance (d_{hkl}) for different planes was determined by using Bragg's law :

$n\lambda = 2d \sin\theta$ ……(3- 1)

Where n is the reflection order, θ is Bragg's angle, and λ is the wavelength of X-ray radiation 1.54056Å.

The data obtained from the XRD measurements can be used to calculate the crystallite size (C.S.) of the prepared samples according to Debye-Scherer's formula [131]:

$D = \frac{0.89\lambda}{\beta \cos\theta}$ .....(3-2)

Where λ is the wavelength of x-ray radiation 1.54056Å, β is the full-width at half-maximum of the peak on the XRD pattern, θ is the diffraction angle, and 0.89 is an Scherer's constant. As shown in Figure (3-11).

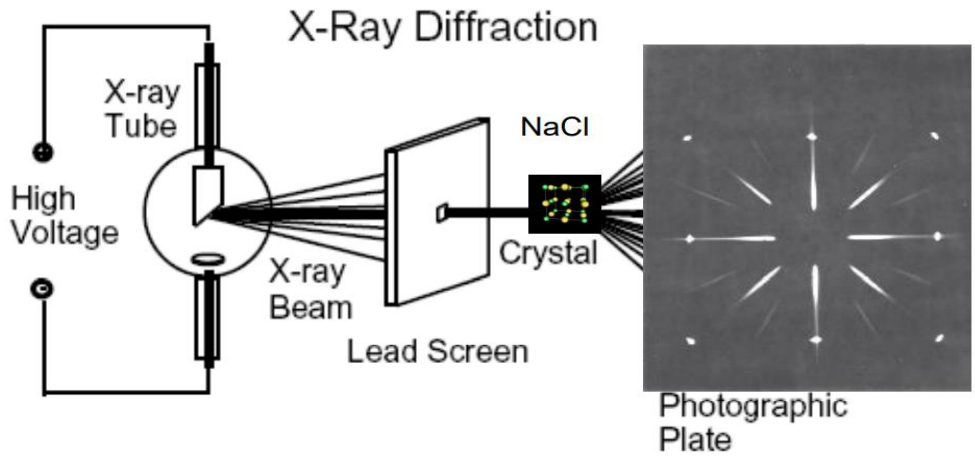

Fig. (3-11): X-Ray Diffraction (XRD) [131].

3-3-2 Atomic force microscopy

in order to study surface roughness and topography of the prepared samples were used AFM. The atomic force microscope is one of the types of scanning probe microscope, where a topographic image of the sample surface can be achieved based on the interactions between the tip and the surface of the sample. It is characterized by imaging almost any type of surface, including polymers, ceramics, composites, glass, and biological samples. AFMs probe the sample and performs measurements in three dimensions on the surface of the sample, and hence can presentation of three-dimensional image of the sample surface and this provides a great advantage over any microscope available previously [135]. this work done in physics laboratory in the College of Science / Mustansiriya University.

3-3-3 Scanning Electron Microscopy

The structural and morphological analysis of any thin film can be performed using scanning electron microscopy (SEM). Scanning Electron Microscope (SEM) uses a focused beam of high energy electrons to generate a variety of signals at the surface of the solid samples. The signals that derive from the electron sample interactions reveal information about the sample,[136] including The texture of the sample,

chemical composition, crystalline structure, and orientation of materials that make up the sample. this work done in physics laboratory in the College of Science / Albasrah University.

3-3-4 Energy Dispersive X-ray Diffraction

Energy-dispersive x-ray spectroscopy (EDX) is an analytical technique that is used to the compositional analysis of elements which contained in the materials. It is a technique used in conjunction with SEM to determine the elemental composition of the final sample. The resulting signals due to the interaction between the primary electron beam and the sample under investigation includes secondary electrons, backscattered electrons, Auger electrons and characteristic x-rays. The characteristic X-ray is a fingerprint of the element from which it is emitted. The emitted X-ray is sensed and collected by the EDX detector [137].

3-3-5 Spectroscopic Measurements (UV-Visible)

Transmission and absorption spectra of the prepared samples were recorded using a computer-controlled UV-visible spectrophotometer (model K-MAC Spectra Academy SV-2100) . This measurement process could be precisely controlled by suitable software installed on a personal computer. The arrangement of this instrument can be modified to measure the fluorescence by putting the light source at 90° with respect to the detector [138]. As well, the light source can be replaced by a laser source to measure the irradiance of the sample. In this case, the test quartz cell should have four transparent sides. this work done in physics laboratory in the College of Science / Babylon University.

3-3-6 Fourier-Transform Infrared Spectroscopy

In order to recognize the bonding modes of the prepared compounds, the FTIR measurements were done by FTIR spectrometer (SHIMADZU FTIR-8400S) containing the prepared samples. this work done in chemistry department in the College of Science / University of Baghdad, These measurements were performed in the spectral range (400 to 4000) cm^{-1} [139].

3-4 Culture Cell line

Cell culture refers to the removal of cells from an animal or plant and their subsequent growth in a favorable artificial environment. The cells may be removed from the tissue directly and dis-aggregated by enzymatic. Primary culture refers to the stage of the culture after the cells are isolated from the tissue and proliferated under the appropriate conditions until they occupy all of the available substrate (i.e., reach confluence). At this stage, the cells have to be sub-cultured by transferring them to a new vessel with fresh growth medium to provide more room for continued growth. After the first subculture, the primary culture becomes known as a cell line, cells with the highest growth capacity predominate, resulting in a degree of genotypic and phenotypic uniformity in the population [140].

3-5 Chemical Material:

The chemical material used in this study are listed in **(Table 3-3)** with their suppliers.

Table (3-3): List of Chemicals Used in the Study

Chemical	Company	Country
Alcohol spray (ethanol 70%)	AMEYA FZE	UAE
Dimethyl sulfoxide (DMSO)	Roth	Germany
Fetal bovine serum (FBS)	Gibco	UK
Gentamycin (80 mg vial)	The Arab pharm.	Jordan
MTT(3-(4,5-Dimethylthiazole-2-yl)-2,5-diphenyl-2H-tetrazolium bromide) dye powder	Roth	Germany
Phosphate buffer saline tablet	Gibco	UK
Roswell Park Memorial Institute-1640 (RPMI-1640) powder medium	Gibco	UK
Sodium bicarbonate powder	Ludeco	Belgium
Trypsin- Ethylenediaminetetraacetic acid (EDTA) powder	US biological	USA
Cisplatin	GSL	India

3-6 Instruments and Tools:

The instruments and tools used in the study are listed in **(Table 3-4)** with their origins:

Table (3-4): List of Instruments and Tools Used in the Study

instrument or tool	Company	Country
Autoclave	Jeiotech	Korea
Automatic micropipettes (different sizes)	Human	Germany
Cell culture flask (25ml)	SPL	Korea
Cell culture plate (96- wells)	SPL	Korea

Digital camera	Sony	Japan
Distiller	ROWA	Germany
Double distillation water stills	GFL	Germany
Electric oven	Memmert	Germany
ELISA Reader	Human	Germany
(Sterile freezing vial (1.5 ml	Biofil	Australia
Flow cytometer (BriCyte E6)	Mindray	China
Incubator	Memmert	Germany
Inverted microscope	T.C Meiji techno	Japan
Laminar air flow cabinet	Labtech	Korea
Liquid nitrogen container GT38	Air Liquide	France
Magnetic stirrer	Labinco	Netherland
Microcentrifuge	Memmert	Germany
Millipore filter (0.45, 0.22μm)	Biofil	Australia
PH Meter	WTW	Germany

3-7 Methods-Preparation of Reagents and Solutions:

3-7-1 Phosphate Buffer Saline (PBS):

The PBS was prepared according to Gibco manufacturer manual by dissolving one tablet of PBS in 500 ml deionized distilled water (DDW) with stirring constantly on a magnetic stirrer at room temperature, the pH will be 7.45 and requires no adjustment. Sterilization was done by autoclaving and kept sterile in a closed bottle until use.

3-7-2Gentamycin Stock Solution:

Gentamycin vial of 40 mg/ ml solution was considered as stock solution and stored at 4 C˚ for uses. The working concentration of gentamycin in the medium is 50 µg/ml .

3-7-3 Trypsin Solution:

According to US Biological directions, A weight of 10.1 gm of trypsin powder was dissolved in 900ml of DDW and constantly mixed by stirring at room temperature. The pH of the solution was adjusted to 7.2, and the volume completed to one liter. The solution was sterilized by filtration using 0.45 and 0.22 µm millipore filters subsequently. The content was stored at (- 20C˚).

3-7-4 MTT Solution:

A weight of 0.5 g of MTT powder was dissolved in 100 ml PBS to obtain a concentration of 5 mg/ml. Then the MTT solution was sterilized by filtration through a 0.2 µm millipore filter into a sterile and light protected container and stored at 4°C for frequent use or at (-20)°C for long term storage [132].

3-8 Preparation of Tissue Culture Medium:

3-8-1 Preparation of Serum-Free Medium:

Liquid RPMI-1640 medium was prepared from powdered RPMI-1640 medium according to the Gibco product manual as the following: From the RPMI-1640 powdered medium, 10.43 g was dissolved in approximately 900 ml of DDW in a volumetric flask. The other components include: 2 g sodium bicarbonate powder or according to need and 1.25 ml from gentamycin stock solution had been added with continuous stirring. The volume was completed by DDW to one liter and

the pH of the medium adjusted to 7.4. Sterilization was done by 0.4 and 0.2 μm Millipore filters subsequently. After the end of the procedure, 5 ml of the medium was incubated at 37 ºC in a sterile flask for 4 days with daily examination for signs of bacterial and fungal contamination. It was considered sterile only in case of no signs of contamination during the four days of incubation. Then the medium was stored at 4ºC until use.

3-8-2 Preparation of Serum-Medium:

Serum-medium was prepared as described in (3.8.1) with the addition of 10% FBS.

3-8-3 Preparation Of Colon Cancer

prostate PC3 and MDCK cell lines in frozen vials were obtained from Tissue Culture Laboratory in the College of Medicine / University of Babylon.

3-9 Harvesting and Sub-culturing Of Colon Cancer

Harvesting is a technique that uses the proteolytic enzyme trypsin to detach and disaggregate the adherent monolayer cells from the bottom of the culture flask. It was performed whenever the cells need to be harvested for cell counting and sub-culturing of the cell line. This procedure was done according to the following:

1- Cells were examined using the inverted microscope to ensure that the cells are healthy and sub-confluent (in the exponential phase of growth) and are free from contamination.

2- The spent medium was removed using a pipette and wash the monolayer with a sufficient volume of pre-warmed trypsin- solution to ensure the removal of all media from the flask. This washing step was repeated if the cells were known to adhere strongly.

3- Appropriate volume of trypsin- solution was added into the washed cell monolayer using (1-2 ml) per 25-cm^2 flask. Flask was rotated to cover the monolayer with trypsin.

4- The flask was returned back to the incubator at 37°C to allow the cells to detach from the inside surface of the flask (the length of time depends on the cell line, but usually this will occur within 2–10 minutes).

5- The cells were examined using an inverted microscope to ensure that all the cells are detached and in suspension. The side of the flasks may be gently tapped to release any remaining attached cells.

6- Inactivate the trypsin by adding an equal volume of serum-containing medium to the flask.

7- According to the required density, an aliquot of cells was transferred to a new labeled flask containing a pre-warmed serum-containing medium (5–7ml for a 25-cm^2 flask).

9- The flask was incubated at 37C°.

10- This process was repeated as demanded by the growth characteristics of the cell line, as shown in figure (3-12):

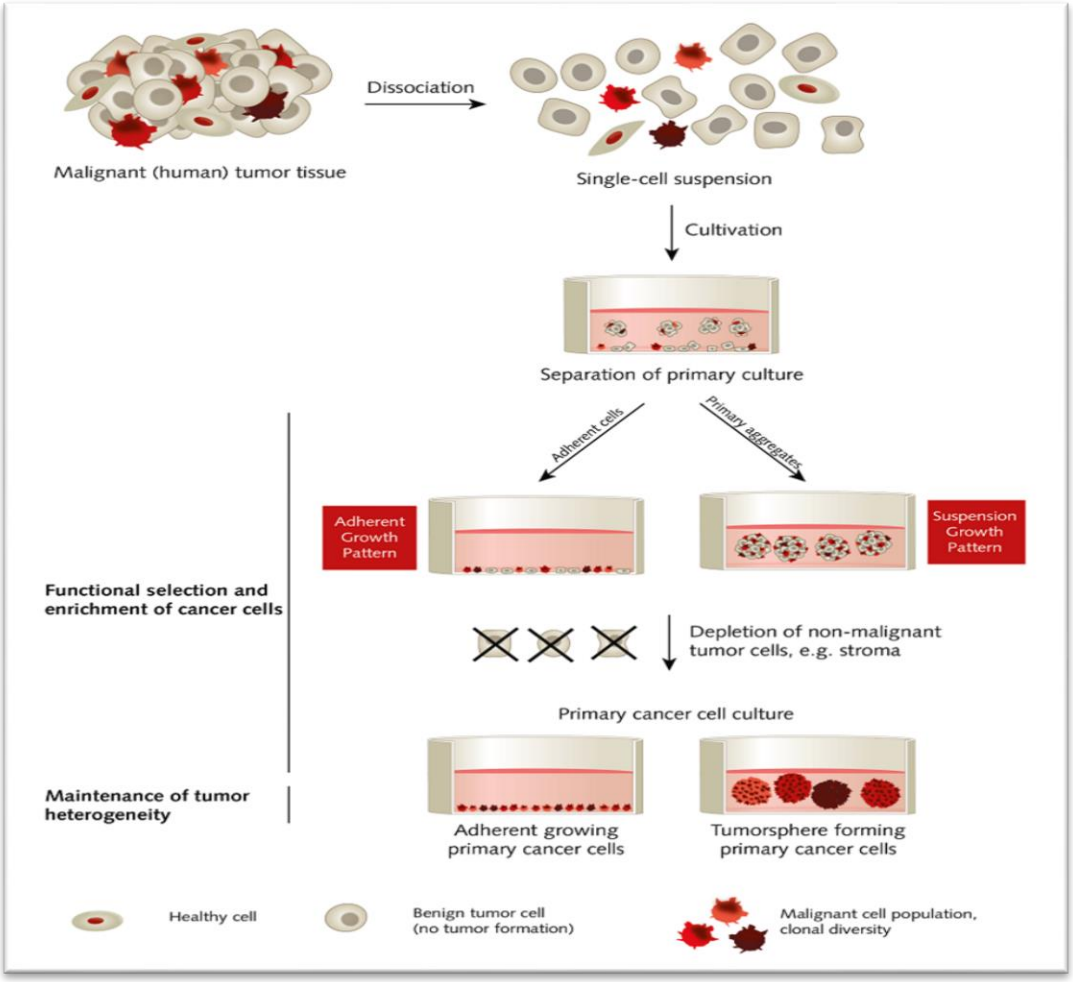

Fig.(3-12): Preparation Of Colonic Prostate PC3.[141]

3-10 Thawing of Colon Cell lines:

The frozen cell line vial was removed from liquid nitrogen container with caution and directly placed into a beaker containing pre-warmed (37°C) sterile DDW. The vial was removed from the water before the ice floccule dissolved completely, then it was wiped with 70% ethanol. Without delay, the cell suspension content of the vial was pipetted under laminar flow cabinet into a 15 ml sterile plastic centrifuge tube containing 10 ml of pre-warmed serum-free medium. Centrifugation was done at 1000 rpm for 5 minutes and the supernatant was aspirated and decanted. The cells pellet was re-suspended into 5ml warm (37C°) serum-medium

and transferred into 25 ml size cell culture flask, incubated at 37C˚ and the serum medium replaced on the next day.

A solution of a nanoparticles with distilled water , an appropriate amount of a specific substance in a specific volume of nanoparticles at a concentration (1000) µg of nano powder is dissolved in a volume of 1 cm^3)of solvent (water), according to the following relationship [142]:

$$\frac{C \times V \times M.W}{1000} \quad \ldots\ldots\ldots\ldots\ldots\ldots\ldots \quad (3-3)$$

w_{m} = Nano powder weight

C: the concentration to be prepared in mol

V: the volume of the solvent cm^3 to be added to the substance.

M.W: The molecular weight of the dye used is gm/mol.

To dilute the prepared (1000, 500, 250, 125, 62.50, 31.25) µg/ml this is done using the following relationship, which is called the dilution relationship:

$C_1V_1 = C_2V_2$ ……..(3-4)

Where :

C_1: First concentration.

C_2: second concentration.

V_1: the necessary volume of the first concentration.

V_2: The volume needed to be added to the first concentration to obtain the second concentration. As shown in figure (3-13):

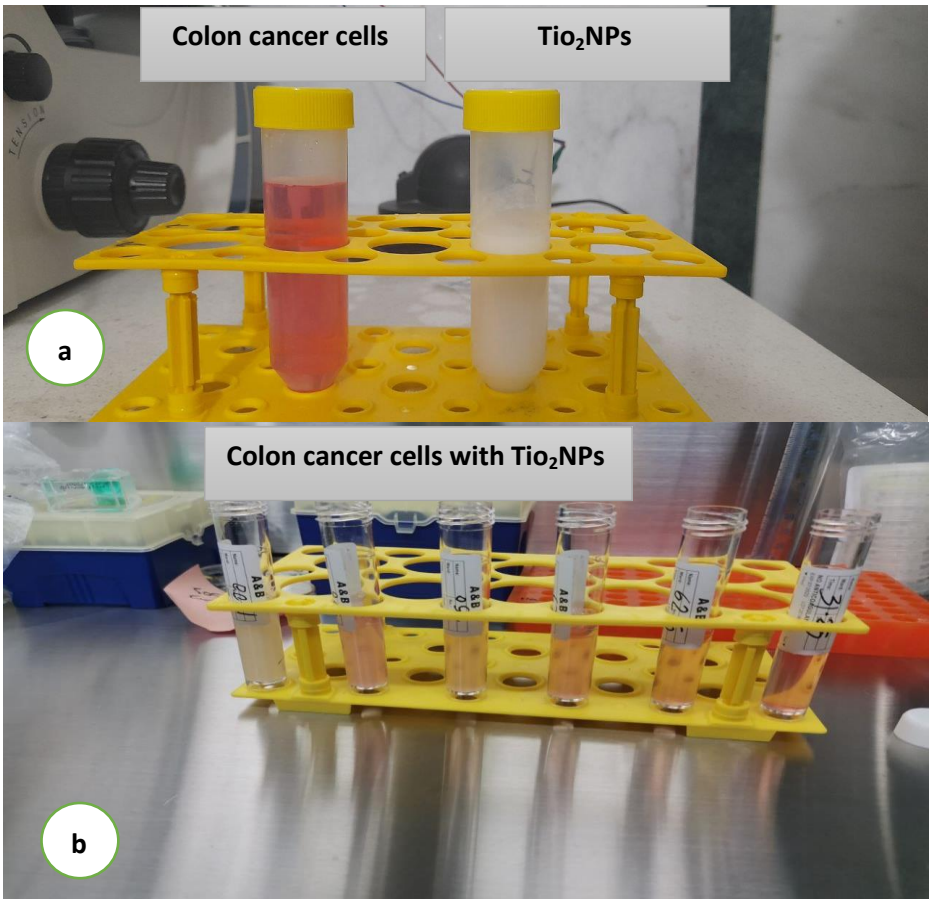

Fig. (3-13):a) colon cancer cell without Tio_2NPs

b) Colon cancer cells with Tio_2NPs.

3-11 Cytotoxicity assays:

3-11-1 MTT Assay Principle:

The general purpose of the MTT assay is to measure viable cells in relatively high throughput (96-well plates) without the need for elaborate cell counting. Therefore, the most common use is to determine the cytotoxicity of several drugs at different concentrations. The principle of the MTT assay is that for most viable cells mitochondrial activity is constant and thereby an increase or decrease in the number of viable cells

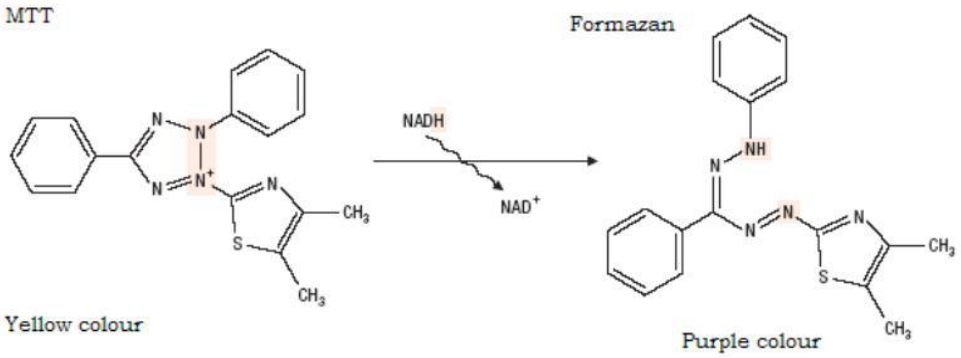

Figure (3-14): Principle of MTT Assay [132]

is linearly related to the mitochondrial activity, as shown in figure (3-14).The mitochondrial activity of the cells is reflected by the conversion of the pale-yellow tetrazolium salt (MTT dye) into dark purple formazan crystals by NADH which can be solubilized for homogenous measurement. Thus, any increase or decrease in viable cell number can be detected by measuring formazan concentration reflected in optical density (absorbance) using a plate reader at 570 nm. The darker the solution, the greater the number of viable and metabolically active cells [132].

3-11-2 Procedure:

1- At the end of the drug exposure period, the medium was removed from the wells and then the cells were washed with PBS. A blank control was carried to assess unspecific formazan conversion.

2- A volume of 1.2 ml of MTT solution (5 mg/ ml) was added to 10.8 ml medium to obtain final concentration of 0.5 mg/mL. Then, 200 µl of the resulting solution was added in each well.

3- The plate was incubated for 3 hours at 37°C until intracellular purple formazan crystals were visible under the inverted microscope.

4- The supernatant was removed and 100 µl DMSO was added in each well to dissolve the resultant formazan crystals.

5- The plate was incubated at room temperature for 30 minutes until the cells have lysed and purple crystals have dissolved.

6- Absorbance was measured by a microplate reader at 570 nm. The absorbance reading of the blank must be subtracted from all samples. Absorbance readings from test samples must then be divided by those of the control and multiplied by 100 to give percentage cell viability or proliferation. Absorbance values greater than the control indicate cell proliferation, while lower values suggest cell death or inhibition of proliferation. Percent of cell viability or percent of inhibition was calculated by the following formula:

$$\% \text{ viability} = (AT - AB) / (AC - AB) \times 100\%$$

Where, AT = Absorbance of treated cells (drug).

AB = Absorbance of blank (only medium).

AC = Absorbance of control (untreated).

$$\% \text{ Inhibition} = 100 - \% \text{ viability}$$

3-12 Statistical Analysis:

Means and standard deviation were calculated for the experimental group. The statistical significance of the differences between the data obtained from the control and that obtained from the experimental group was analyzed via analysis using One Way Analysis of Variance using the SPSS 25 computer program (SPSS). P-Values < 0.05 were considered to be statistically significant. As shown in figure (3-15):

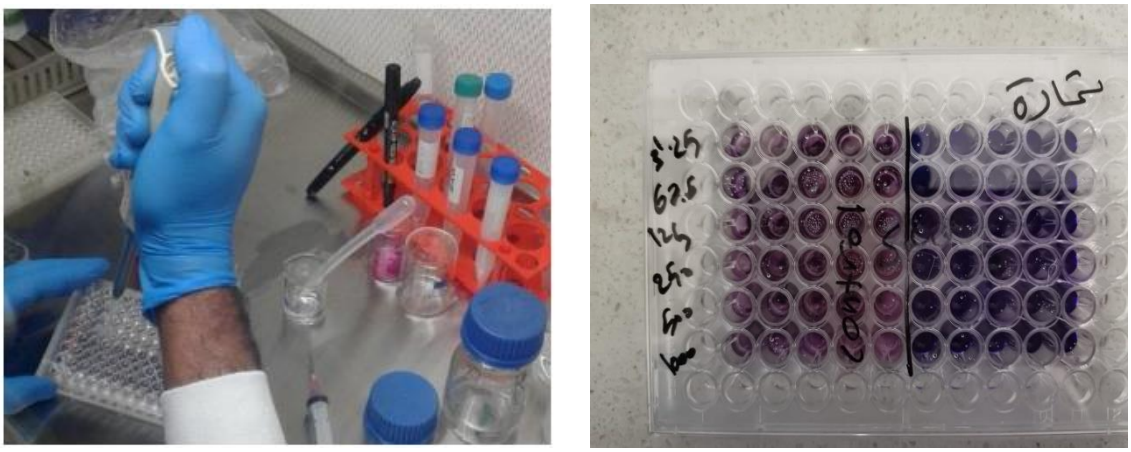

Figure (3-15) :The 96 well plates for MTT assay test

3-13 Description of LIF Arrangement Technique

Figure (3-16) shows the arrangement of LIF setup and as an indication of each part of it:

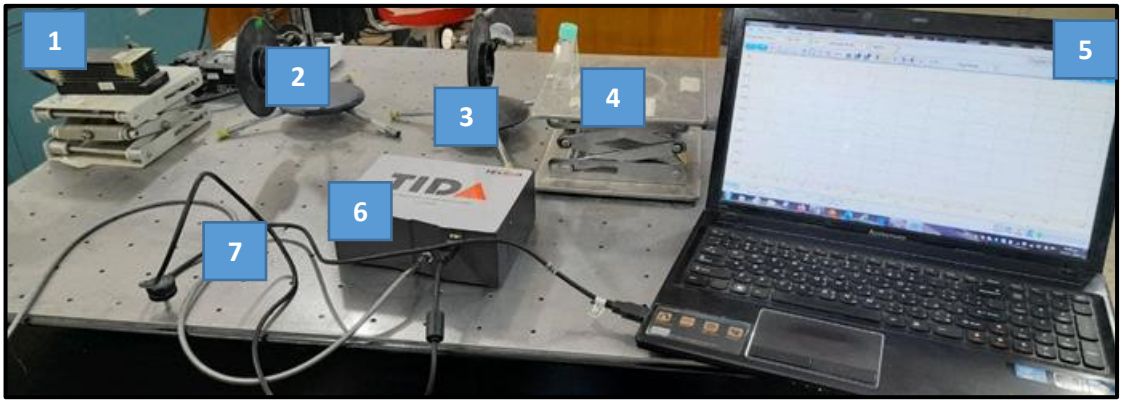

Fig.(3-16) Parts of the LIF spectroscopy system.

The main parts are:

1- A CW diode laser source, with (473 nm) fundamental wavelength, for sample irradiation.

2-Aperture to control the diameter of the laser beam.

3- A light lens is used to illuminate the laser on the surface of the sample with a focal length (f =10 cm).

4- A plane surface for placing the sample for the purpose of examination. The distance between the laser and the sample (10cm).

5- A computer to run the spectrum analyzer software that shows the data as a graph of wavelength as a function of intensity. Hence, the possibility of storing detailed data for the spectrum.

6- The optical fiber holder is divided into circular angles (360°), to control the placement of the optical fiber at the best angle for receiving the plasma spectrum.

7 - The sample under study and targeted by diode laser and located under the arm carrying it.

3-13-1 laser Source

The laser source used in the LIF system is a diode laser. The table (3-5) shows the parameters of the laser used in this technology:

Table (3-5): specifications of the laser source (diode) used in the technology

Mode laser	CW
laser Wavelength	473 nm
Optical Output Power	100 mW
Threshold Current	20 mA
Applied voltage	220 v

3-13-2 Optical fiber

A fiber-optic wire is used in the LIF technique to collect the spectrum emitted from the sample to be transferred to the spectrometer. It is set at an angle of 90 from the sample position. The spectrum emitted from the sample is transmitted through the fibers using the phenomenon of total reflection, and this allows the introduction of a sufficient amount of emitted spectrum into the spectrum analyzer. [143]

4-1 Part One

In this part, the result and discussion of thickness measurement and deposition time of TiO_2NPs using DC sputtering technique are studied and discussed. Structures properties of TiO_2NPs (XRD, FTIR, AFM, SEM, and EDX) and Spectral properties are described in this part.

4-2 Thickness and Time of D.C Sputtering for TiO_2 NPs.

This section show the effects of working gas pressure, gas mixing ratio, inter-electrode spacing, and film thickness on the structural and optical properties of synthesized samples. The results showed that as the deposition time increased, the thickness increased, as shown in the table (4-1).

Table (4 -1): Thickness and the Time of D.C Sputtering of (TiO_2 NPs)

Material	Deposition Time (h)	Thickness(nm)
TiO_2	1	106.4
	1:30	159.6
	2	190.0
	2:30	209.0
	3	212.8

4-3 Characterization of TiO_2 NPs

The structural and spectral properties of the produced samples were measured in this study. X-ray diffraction (XRD) patterns, Fourier-transform infrared spectroscopy (FTIR), atomic force microscopy (AFM), scanning electron microscopy (SEM), Energy-Dispersive X-Ray (EDX)

Spectroscopy, Dispersion Curves of Nanostructured Thin Films, and UV-Visible spectroscopy are among the tests performed.

4-3-1 XRD Patterns of TiO_2 NPs

The use of X-ray diffraction to identify the crystal structure and crystallinity is critical. Strong diffraction peaks were observed in the XRD patterns for TiO_2 nanoparticles of various sizes, showing TiO_2 in the anisate phase generated at a gas mixing ratio of 50:50 and a chamber temperature of 400°C. The diffraction peaks at 25.2°, 37.8°, 48.1°, 53.9°, 55.1°, 62.8°, 68.9°, 70.1°, and 75° corresponded to crystal planes (101), (004), (200), (105), (211), (118), (116), (220), and (125), which are in agreement with the standard spectrum [161], as shown in figure (4-1). Debye-equation Scherer's was used to calculate the average crystallite size of the composite [64]. The **TiO_2NPs** thin film's average crystallite size was calculated according to Debye-Scherer's formula equation (3-2) to be 17.74 nm, as shown in figure (4-1):

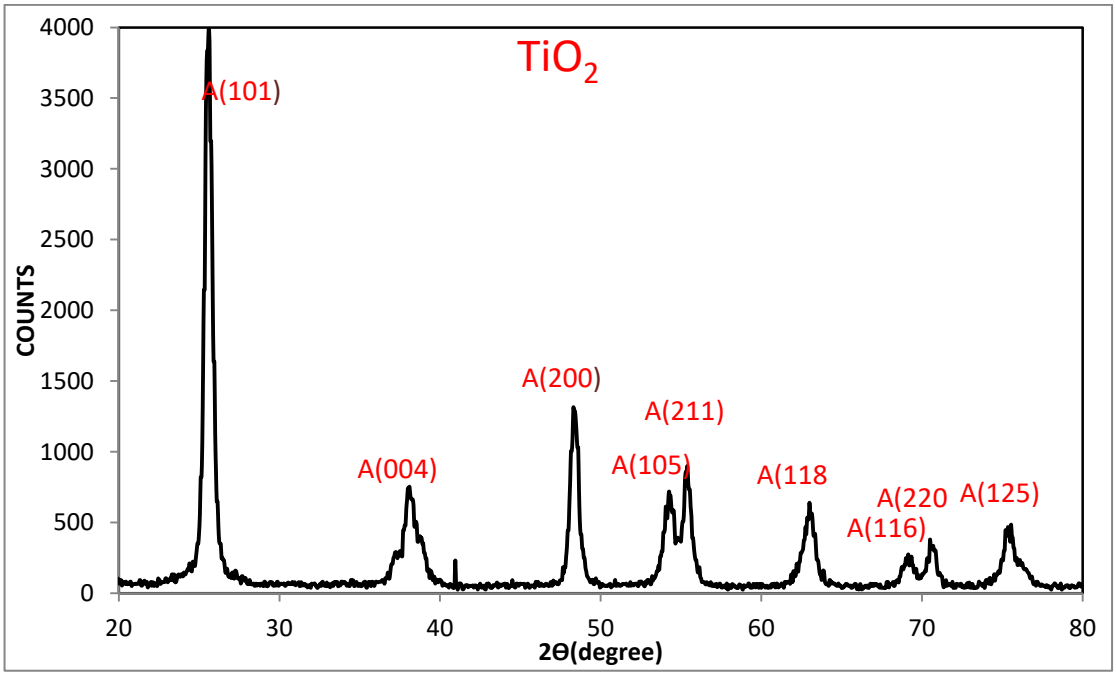

Fig. (4-1):The XRD patterns for anatase phase of TiO_2 NPs thin films prepared at gas mixing ratio 50:50 and inter-electrode 4 cm

4-3-2 FTIR Spectra of TiO_2 NPs Films

For a long time, FTIR spectra have been used to provide information on the nature of metal oxides. The stretching and bending vibrations of the OH group cause the peaks at 3450 cm^{-1} and 1620 cm^{-1} in the spectra, as seen in the figure (4-2). For all of the produced samples, the structure al of TiO_2NPs was clearly visible in these spectra. The peak at 408.91 cm^{-1} is attributed to Ti-O-Ti bands in the TiO_2NPs lattice [134], while the band assigned to Ti-O stretching vibration was seen at roughly 447 and 667 cm^{-1}. Because of the optimal working conditions utilized in the sputtering equipment, FTIR confirms that there are no contaminants within the prepared samples.

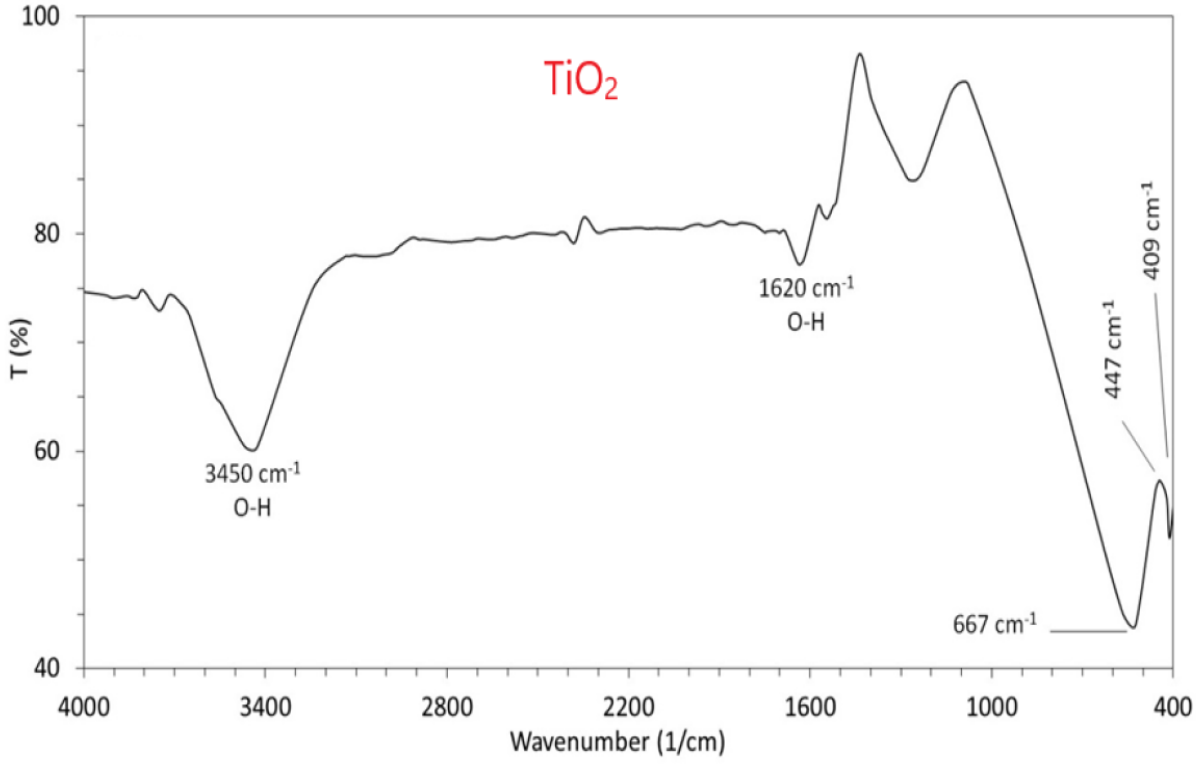

Fig. (4-2):The FTIR spectra for TiO_2NPs thin films prepared at gas mixing ratio 50:50.

4-3-3 AFM Results of TiO_2NPs Films

There were various grain sizes in the TiO_2NPs thin film had an anatase structure, which was discovered. Before reaching the substrate surface, these high-energy particles are gas-scattered as a result of collision interactions between the target and the substrate [135] as shown in figure (4-3), the produced TiO_2NPs nanostructures had a Core Roughness Depth (sk) of 15.1 nm and a root-mean-squared roughness (sq) of 17.5 nm, where sk > sq .

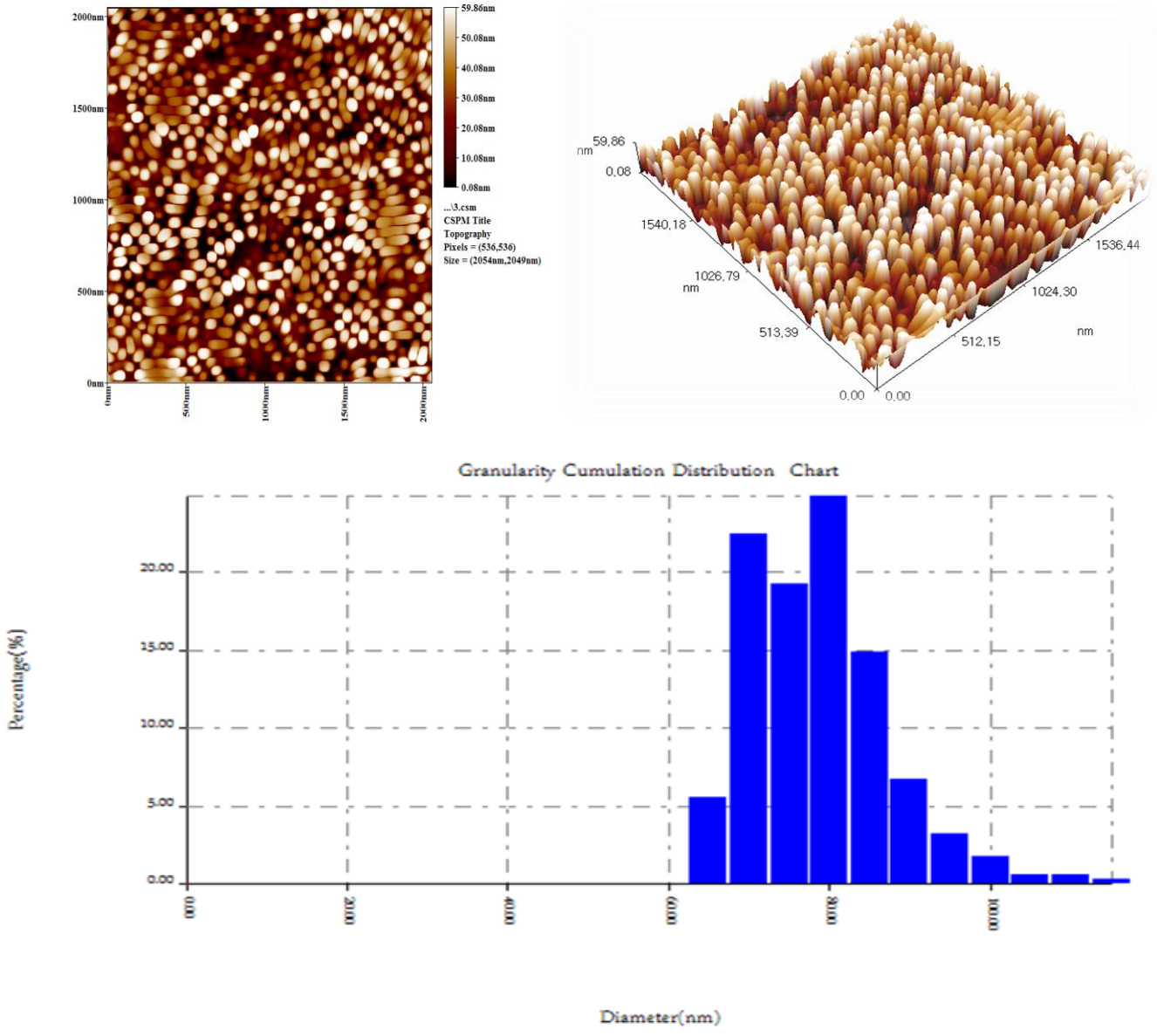

Fig. (4-3): The three dimensional AFM micrographs and granularity cumulating distribution of TiO_2NPs thin film

4-3-4 SEM Measurements of TiO_2NPs Films

Scanning electron microscopy (SEM) was used to determine the surface profile and particle size of the thin films that had been manufactured (SEM). The first feature seen in these photos is homogeneous particle distribution, which is one of the most fundamental advantages of the DC magnetron sputtering approach for nanostructure fabrication. Another noteworthy finding is the lack of aggregation across the scanned sample . This could be due to the heat sink mechanism used in TiO_2NPs samples to prevent the anatase phase from changing to rutile. This can be explained as follows: in a single phase structure, such as the anatase TiO_2NPs sample obtained in this study. In the SEM images, the nanoparticles have a hexagonal form in the structure [136], figure(4-4):

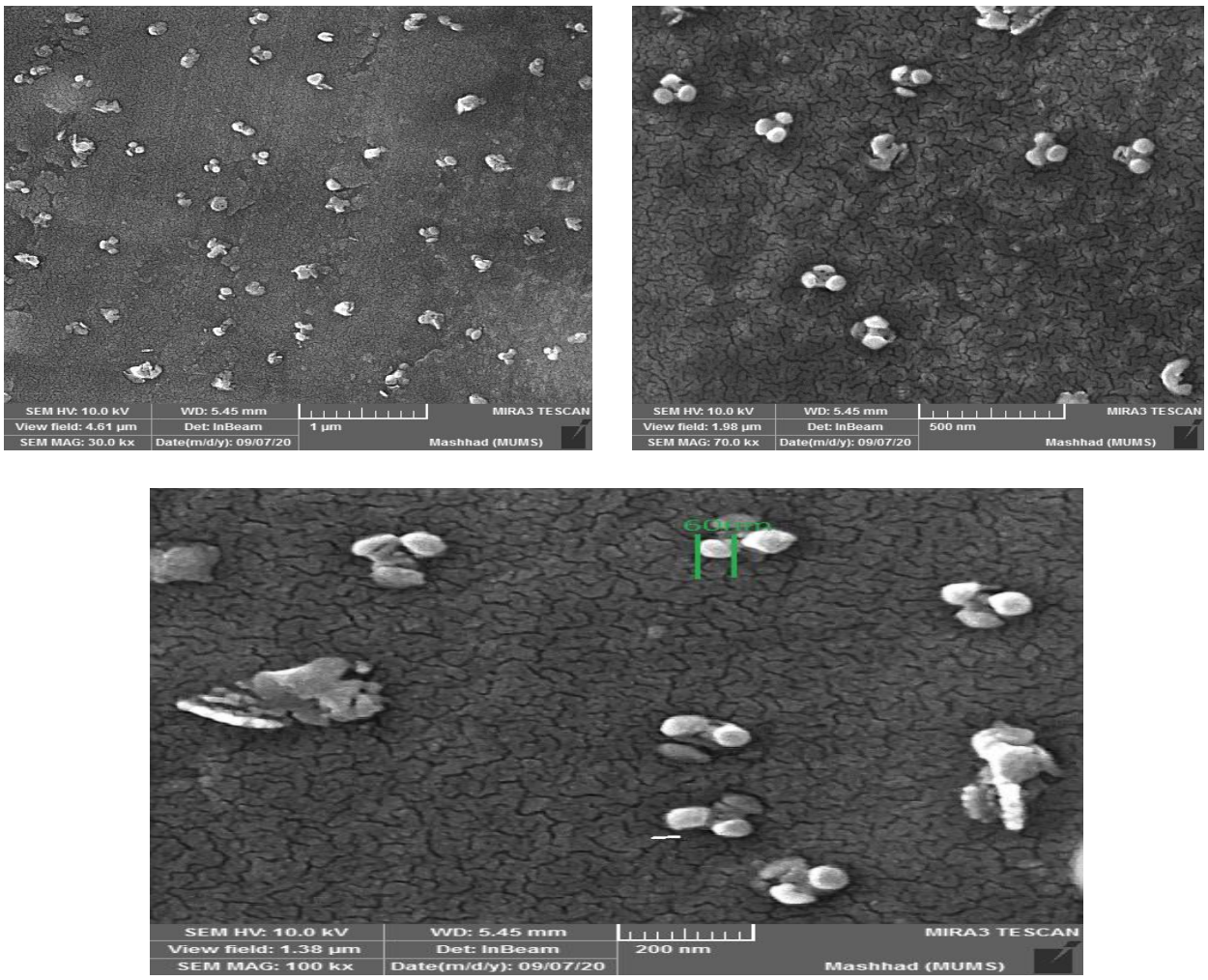

Fig. (4-4):The SEM images of TiO_2 thin film prepared.

4-3-5 EDX measurements of TiO_2NPs Films

The produced samples' energy-dispersive x-ray (EDX) spectra were recorded and analyzed .The table (4-2) shows a summary of the elemental compositions in the TiO_2NPs sample. The weight ratio of Ti:O was found to be 46.77: 50.79, based on the availability of Ti and O in the final sample. These findings supported the stoichiometry of TiO_2NPs molecules since they matched the chemical bonding arrangement of the compound perfectly. It was observed that the prepared TiO2NPs samples were all most pure, which was corroborated by the atomic integration of Ti and O atoms. This feature is especially useful for investigations involving physical and chemical features and processes. The EDX spectrum present in figure (4-5):

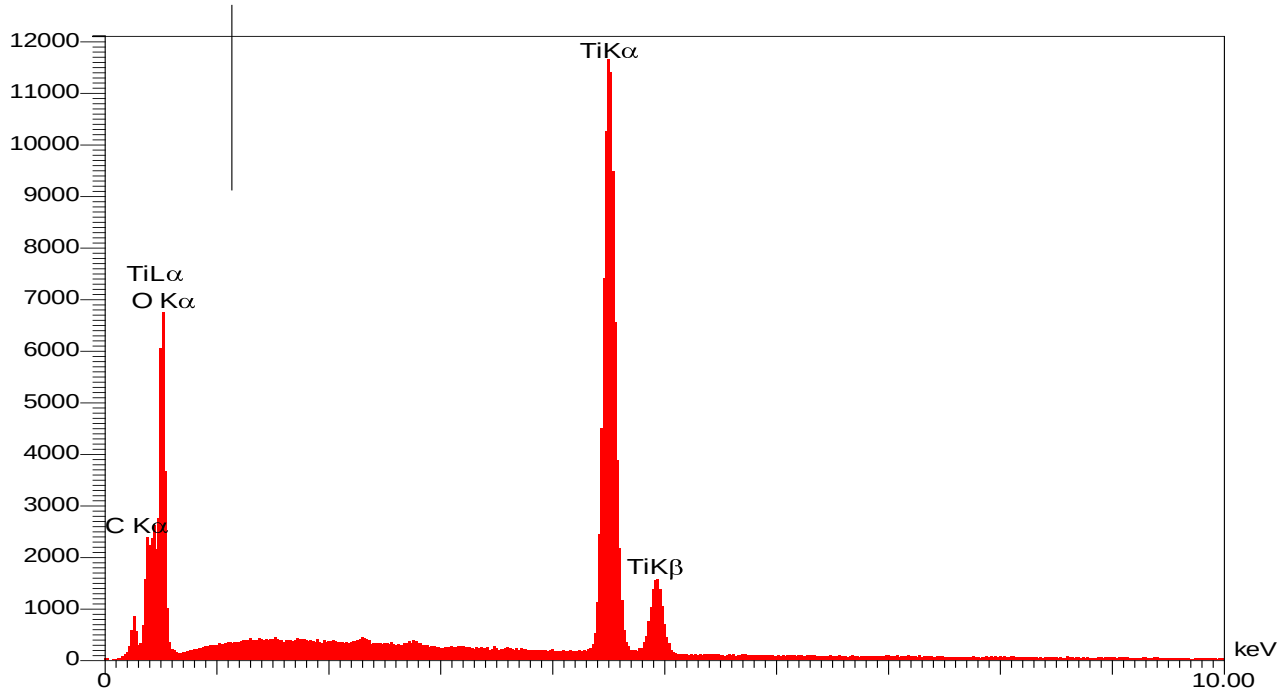

Fig.(4-5) :The EDX results of TiO_2NPs thin film prepared

Table(4-2):Quantitative Results of TiO_2NPs by EDX Spectroscopy

Element	Line	W%	A%
C	Kα	2.44	4.67
O	Kα	50.79	72.91
Ti	Kα	46.77	22.42
		100.00	100.00

4-3-6 Absorption and Fluorescence Spectra of TiO_2 NPs

Absorption and fluorescence spectra of TiO_2 films of the anatase phase nanocrystal line as shown in Fig. (4-6). Nanomaterials were used in this research as a treatment using them to kill colon cancer cells. Fluorescence and absorption spectra were studied to clarify the difference between them and the fluorescence and absorption spectra of colon cancer cell carcinomas to obtain a more accurate diagnosis. Compared with other studies, a blue shift occurred with absorbance [137]. Figure (4-6a) shows the absorbance spectrum of TiO_2NPs using UV-visible spectroscopy in distilled water plotted against the wavelength (λ). The wavelength has the highest absorption (0.941) is (300 nm), because the absorption depends on the particle size , this agreement with Literature survey [44]. Figure (4-6b) shows the fluorescence spectrum of TiO_2NPs using fluorescence spectroscopy (Spectra Academy). The wavelength at the highest fluorescence (9.579) equals (340) nm, peak at a longer wavelength is attributed to the dipole Plasmon resonance of the TiO_2NPs. As the antiparticle spacing decreases, the first peak becomes weaker while the second peak intensifies and shifts to longer wavelengths. The maximum peak shift is observed if the antiparticle distance approaches zero, at which point the electrodynamic interaction between the nanoparticles is at a maximum. the fluorescence emission of semiconductors is mainly produced when the photo induced electrons and holes are rearranged, Thus, the grafting can lead to the separation of the photo induced electrons on the surface of TiO_2 and thus prevent their recombination, which leads to the enhancement of the photocatalytic activity, this agreement with Literature survey [47]

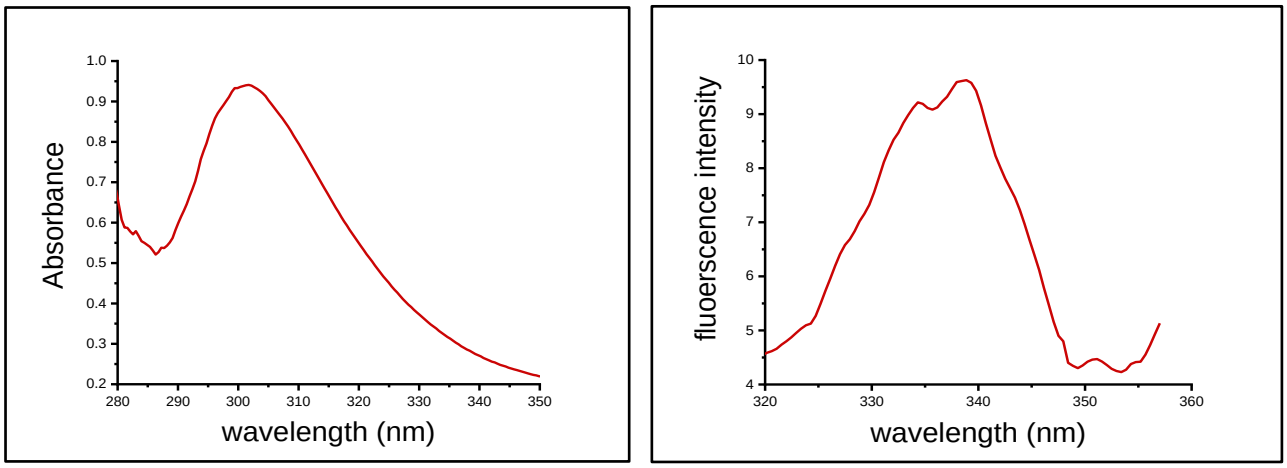

Fig. (4-6):a) absorption spectra for the prepared sample of TiO_2 NPs , b) Fluorescence spectra for the prepared sample of TiO_2 NPs

Table(4-3): Absorption and Fluorescence of TiO_2 NPs

	λ_{max} (nm)	Intensity
Absorbance	300	0.941
Fluorescence	340	9.579

4-4 Part Two

This part shows a fluorescence spectra and absorption spectra for colon cancer cells after treatment with TiO_2NPs were studied by using the fluorescence and UV- visible spectroscopy to compare with laser induced fluorescence (LIF) technique.

After completing the preparation of colon cancer cell samples and treating them with different concentrations (1000, 500, 250, 125, 62.50, 31.25) µg/ml of TiO_2NPs, and to ensure the possibility of a spectroscopic study, specific samples were taken and their absorption spectrum was measured using (uv- visible) spectroscopy (deuterium and xenon lamps) as well as their emission spectrum using a fluorescence spectrometer

(xenon lamps). Both spectrometers use a source of ordinary electromagnetic radiation It was found by measuring the absorption spectra that it is possible to conduct a spectroscopic study using the absorption spectrometer, and it is not possible to conduct the study and diagnosis using the fluorescence spectrometer. Therefore, the study resorted to using the laser induced fluorescence technique to study the emission spectra to diagnose biochemical samples and this is identical to most of the previous studies [138,139] ,as in figures (4-7 a) and (4-7b).

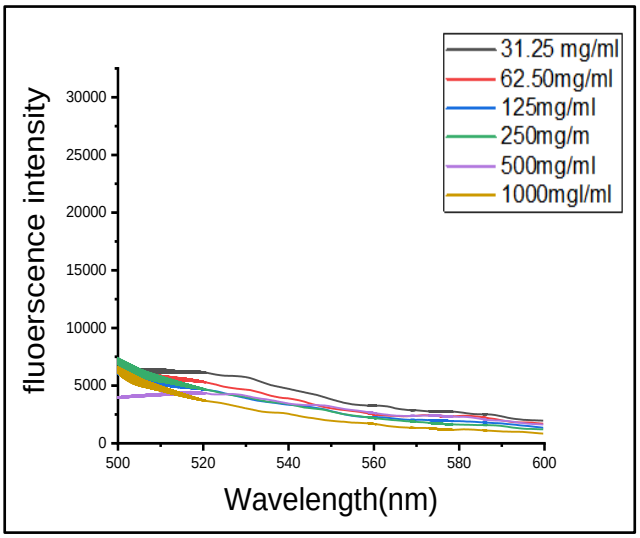

(a)

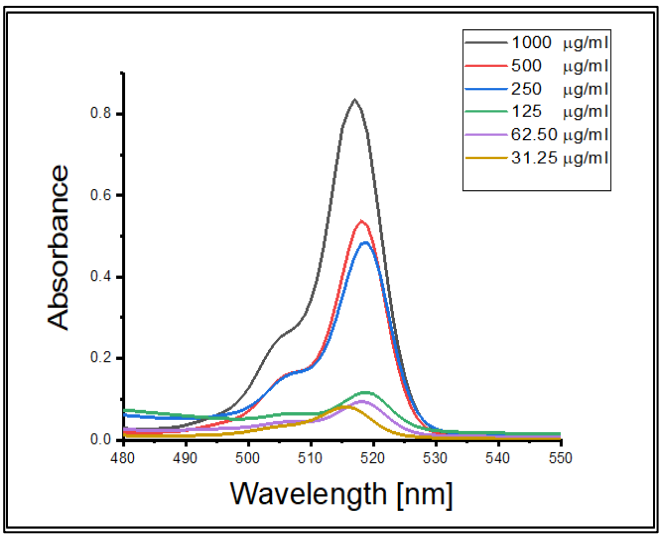

(b)

Figure (4-7): a) fluorescence spectra of colon Cancer for counting different concentrations (1000, 500, 250, 125, 62.50, 31.25) µg/ml. b) Absorbance of colon Cancer for counting different concentrations (1000, 500, 250, 125, 62.50, 31.25)

4-5 Part Three

This part shows and discusses absorbance spectrum by using UV-Visible spectrometer as a diagnostic method for the Comparison of the absorbance spectrum of live and dead colon cancer cells and As well as studying the absorbance spectrum spectra each chemical compound that was used in the tissue culture of cells that include the nutrient medium (RMPI 1640) of colon cancer cells , trypsin and colon cancer cells In

order to accurately determine the absorbance spectrum of colon cancer cells and distinguish it from the absorbance spectrum of the rest of the components contained within the cell culture complex of colon cancer cells before and after treatment with TiO_2NPs. Also, the optical properties of all the prepared samples were measured, which include (reflectivity, refractive index absorption coefficient, Transmission) . (LIF) technique the spectra of the prepared samples were studied. To study the effect of exaction wavelength in diagnosing colon cancer cells, three wavelengths (403, 473, 532) nm were used. Live and dead colon cancer cells were classified by laser-induced fluorescence (LIF) . The LIF of the nutrient medium (RMPI 1640) of colon cancer cells as well as trypsin were studied. The (LIF) of colon cancer cells were measured after treatment with nanomaterials, and there was a lower number of cancer surviving cells than the initial number due to the presence of a concentration multiplier of TiO_2NPs.

4-5-1 Comparison of the Absorbance Spectrum of Living and Dead Colon Cancer Cells without TiO_2NPs Treatment (Control Colon Cancer Cells)

The result in figure (4-8) shows the comparison of the absorbance spectrum between living and dead cells of colon cancer cells by using UV-Visible spectrometer. When preparing these cells by the method of tissue culture of cells, these cells live for four hours at most, and then died due to different reasons. Where it was possible to clarify the difference and diagnose these cells using UV-Visible spectroscopy. The red line represents the absorbance of dead cells and the black line represents the absorbance of living colon cancer cells. It was observed that the absorbance of living cells (0.957) at a wavelength of 522 nm was higher than the absorbance of dead cells (0.571) at a wavelength of 524

nm . In living cells, the reason for the high absorbance is due to the presence of cancer cells in addition to other chemicals present in the cancer cell formation compound. As for dead cells, the absorbance mostly refers to the chemical compounds found in the compound, where the absorbance of dead cells is very low

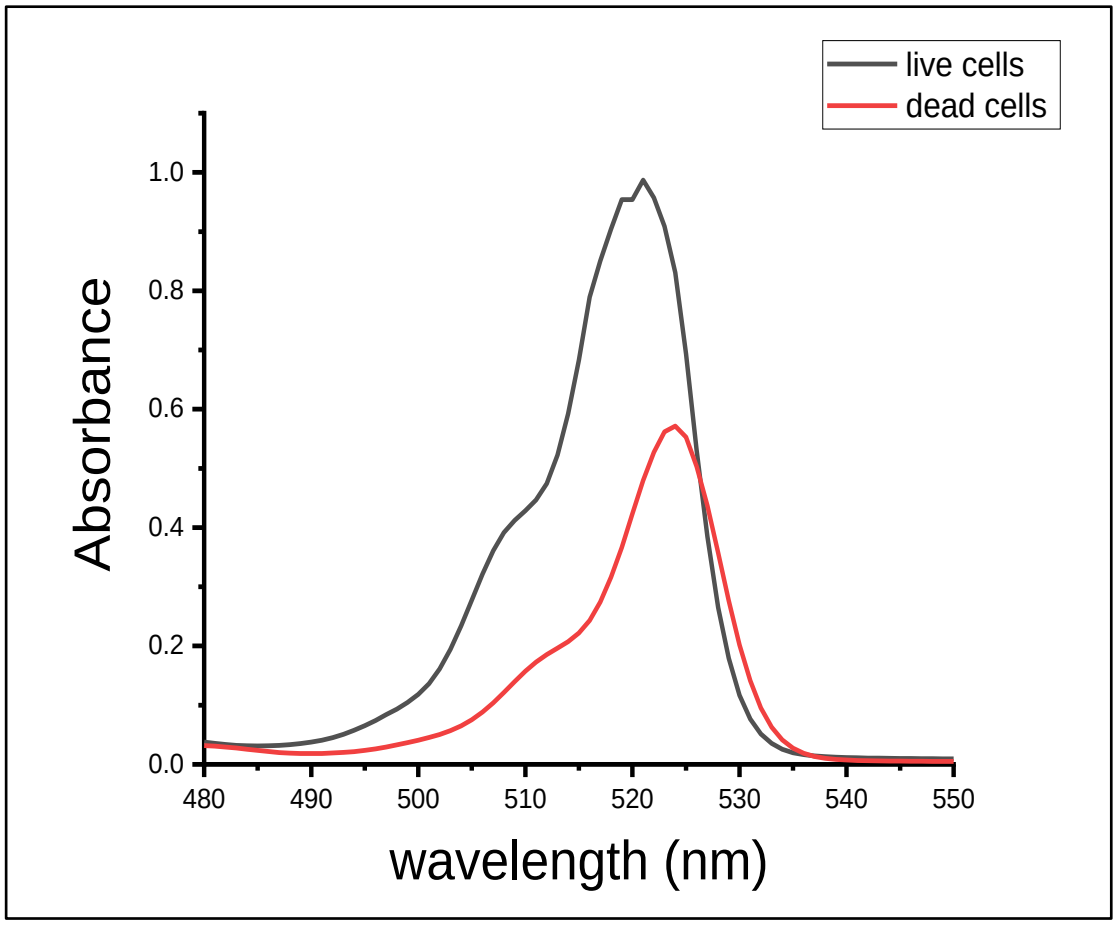

Fig.(4-8): Absorbance spectra of live and dead colon cancer cells culture

Table(4-4): Absorbance of live and dead colon cancer cells culture

Material	λ_{max} (nm)	Absorbance
Living cells	522	0.957
Dead cells	524	0. 571

4-5-2 Absorbance Spectrum of The Nutrient Medium (RMPI 1640)

Figure (4-9) shows absorbance spectrum of the nutrient medium (RMPI 1640) of colon cancer cells culture, (RMPI 1640) medium represents the major component of all cell culture cultures as it is the food medium for tumor cells, To evaluate the effect of this medium on the absorption results at diagnosis, the absorbance spectrum of (RMPI 1640) medium were calculated. Where the highest absorption of the (RMPI 1640) medium is (0.329) at the wavelength (452 nm) .

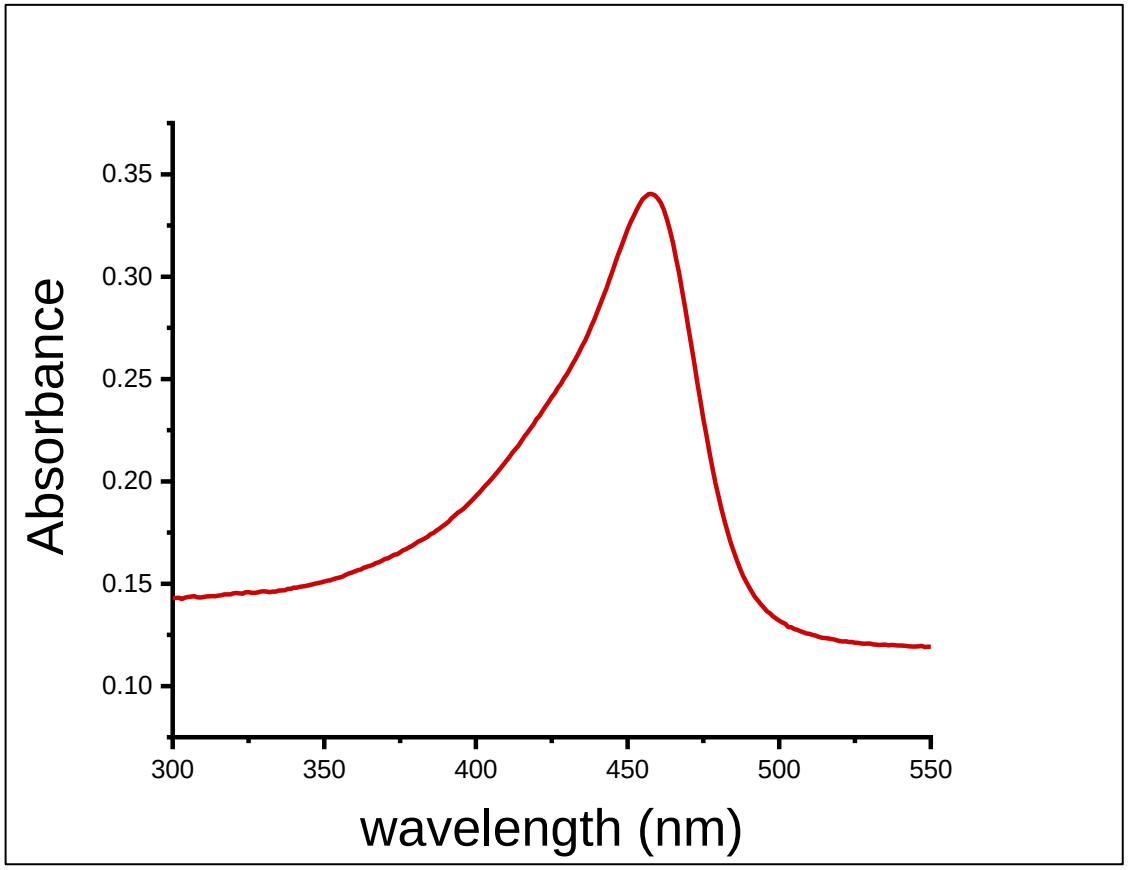

Fig.(4-9): Absorbance Spectrum of The Nutrient Medium (RMPI 1640).

Table(4-5): Absorbance Spectrum of (RMPI 1640) 1640 Medium

λ_{max} (nm)	Absorption
452	0.329

4-5-3 Absorption Spectra of Colon Cancer Cells and Trypsin

Trypsin is widely used for cell dissociation which breaks down proteins to separate or detach cells from the culture vessel. This process is important when cells need to move from vessel to vessel, and when complete, the cells will become suspended and appear rounded. Since trypsin is one of the chemical compounds found in colon cancer cells, the absorbance spectrum of trypsin were measured and compared with the absorbance spectrum of colon cancer cells.

Figure (4-10), the red line represents the absorbance spectrum of trypsin (0.261) at a wavelength (326 nm) and the black line represents the absorbance spectrum of colon cancer cells with trypsin (0.957) at a wavelength (522nm).

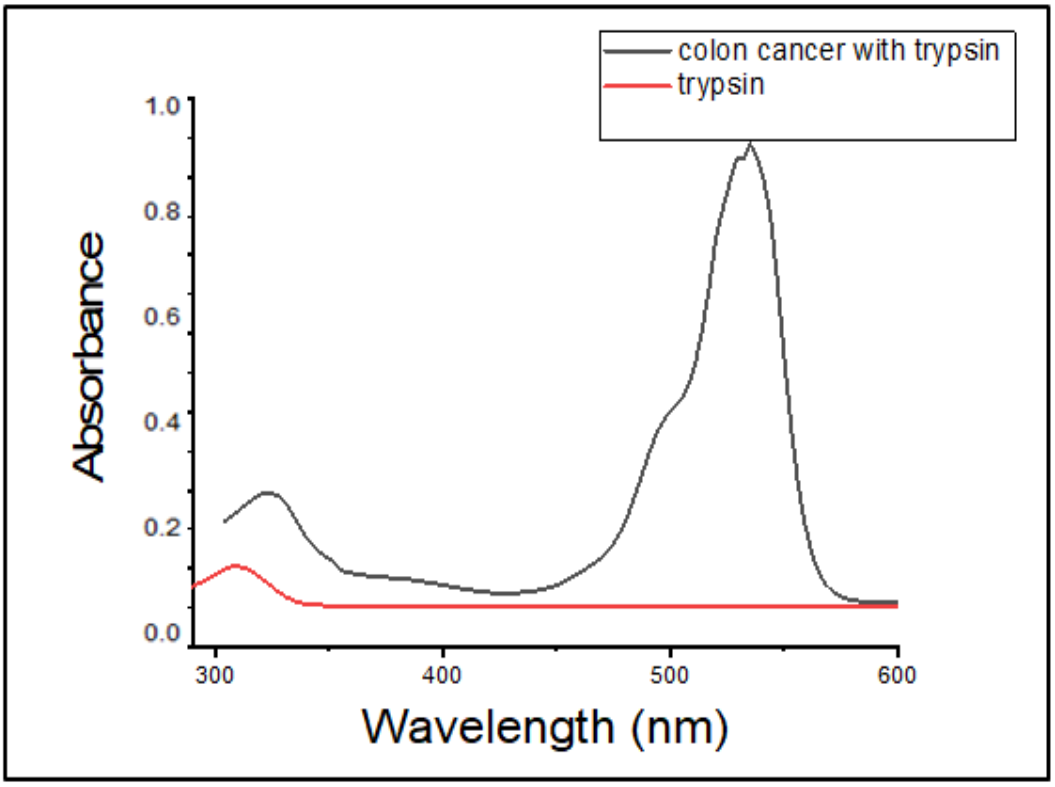

Fig.(4-10): Absorbance Spectrum of Colon Cancer Cells and Trypsin

Table(4-6): Absorption Spectra of Colon Cancer Cells and Trypsin

Material	λ_{max} (nm)	Absorption
Colon cancer with trypsin	522	0.957
Trypsin	326	0.261

4-5-4 Absorbance Spectrum of the Colon Cancer Cell with TiO_2 NPs Treated

This part shows and discusses the absorbance spectrum of colon cancer cell behavior after treatment with TiO_2NPs and for counting different concentrations (1000, 500, 250, 125, 62.50, 31.25) µg/ml of the nanomaterial. Figure (4-11) shows the absorbance spectrum of the nanomaterial interaction mixture with the cancer cell compound were recorded. absorbance spectrum were recorded for all components of the compound separately (trypsin, nanomaterial, the nutrient medium (RMPI 1640) of colon cancer cells). It was noted that the highest absorbance was obtained (0.836) at a concentration (1000 µg/ml) of the nanomaterials at a wavelength (517nm) and the lowest absorbance was obtained (0.081) at a concentration (31.25 µg/ml) of the nanomaterials at a wavelength (515nm). So observed that the higher the concentration of the nanomaterial in the solution, the higher the absorbance. because of increased in the concentration, the solution became darker, so the absorbance becomes high in addition to other physical phenomena such as scattering and reflectivity. Compared with the absorbance of the cancer cells compound before they were treated with nanomaterials, the control compound had a high absorbance close to the absorbance of the compound after adding the nanomaterial at a concentration (1000 µg/ml) This is due to the preparation conditions where the absorbance of the compound was measured after treatment 24 hours after adding the nanomaterial.

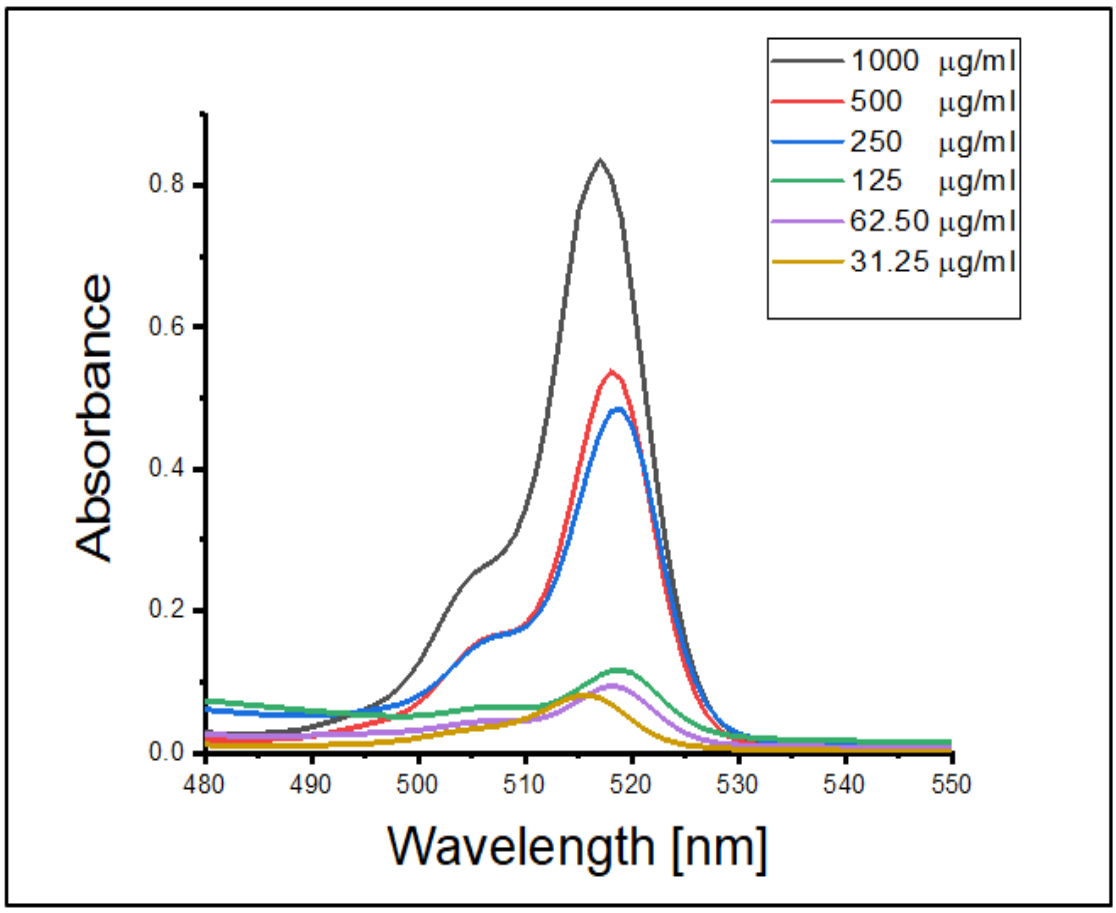

Fig.(4-11): Absorbance of colon Cancer for different concentrations (1000, 500, 250, 125, 62.50, 31.25) µg/ml of TiO_2NPs

Table(4-7): Absorption spectra of colon Cancer for different concentrations (1000, 500, 250, 125, 62.50, 31.25) µg/ml of TiO_2NPs

Concentration (µg/ml)	λ_{max} (nm)	A
Control	522	0.957
1000	517	0.836
500	518	0.583
250	519	0.485
125	519	0.116
62.50	518	0.094
31.25	518	0.081

4-5-5 Laser-Induced Fluorescence (LIF) spectrum of colon cancer cell

This part describes and discusses (LIF) spectrum by using laser induced fluorescence technique as a modern and accurate diagnostic method. The effect of excitation wavelengths (403,473,532) nm for diagnosing colon cancer cells was studied to find out the best wavelength in diagnosis and use it to diagnose the rest of the prepared samples, as well as studying the difference between living and dead colon cancer cells through this technique, as well as studying laser fluorescence (LIF) spectra for each chemical compound that was used in tissue culture. From cells containing nutrient medium (RMPI 1640) for colon cancer cell, trypsin and colon cancer cell medium before and after TiO_2NPs treated.

4-5-6 Effect of Excitation Wavelength to Diagnosing Colon Cancer Cells by Using Laser-Induced Fluorescence (LIF)

Figure (4-12) shows the effect of excitation wavelengths (473, 532 , 403) nm to diagnosis the colon cancer cells in LIF spectrum. It is expected that the use of different wavelengths will lead to the formation of different spectral intensities of the spectra of cells to verify the response of cancer cells to the wavelength used, and this reflects the spectral contents similar to the wavelength used in excitation. From the figure (4-12) , notice the difference between the fluorescence intensities at different wavelengths due to the amount of proteins present in the contents of the colon cancer cell, and this is due to the difference in the characteristic emission wavelengths, corresponding to the different constituting bio-species (fluorophores) that got excited with each excitation wavelength , this agreement with Literature survey [45,49].The blue line represents the emission spectrum obtained at wavelength 403 nm, the red line represents the emission spectrum obtained at wavelength

532 nm, and the black line represents the emission spectrum at wavelength 473 nm. In the case of excitation at wavelength 473 nm, a maximum emission spectrum for colon cancer sample was observed equal to (43680) in contrast to the case of excitation at wavelength 403 nm in which the peak of the emission spectrum is very small equal to (9990). In the emission spectra, there is a component that fluoresces at wavelengths 532 nm and 473 nm, As for the wavelength of 304 nm, the lowest emission was obtained because all the materials inside the colon cancer cell culture compound had the highest absorbance at 473 nm and 532 nm. The spectral shapes were not completely identical at all wavelengths used in the diagnosis, and the difference in the intensity of emission is due to the presence of many biochemical components in the cell sample this agreement with [157 ,158].

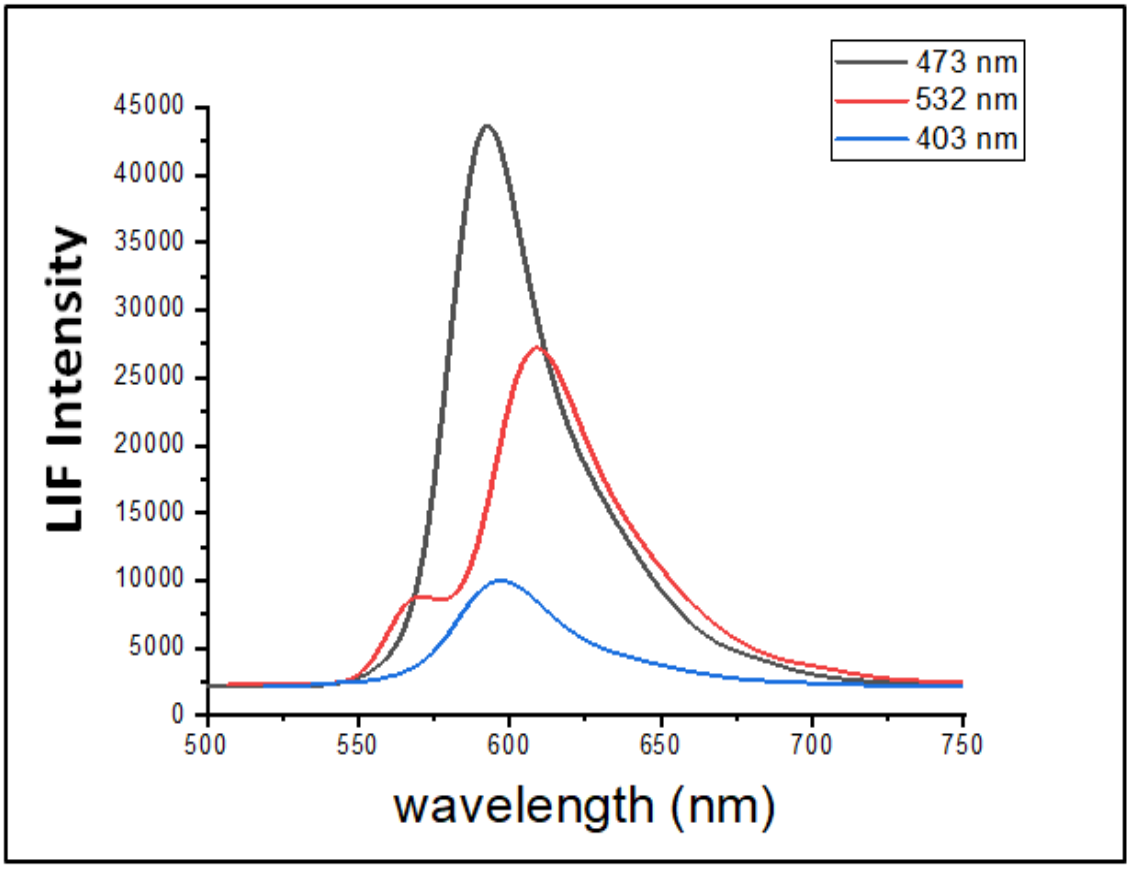

Fig.(4-12): LIF spectrum cancer cell at excitation wavelengths (403,473, 532) nm

Table(4-8): LIF spectrum cancer cell at excitation wavelengths (403,473, 532) nm

Laser source	λ_{max} (nm)	intensity
473 (nm)	600	43680
532 (nm)	609	27220
403 (nm)	597	9990

4-5-7 Comparison of LIF Spectrum of Living and Dead Colon Cancer Cells without TiO_2NPs Treated (Control Colon Cancer Cells)

The prepared colon cancer cells were examined by LIF spectrum using LIF system in the Department of Laser Physics / College of Science for Women / University of Babylon, where the laser wavelength used in the examination was 473 nm (CW laser), and the absorption wavelength of colon cancer cells was 522 nm

Figure (4-13) shows the comparison between living and dead cells of colon cancer cells by using LIF is discussed and explained. Where it was possible to clarify the difference and diagnose these cells using laser induced fluorescence technology. The red line represents the LIF spectrum of dead cells and the black line represents the LIF spectrum of living cells. It was noticed that the LIF spectrum of live cells (27220) at a wavelength of 610 nm is higher than the LIF spectrum of dead cells (16500) at a wavelength of 607 nm, It is observed that the dead cells have an emission spectrum, because the entire composition of the cells is contained within the compound only that the cells have reduced their effectiveness and that this part of the cells has lost its concentration due to dehydration.

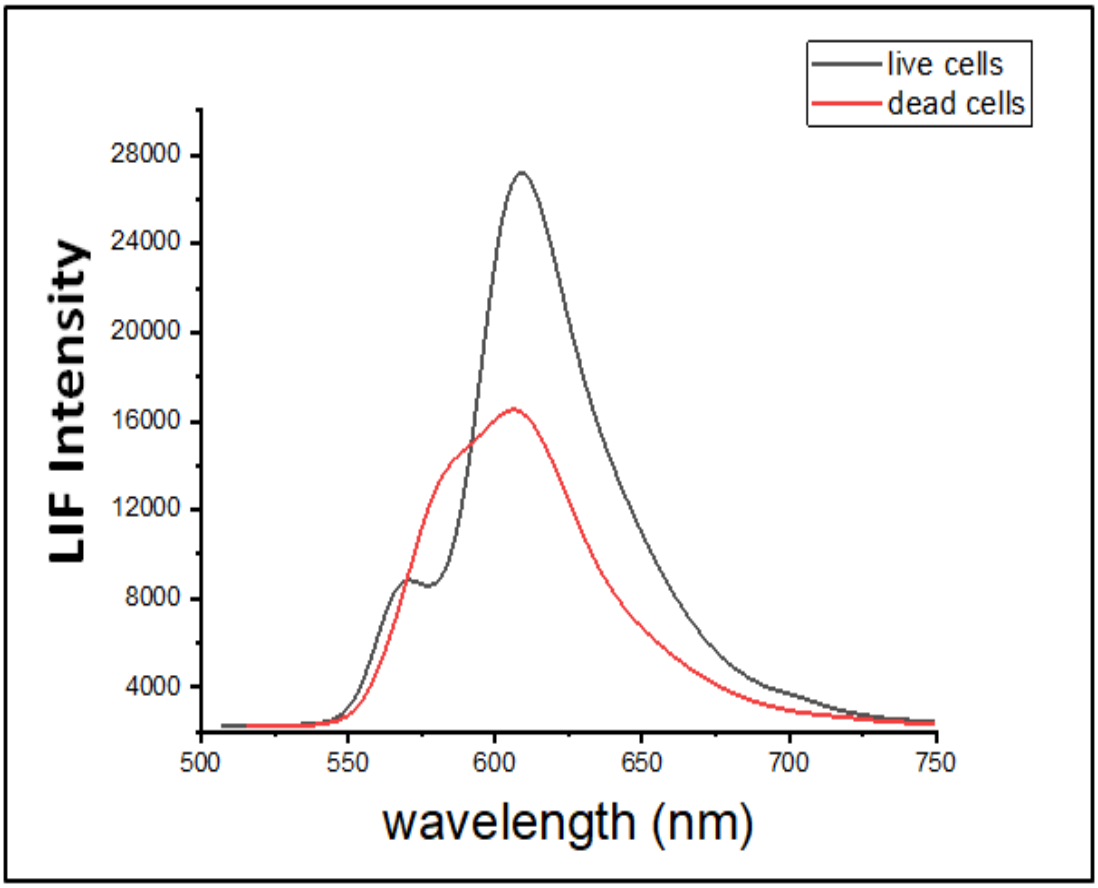

Fig.(4-13): LIF spectrum of living and dead cell colonic Cancer.

Table(4-9): LIF spectrum living and dead cell colonic Cancer.

Material	λ_{max} (nm)	intensity
Live cells	610	27220
Dead cells	607	16500

4-5-8 LIF Spectrum of Colon Cancer Cells Without TiO_2 NPs Treated

This part presents and discusses the behavior of the LIF spectra of a colon cancer cell before the treatment with TiO_2NPs. By knowing the behavior of the LIF spectrum of each chemical compound used in cells

culture for cells that include the nutrient medium (RMPI 1640) for colon cancer cell, colon cancer cell and trypsin.

4-5-8-1 LIF spectrum of the nutrient medium (RMPI 1640) of colon cancer cells

The nutrient medium (RMPI 1640) of colon cancer cells culture can negatively affect the fluorescence assay by causing high levels of fluorescence to the media. To evaluate the effect of this medium on the fluorescence results at diagnosis, figure (4-14) shows LIF spectrum of the rpmi 1640 medium were measured. Where the highest fluorescence of the medium (5620) at the wavelength (526 nm), these results showed a relationship between the wavelengths of the medium with wavelengths of fluorescence from the cancer cell, and the difference in intensity and wavelength was observed .

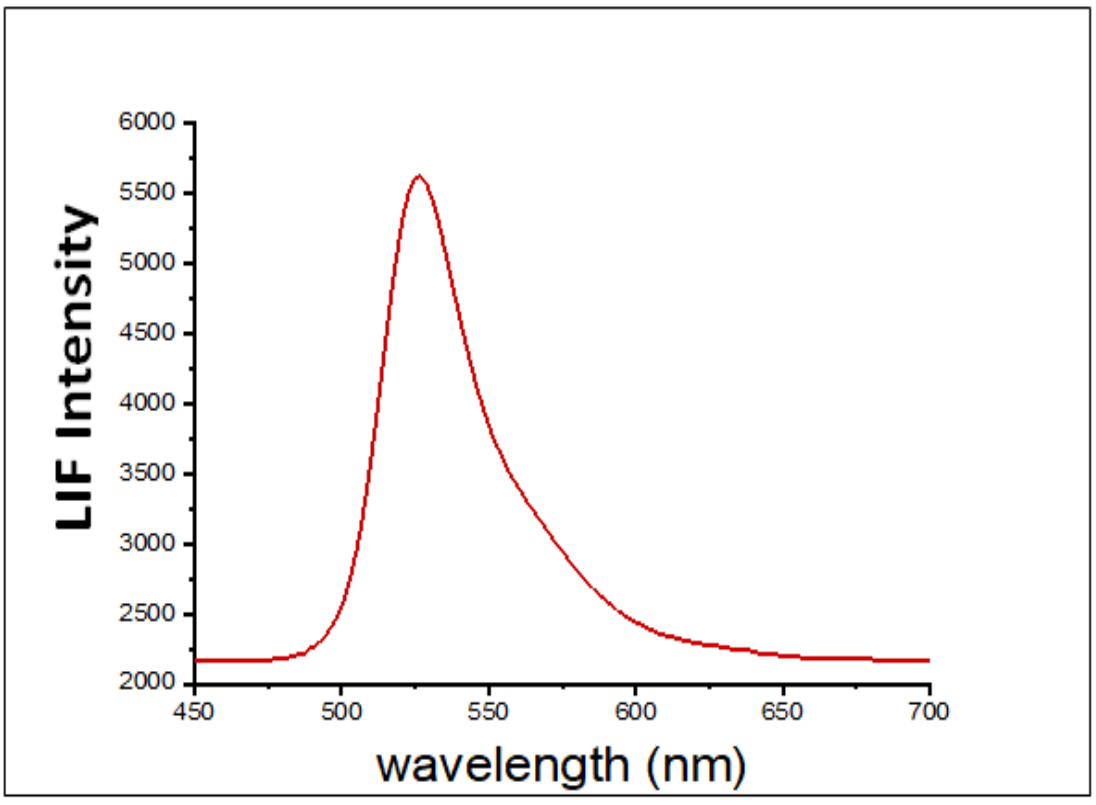

Fig.(4-14): LIF spectrum of nutrient medium (RMPI 1640) of colon cancer cells.

Table (4-10): LIF spectrum of of nutrient medium (RMPI 1640) of colon cancer cells.

λ_{max} (nm)	Intensity
526	5620

4-5-8-2 LIF Spectrum of Colon Cancer Cells and Trypsin

Since trypsin is one of the chemical compounds found in colon cancer cells, the LIF spectra of trypsin were measured and compared with the LIF spectra of colon cancer cells .In figure (4-15) , the red line represents the fluorescence spectrum of trypsin (2990) at a wavelength (409nm) and the black line represents the fluorescence spectrum of colon cancer cells with trypsin (27220) at a wavelength (610nm). It was noted that the effect of trypsin is very low and therefore does not affect the spectrum of cancer cells, this agreement with Literature survey [49].

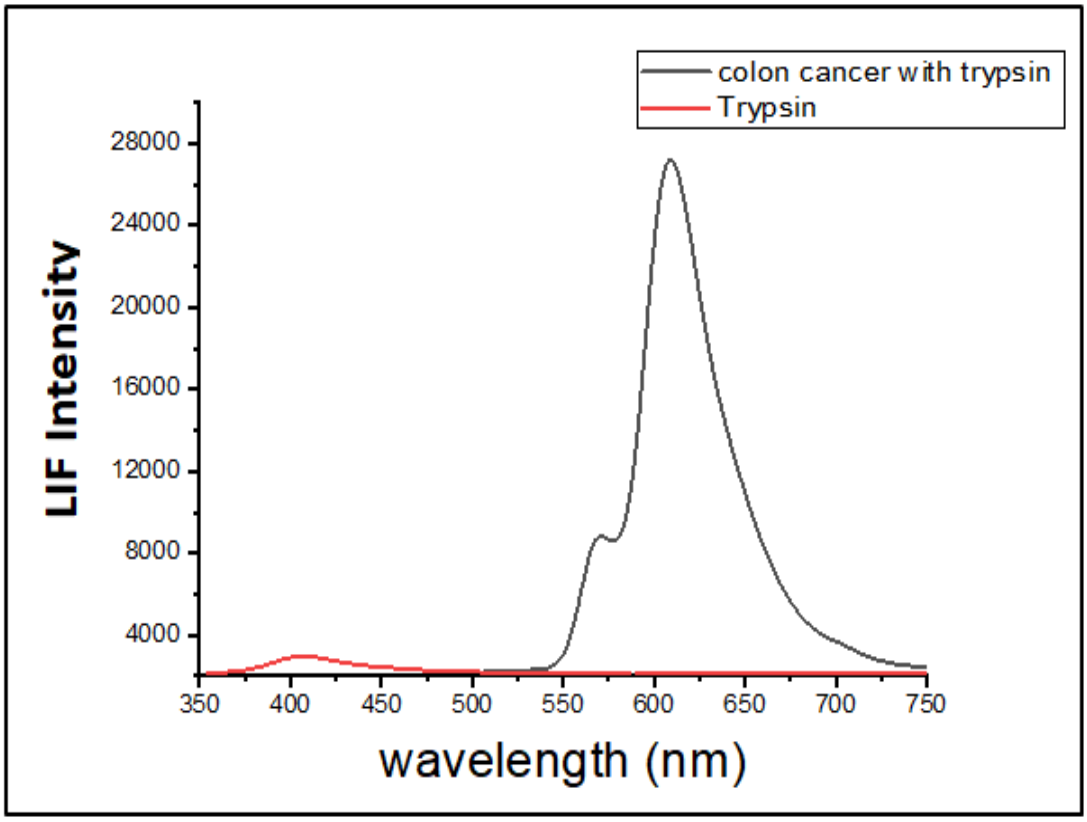

Fig.(4-15): LIF Spectrum Colon Cancer Cell and Trypsin

Table(4-11): LIF Spectrum of colon Cancer Cell and Trypsin

Material	λ_{max} (nm)	intensity
Colon cancer with trypsin	610	27220
Trypsin	409	2990

4-5-9 LIF spectrum the Cancer Cell with TiO_2 NPs treated

This part shows and discusses the LIF spectra of colon cancer cell behavior after treatment with TiO_2NPs and for counting different concentrations (1000, 500, 250, 125, 62.50, 31.25) µg/ml of the nanomaterial by using LIF Technique is show in figure (4-16).

When a biological molecule is illuminated with a specific wavelength, which falls within the absorption spectrum of that molecule, it absorbs this energy and is excited from the ground level to the excited level, and then the molecule returns to the ground state by emitting energy in the form of fluorescence with emissive wavelengths. Colon cancer cells were exposed to different concentrations of nanomaterials for 24 h to test the selectivity of this treatment for cancer cells. The effect of the concentrations used was compared with the control cell before it was treated and diagnosed using the laser induced fluorescence (LIF) technique. Nanomaterials can present antigens or adjuvants to stimulate immune cells, which helps the immune system to efficiently kill cancer cells that resulted in the induction of distinct cellular outcomes. Morphological changes induced by different Tio_2NPs concentrations ((1000, 500, 250, 125, 62.50, 31.25) µg/ml) were distinct in cancer colon cells. It was observed that the concentration of nanoparticles increased, cancer cells died, this agreement with Literature survey [51].

so the intensity of fluorescence decreased, and this corresponds to the statistical analysis. this agreement with [158] .

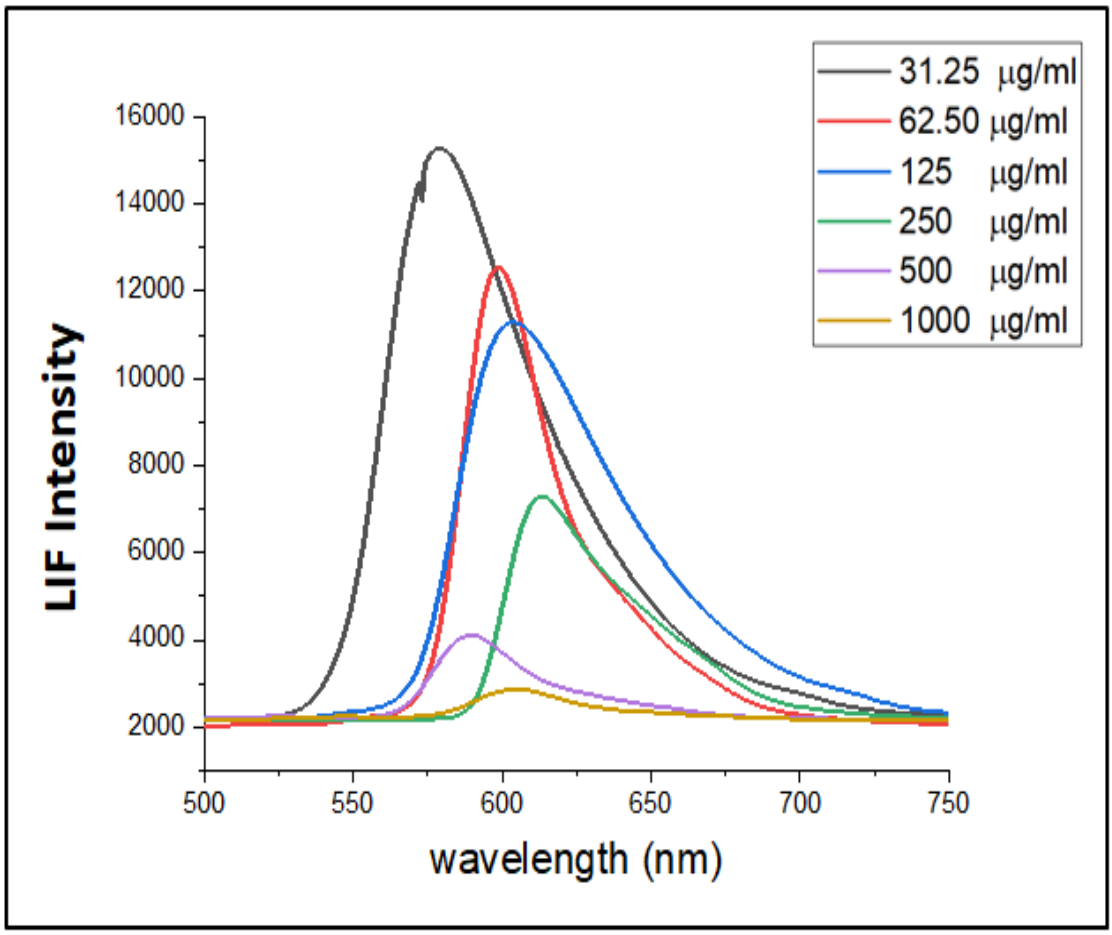

Fig.(4-16): LIF spectrum of colon Cancer for different concentrations (1000, 500, 250, 125, 62.50, 31.25) µg/ml of TiO_2NPs

Table(4-12): LIF spectrum of colon Cancer for different concentrations (1000, 500, 250, 125, 62.50, 31.25) µg/ml of TiO_2NPs

Concentration (µg/ml)	λ_{max} (nm)	intensity
control	610	27220
1000	606	2870
500	589	4110
250	613	7300
125	603	11290
62.50	597	12460
31.25	579	15280

4-6 Part Four

4-6-1 The Morphology of Cancer and Normal Cell

Figure (4-17) shows the biological evaluations of TiO_2 NPs in an initial test using an optic microscope on a culture cell line before doing the MTT experiment on human colon cancer and normal cell culture. Both cell cultures showed signs of cytotoxicity, according to the findings.

Even at a nanoparticle concentration of 31.25 µg/ml, after exposure. In general, nanoparticles have an impact on cell membrane integrity and morphology, and pinocytosis has been considered as the primary mechanism for nanoparticle uptake in cells. The toxicity of TiO_2NPs, which were exposed to successive dilutions of decreasing concentrations, inhibited cell cycle progression. When the concentration of TiO_2NPs on cancer cells is increased, the cells shrink and die, with the highest death occurring at a concentration of (1000 µg/ml). While the effects of (micro-size of TiO_2) Tio_2NPs on normal cells are different, this is due to the fact

that TiO_2NPs with small sizes can enter cancer cells, causing cell shrinkage and death, whereas the presence of TiO_2NPs on the cell membrane of a normal cell, but not inside the cell, causes a change in the shape of the normal cell and death due to Tio_2NPs' toxicity.

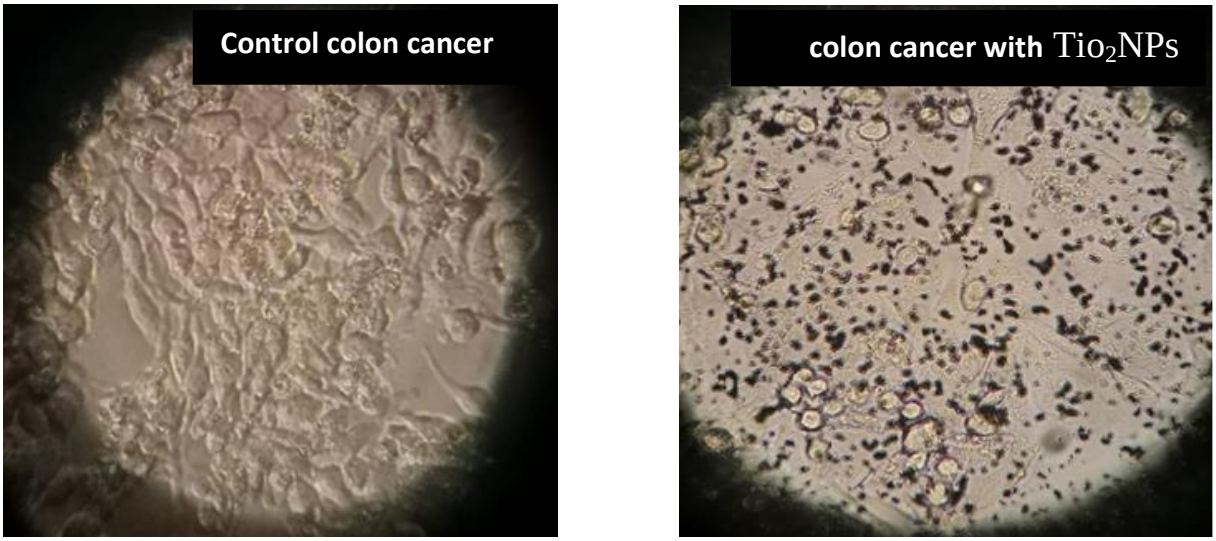

Fig. (4-17): Observations of cancer cell morphological changes after exposure with nanoparticles, the cells were observed by optic microscope directly

4-6-2 The Effect of TiO_2 NPs on Cancer Cell Line

The optical density of cell growth in each well of the microliter plate is determined using the MTT test. The maintenance medium containing the test drug was discarded before the completion of the cytotoxicity assay, and the wells were washed with 100 l of cold Phosphate buffer saline (PBS) using an automated pipette. The surviving human colon cancer cell line cultures are then fixed for 20 minutes at room temperature with 10% buffered formalin. After discarding the fixative solution, 100 l of MTT was added to each well, incubated for 30 minutes, and the absorbance was measured at 620 nm. The MTT assay measures cell proliferation in response to varying doses of TiO_2NPs in the culture media. Cells cultivated in TiO_2NPs-containing medium for 48 hours had

a lower survival rate than cells cultured in control medium (0 g/ml). At lower concentrations of TiO_2NPs (31.25 g/ml), there were obvious changes in cell survival, and as the concentration climbed (62.50 g/ml), there was a modest change in cell survival, but as the concentration reached (125,250, 500, and 1000) g/ml, cell survival dropped dramatically. Normal cells grown for 48 hours in media containing TiO_2NPs exhibit a modest decrease in viability. There is a consistent change in cell viability with (125, 250, 500, and 1000) g/ml TiO_2NPs concentration, and this change is distinct from that of cancer cells, as shown in Figure (4-18).

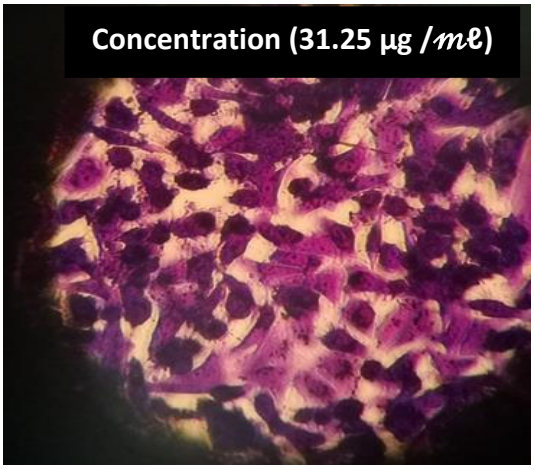

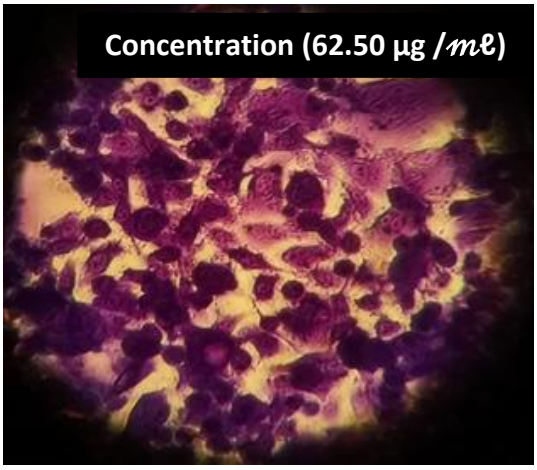

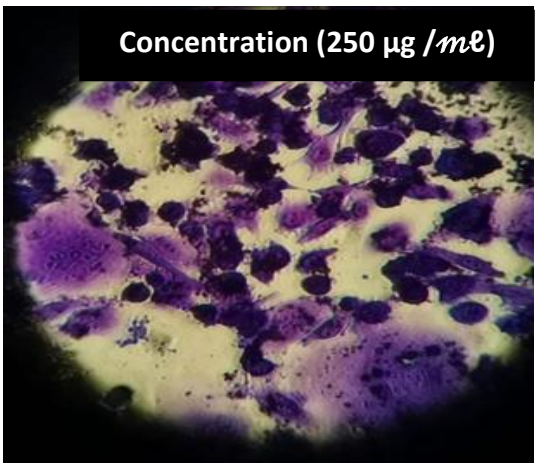

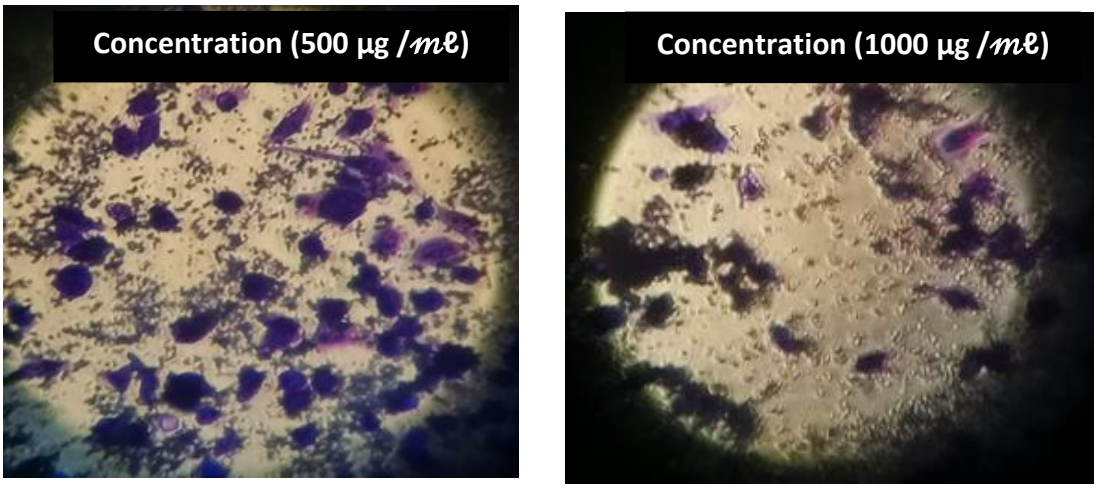

Fig. (4-18): Observations of colon cancer cell morphological changes after exposure with different concertation nanoparticles for 24 hours, the cells were observed by optic microscope directly.

4-6-3 The Cell Viability Analysis of Colon Cancer Cell by MTT Assay

The MTT test was used to assess the viability of human colon cells exposed to serial doubling increases in Tio2 nanoparticle concentrations ranging from 31.25 to 1000 g/ml. Nanoparticles' considerable suppression of cell viability was clearly detected in a dose-dependent manner. The cytotoxicity of TiO_2NPs against cancer cells was size dependant. Figure (4-19) shows the cell viability of TiO_2NPs with a minimal serial doubling increase. The cell survival rate diminishes as the concentration ofnanoparticles rises. The viability of cells dropped marginally as the concentration of TiO_2 nanoparticles was raised, this agreement with Literature survey [53].

.

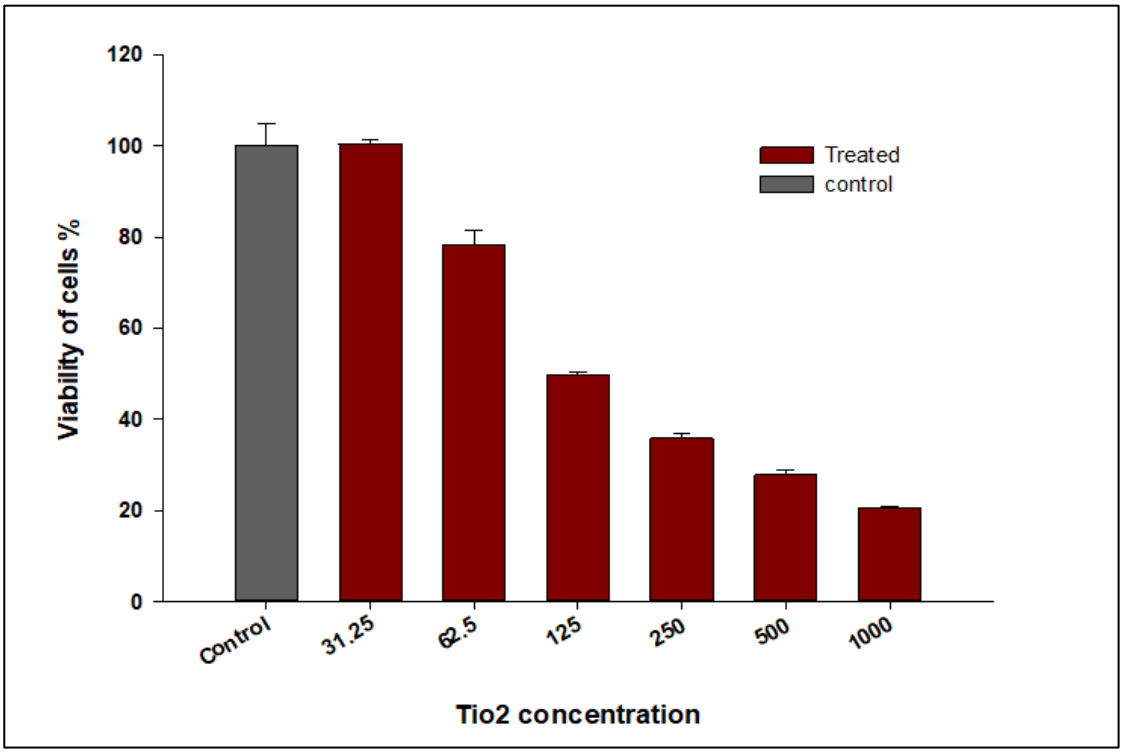

Fig.(4-19): viability of colon Cancer for counting different concentrations (1000, 500, 250, 125, 62.50, 31.25) µg/ml

To compare the three diagnostic techniques that include absorption spectroscopy, laser induced fluorescence spectroscopy and microscopy, three samples treated with nanomaterial were taken and measured by these three techniques to illustrate the difference in diagnosis.

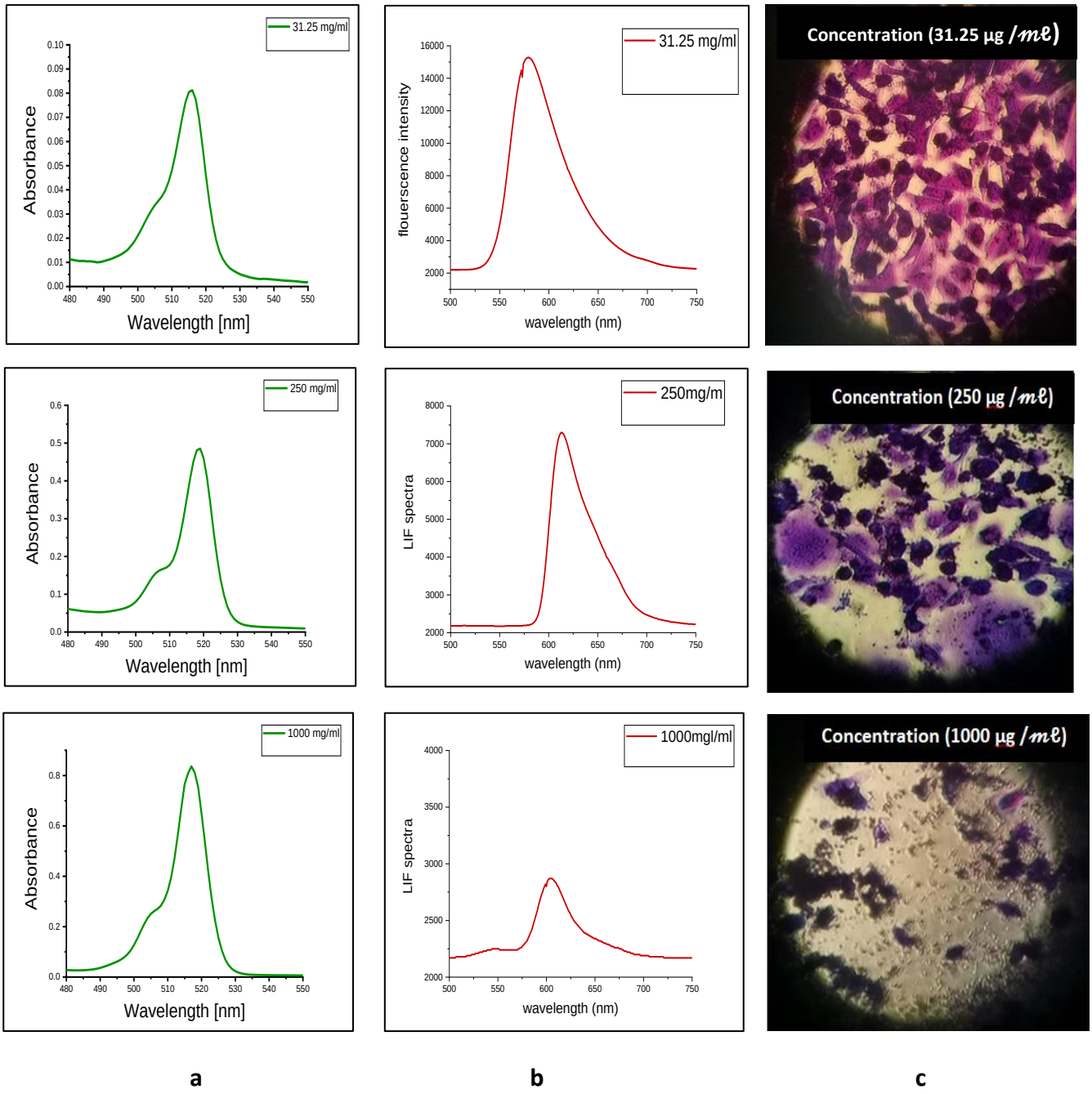

Fig.(4-20): Comparison of the three diagnostic techniques of colon Cancer: (a) absorbance, (b) LIF, (C) microscopy

Figure (4-20) shows the difference in diagnosis using three techniques: absorption spectroscopy, laser induced fluorescence (LIF) and microscopy. It was concluded that the laser induced fluorescence technique is the best technique in accurate diagnosis. It was observed that when changing the concentration of the nanomaterial, there is a change in the intensity and shift in the wavelength, and this is not present in the absorption spectra, where it was noted that the intensity changes with the stay of the wavelength constant, and this indicates that Accuracy in diagnosis.

4-7 Conclusion

Based on the results obtained by diagnosing colon cancer cells before and after adding the nanomaterial using LIF.

1- It was observed that by using a laser with a wavelength of 473 nm, the highest fluorescence of colon cancer cells was obtained, so this wavelength was used in diagnosing the rest of the samples.

2- Comparison between the live cells and dead cells of colon by using absorbance and LIF spectrum of colon cancer

3- Show the absorbance and fluorescence of the components of the medium in which colon cancer cells were implanted, as well as the absorbance and fluorescence of colon cancer cells with the components of the medium in order to know the true spectrum of colon cancer and diagnose it with high accuracy away from the components of the medium in which these cells live.

4-The absorbance of colon cancer cells after adding several concentrations of the nanomaterial (1000, 500, 250, 125, 62.50, 31.25) µg/ml. It is observed that the higher the concentration, the greater the absorbance, and this corresponds to the fluorescence spectra .

5- The fluorescence spectra of colon cancer cells after adding several concentrations of the nanomaterial (1000, 500, 250, 125, 62.50, 31.25) µg/ml, where the best results were obtained, which correspond to the statistical analysis of the cells

6- At high concentrations, it was observed that the fluorescence spectrum was very low, and this indicates the destruction of cancer cells, due to the small size of the nanomaterial that can penetrate into the cell and spread into the cytoplasm of the cell. The desire of this thesis was to determine the best concentration of nanoparticles, which results in the optimal solution for treating cancer. The results showed the best concentration 250 µg/ml that gives the maximum number of destroyed cancer cells.

4-8 Recommendations and Future Work

1-The use of the (LIF) system in diagnosing different types of cancer, such as breast cancer and kidney cancer

2-The use of the (LIBS) system in diagnosing colon cancer and other types of cancer

3-because tumor vasculature is irregular in comparison to normal tissue, the nanoparticle dispersion in the tumor is still higher by high concentration than in healthy cells around the tumor tissue, therefore we can leverage this the ability to detect cancer tumors using X-rays.

Reference

[1] R. W. **Wood**, "The fluorescence of sodium vapor and the resonance radiation of electrons", Philosophical Magazine, vol. 10, P.513, (1905).

[2] W. Daily., ”Laser Induced Fluorescence Spectroscopy in Flames”, Prog. Energy Combust. Sci. Vol. 23, P.P. 133-199, (1997).

[3] Richard N. Zare,” My Life with LIF: A Personal Account of Developing Laser-Induced Fluorescence”, Annu. Rev. Anal. Chem. 5.1 (2012).

[4] J. Thaddeus Salmon and Normand M. Laurendeau, “Quenching-independent fluorescence measurements of atomic hydrogen with photoionization controlled-loss spectroscopy”, Optics Letters, Vol. 11, No. 7, (1986).

[5] Paul E liao, Red Bank , Paul L. Kelley, Ivan P. Kaminow, Holmdel,” Tunable Lasers handbook” F. J. Duarte Eastman Kodak Company Rochesrer, New York, (1995).

[6] Richard N. Zare1 and Samuel Kim,” Microfluidic platforms for single-cell analysis”, Annu. Rev. Biomed. Eng, (2010).

[7] Andreas Ehn , Jiajian Zhu , Xuesong Li , and Johannes Kiefer,” Advanced Laser-Based Techniques for Gas-Phase Diagnostics in Combustion and Aerospace Engineering”, Applied Spectroscopy, Vol. 71, No.(3) (2017).

[8] McMillen, D. F., Lewis, K. E., Smith, G. P., and Golden,”Quantitative laser Diauostics for Combustion Chemistry and Propulsion”, D. M., J. Phys. Qhem., Vol. 86, No. 709, (1982).

[9] W. Denk, D. W. Piston, and W. W. Webb, “in Laser-Scanning Microscopy”, Handbook Of Biological Confocal Microscopy, James B. Pawley, Springer Science Business Media, LLC, New York, (2006)

[10] R. J. Cattolica, D. Stepowski, D. Puechberty, and M. Cottereau, "Laser-Induced Fluorescence of the CH Molecule in a Low Pressure Flame," J. Quant. Spectrosc. Transfer 32, 363-370 (1984).

[11] Yuncong Chen, Yang Bai, Zhong Han, Zijian Guo, "Photoluminescence imaging of Zn2+ in living systems", Chemical Society Reviews, vol. 44, No.(14), (2015).

[12] G. A. Blab, P. H. M. Lommerse, L. Cognet, S. H. Harms, and T. Schmidt, “Two- Photon Excitation Action Cross-Sections of the Autofluorescent Proteins,” Chem. Phys. Lett., vol. 350, P.P 71-77, (2001).

[13] Masters BR.; So PTC; Gratton.E, "Multiphoton excitation fluorescence microscopy and spectroscopy of in vivo human skin". Biophysical Journal, Vol. 72, No. (6), P.P 2405-2412, (1997).

[14] Bewersdorf J, Rainer P, Hell SW "Multifocal multiphoton microscopy". Optics Letters, Vol. 23 , No.(9),P.P 665-667, (1998).

[15] Khadria A, Coene Y, Gawel P, Roche C, Clays K, Anderson HL "Push–pull pyropheophorbides for nonlinear optical imaging". Organic and Biomolecular Chemistry, Vol.15No. (4), P.P 947-956, (2017).

[16] Reeve JE, Corbett AD, Boczarow I, Wilson T, Bayley H, Anderson HL "Probing the Orientational Distribution of Dyes in Membranes through Multiphoton Microscopy". Biophysical Journal, Vol.103, No. (5), P.P 907–917, (2012).

[17] P. Cheng, J. B. Pawley "The Contrast Formation in Optical Microscopy", Handbook Of Biological Confocal Microscopy New York, P. P. 162–206, (2006).

[18] V. Helms "Fluorescence Resonance Energy Transfer". Principles of Computational Cell Biology. Weinheim, P. P. 202, (2008).

[19] W. H. Freeman and D.C. Harris "Applications of Spectrophotometry". Quantitative Chemical Analysis New York, P.P. 419–44, (2010).

[20] Zheng J "Spectroscopy-based quantitative fluorescence resonance energy transfer analysis" , Methods in Molecular Biology. Vol. 337. No.14, P. P.65–77, (2006).

[21] Andrews DL, "A unified theory of radiative and radiationless molecular energy transfer" , Chemical Physics. Vol.135, No. (2), P.P 195–201, (1989).

[22] Andrews DL and Bradshaw DS "Virtual photons, dipole fields and energy transfer: A quantum electrodynamical approach" , European Journal of Physics. Vol. 25, No. (6), P.P 845–858. (2004).

[23] Jones GA, Bradshaw DS "Resonance energy transfer: From fundamental theory to recent applications". Frontiers in Physics, Vol. 7,P.P. 100, (2019).

[24] Förster T, "Intermolecular energy migration and fluorescence”.,Annalen der Physik (in German),Vol. 437, No. (1–2), P.P 55–75,. (1948).

[25] Valeur B, Berberan-Santos M "Excitation Energy Transfer". Molecular Fluorescence: Principles and Applications, 2nd ed. Weinheim, P.P. 213–261, (2012).

[26] Helms V "Fluorescence Resonance Energy Transfer". Principles of Computational Cell Biology. Weinheim: P. P 202, (2008).

[27] S. E. BRASLAVSKY, ”Glossary of Terms Used in Photochemistry “ Pure Appl. Chem., Vol. 79, No. 3, P.P 293–465, (2007).

[28] Dalmas, O., Do Cao, M.-A., Lugo, M. R., Sharom, F. J., Di Pietro, A., & Jault, J.-M.,”Time-Resolved Fluorescence Resonance Energy Transfer Shows that the Bacterial Multidrug ABC Half-Transporter BmrA Functions as a Homodimer”, Biochemistry, Vol.44, No.(11), P.P 4312–4321, (2005).

[29] Schaufele F, Demarco I, Day RN "FRET Imaging in the Wide-Field Microscope". FRET Microscopy and Spectroscopy. P. P. 72–94, (2005).

[30] Lee S, Lee J, Hohng S "Single-molecule three-color FRET with both negligible spectral overlap and long observation time". Plos One, Vol.5, No. (8), (2010).

[31] C. King; B. Barbiellini; D. Moser & V. Renugopalakrishnan "Exactly soluble model of resonant energy transfer between molecules". Physical Review B., Vol.85, No (12), (2012).

[32] Förster T "Delocalized Excitation and Excitation Transfer". ,Modern Quantum Chemistry, Academic Press. P.P. 93–137,(1965).

[33] Clegg R "Förster resonance energy transfer—FRET: what is it, why do it, and how it's done". Laboratory Techniques in Biochemistry and Molecular Biology,Vol.33, pp. 1–57, (2009).

[34] Varnakavi. Naresh , and Nohyun Lee ," A Review on Biosensors and Recent Development of Nanostructured Materials-Enabled Biosensors", sensors,Vol. 21, No.(4), P.P. 1109, (2021).

[35] Majoul I, Jia Y, Duden R "Practical Fluorescence Resonance Energy Transfer or Molecular Nanobioscopy of Living Cells". Handbook Of Biological Confocal Microscopy . P.P. 788–808, (2006).

[36] Saul Theodore Emmanuel Jones ,"Photo physics of small molecule organo-metallic complexes for OLED applications", hand book Archived from the original , 2019.

[37] Szöllősi J, Alexander DR "The Application of Fluorescence Resonance Energy Transfer to the Investigation of Phosphatases". Methods in Enzymology. Vol. 366. P.P. 203–24,(2007).

[38] Periasamy A "Fluorescence resonance energy transfer microscopy: a mini review" , Journal of Biomedical Optics. Vol. 6 ,No.(3),(2001).

[39] Paolo Bettotti, "Nanodevices for Photonics and Electronics Advances and Applications," Taylor & Francis Group,2015.

[40] G. K. Rajan, "In-Situ Tailoring of The Morphological and Magnetic Properties of Co and CoFe Thin Film Systems," thesis Phd, SRM University, Kattankulathur, 2014.

[41] Qiaobao Zhang, Kaili Zhang , Daguo Xu, Guangcheng Yang, Hui Huang, Fude Nie, Chenmin Liu, Shihe Yang , "CuO nanostructures: Synthesis, characterization, growth mechanisms, fundamental properties,

and applications," Prog. Mater. Sci., Vol. 60, No. 1, P.P. 208–337, (2014).

[42] S. K. Ghoshal, M. R. Sahar; M.S.Rohani, and S. Sharma, , "Optoelectronics–Devices and Applications", Nanophotonics for 21 century, Textbook,(2011).

[43] A. F. Koenderink and A. Polman, "Nanophotincs: Shrinking Light-based technology," Light And Optics, . Vol. 348 ISSUE 6234. (2015).

[44] Fu-Hua Wang and Takashi Yoshitake, "Determination of conjugation efficiency of antibodies and proteins to the superparamagnetic iron oxide nanoparticles by capillary electrophoresis with laser-induced fluorescence detection" Karolinska Institutet, 171 76 Stockholm, Sweden; 2003.

[45] Moon S. Kim, Alan M. Lefcourt, and Yud-Ren Chen," Multispectral laser-induced fluorescence imaging system for large biological samples Vol. 42, pp. 3927-3934, (2003).

[46] Yinhua Jiang, Juan Kang and Yarui Wang," Rapid and Sensitive Analysis of Trace Leads in Medicinal Herbs Using Laser-Induced Breakdown Spectroscopy–Laser-Induced Fluorescence (LIBS-LIF)" First Published ,(2019).

[47] Chan Kyu Kim and Rajamohan R Kalluru, "Gold-nanoparticle-based miniaturized laser-induced fluorescence probe for specific DNA hybridization detection: studies on size-dependent optical properties" Mississippi State University,Research Boulevard, Starkville, (2006).

[48] Joshi-Deepak and KumarAnil K.MainiRamesh, " Detection of biological warfare agents using ultra violet-laser induced fluorescence LIDAR", Molecular and Biomolecular Spectroscopy, , Pages 446-456, (2013).

[49] Jagdish P. Singh∗, Sunil K. Khijwania∗∗, Chan Kyu Kim, Fang-Yu Yueh Shane C. Burgess, "Laser-induced Fluorescence (LIF) Based Optical Fiber Probe for Biomedical Application" College of Veterinary Sciences Mississippi State University, (2014).

[50] Jorge Marques da Silva 1, and Andrei Borissovitch Utkin, " Application of Laser-Induced Fluorescence in Functional Studies of Photosynthetic Biofilms" Universidade de Lisboa, Campo Grande, 1749-016 Lisbon, Portugal, (2018).

[51] Siqi Guo, Yu Jing, Incline. Berkus," Nano-pulse stimulation induces potent immune responses, eradicating local breast cancer while reducing distant metastases" Frank Reidy Research Center for Bioelectrics, Old Dominion University, (2018).

[52] Valentina Gabbarini, Riccardo Rossi, "Laser-induced fluorescence (LIF) as a smart method for fast environmental virological analyses: validation on Picornaviruses",(2019).

[53]. Fatemeh Ghasemi, Parviz Parvin and Maryam Lotfi, " Laser-induced fluorescence spectroscopy for diagnosis of cancerous tissue based on the fluorescence properties of formaldehyde ", Citation Fatemeh Ghasemi et al Laser Phys, (2019).

[54]. Jung GR, Kim KJ, Choi CH, Lee TB, and Han H., " Effect of betulinic acid on anticancer drug-resistant colon cancer cells", Basic Clin Pharmacol Toxicol, Vol.101, No.(4), P.P. 277- 285, (2007).

[55] Yinhua Jiang, Juan Kang, Yarui Wang, Yuqi Chen, and Runhua Li, “Rapid and Sensitive Analysis of Trace Leads in Medicinal Herbs Using Laser-Induced Breakdown Spectroscopy”, Hand book Laser-Induced Fluorescence (LIBS-LIF) ,(2019).

[56] Ahmed L.Abdel Gawad and Yasser El-Sharkawy," Classification of dental diseases using hyperspectral imaging and laser induced fluorescence" Photo diagnosis and Photodynamic Therapy , P.P 128-135, Vol. 25, (2019).

[57] Nicholas C. Speller, Thomas Cantrell, and Amanda M Stockton, " A modular, easy-to-use micro capillary electrophoresis system with laser-induced fluorescence for quantitative compositional analysis of trace organic molecules" ,Hand book Laser-Induced Fluorescence (LIBS-LIF) ,(2019).

[58] Oloche Owoicho, Charles Ochieng' Olwal and Osbourne Quaye, " Potential of laser-induced fluorescence-light detection and ranging for future stand-off virus surveillance", Microb Biotechno, Vol. 14, No.(1), P.P.126-135, (2021).

[59] Groenhuis RAJ, Ferwerda HA, Ten Bosch JJ," Scattering and absorption of turbid materials determined from reflection measurements. 1: theory, Vol.22, No.24, P.P 5662, (1983)

[60] Mehdi Hamamda, Pierre Pillet, Hans Lignier and Daniel Comparat," Ro-vibrational cooling of molecules and prospects", Journal of Physics B: Atomic, Molecular and Optical Physics, Vol. 48, No. 18, (2015).

[61] N. Zare. "My Life with LIF: A Personal Account of Developing Laser-Induced Fluorescence", Annu. Rev. Anal. Vol. 5 , No.1 ,(2012).

[62] Winefordner, J. D., Gornushkin, I. B., Correll, T., Gibb, E., Smith, B. W., & Omenetto, N. "Comparing several atomic spectrometric methods to the super stars: special emphasis on laser induced breakdown spectrometry, LIBS, a future super star." Journal of Analytical Atomic Spectrometry, Vol. 19, No.9, P.P. 1061, (2004).

[63] Patricia Bargiela-Pérez 1 , Jorge González-Merchán 2 , Rosa Díaz-Sánchez 2 , Maria-Angeles Serrera-Figallo 1 , Gerd Volland 1 , Martin Joergens 1 , Jose-Luis Gutiérrez-Pérez 3 , Daniel Torres-Lagares," Prospective study of the 532 nm laser (KTP) versus diode laser 980 nm in the resection of hyperplastic lesions of the oral cavity," Med Oral Patol Oral Cir Bucal, Vol.23, No. (1), P.P. 78-85(2018).

[64] Hamid Farrokhi1, Thazhe Madam Rohith1, Jeeranan Boonruangkan, Seunghwoi Han, Hyunwoong Kim, Seung-Woo Kim & Young-Jin Kim, "High-brightness laser imaging with tunable speckle reduction enabled by electroactive micro-optic diffusers", Scientific Reports, Vol.7, No.(1), (2017).

[65] Mikko Lehtinen "Design of Diode Laser LifetimeTest Device", Master's Thesis, Tampere University, Electrical Engineering, (2019),

[66] Rai, V. N., and S. N. Thakur. "Physics of plasma in laser-induced breakdown spectroscopy." Handbook Laser-induced breakdown spectroscopy (2007).

[67] Singh, Jagdish P., and Surya Narayan Thakur, eds." Laser-induced fluorescence", handbook Physics and dynamics of plasma in laser-induced breakdown spectroscopy Elsevier,(2020).

[68] Richeng Lin1,4, Wei Zheng 1,4✉, Liang Chen2,4, Yanming Zhu1 , MengXuan Xu3, Xiaoping Ouyang2 & Feng Huang, "X-ray radiation excited ultralong (>20,000 seconds) intrinsic phosphorescence in aluminum nitride single-crystal scintillators", Nature Communications, Vol.11, No.(1), (2022).

[69] Hellen C. Ishikawa-Ankerhold, Richard Ankerhold, and Gregor P. C. Drummen," Advanced Fluorescence Microscopy Techniques—FRAP, FLIP, FLAP, FRET and FLIM", National library of medicine , Vol.17, No.(4), P.P.4047–4132, (2012).

[70] Siyuan Qin , Jingwen Jiang1, Yi Lu , Edouard C. Nice , Canhua Huang, Jian Zhang, and Weifeng He," Emerging role of tumor cell plasticity in modifying therapeutic response", Signal Transduction and Targeted Therapy,Vol. 5, No.(1), (2020).

[71]. M. Andresen, A. C. Stiel, J. Fölling, D. Wenzel, A. Schönle, A. Egner, C. Eggeling, S. W. Hell, and S. Jakobs, «Photoswitchable fluorescent proteins enable monochromatic multilabel imaging and dual color uorescence nanoscopy», Nature Biotechnology, Vol. 26, P.P. 1035-1040, (2008).

[72]. G. S. Filonov, K. D. Piatkevich, L.-M. Ting, J. Zhang, K. Kim, and V. V. Verkhusha, «Bright and stable near-infrared fluorescent protein for in vivo imaging», Nature Biotechnology, Vol. 29, P.P. 757-761, (2011).

[73] hang, J.-B., Chen, F., Yoon, Y.-G., Jung, E. E., Babcock, H., Kang, J. S., … Boyden, E. S.," Iterative expansion microscopy", Nature Methods, Vol.14, No.(6), P.P.593–599, (2017).

[74 Gitis, Vitaly; Rothenberg, Gadi, Gitis, Vitaly," Rothenberg, Gadi (eds.):, Handbook of Porous Materials. Singapore: World Scientific. pp. 63–64, (2020).

[75] Wei YanORCID, Yangrui Huang,Luwei Wang *,Jin Li,Yong Guo,Zhigang Yang andJunle ,"Multi-Color Two-Photon Microscopic Imaging Based on a Single-Wavelength Excitation" ,Two-photon laser scanning microscope Science , Vol. 12, No.(5),P.P. 307, (2022).

[76] Enderlein J, Gregor I, Patra D, Fitter J.,” Art and artefacts of fluorescence correlation spectroscopy”, Curr Pharm Biotechnol, Vol. 5 P.P 155–161 , (2004)

[77] Fernandez-Suarez M, Ting AY. “Fluorescent probes for superresolution imaging in living cells”, Nat Rev Mol Cell Biol , Vol.9: P.P.929–943, (2008).

[78] El-Azazy, M. S.” Analytical Calibrations: Schemes, Manuals, and Metrological Deliberations. ”Handbook Calibration and Validation of Analytical Methods - A Sampling of Current Approaches. (2018).

[79], Dimofte, A., Finlay, J. C., & Zhu, T. C. “A method for determination of the absorption and scattering properties interstitially in turbid media”, Physics in Medicine and Biology, Vol. 50, No.(10), P.P. 2291–2311. (2005).

[80] Aimable Samuel, Cheng Jessica, Arnold Kevin Aptowicz and Yong Lepan, “Review of elastic light scattering from single aerosol particles and application in bioaerosol detection” Journal of Quantitative Spectroscopy and Radiative Transfer, Vol. 279, (2022).

[81] Koochesfahani, M., Cohn, R., MacKinnon, C., & Koochesfahani, M. Simultaneous whole-field measurements of velocity and concentration fields using a combination of MTV and LIF. Measurement Science and Technology, Vol.11, No.(9), P.P.1289–1300, (2000).

[82] Bulska, E., & Ruszczyńska, A,”Analytical Techniques for Trace Element Determination”, Physical Sciences Reviews, Vol.2,No.(5),(2017).

[83] Iyad Safi , “A study of reactive magnetron sputtering of alloy transparent conducting oxides from elemental targets”, PhD thesis , Loughborough University, (1997).

[84] Kiyotaka Wasa, Isaku Kanno, and Hidetoshi Kotera, “Handbook of Sputter Deposition Technology,Fundamentals and Applications for Functional Thin Films, Nanomaterials, and MEMS,” Second Edition, Vol.53, No.9.(2013).

[85] O. O. Abegunde, E. T. Akinlabi, O. P. Oladijo, S. Akinlabi, and A. U. Ude, “Overview of thin film deposition techniques,” AIMS Mater. Sci., Vol. 6, No. 2, P.P. 174–199, (2019),

[86] Gareth William Hall, “Control of the properties of semiconducting thin films deposited using magnetron sputtering,” PhD thesis, Loughborough University , (1993) .

[87] James Mbiyu, “ Fundamental Processes in Growth of Reactive DC Magnetron Sputtered Thin Films,” thesis approved by the faculty of mathematics, computer science and natural sciences of Rheinisch - Westflischen Technische Hochschule Aachen ,(2004)

[88] A. Iles and N. Pamme, “Sputtering for Film Deposition,” Encyclopedia of Microfluidics and Nanofluidics, Encycl. Microfluid. Nanofluidics, P.P. 1–9, (2013).

[89] S. K. PANDIAN, “Preparation and Characterization of Titanium Based Coatings By Direct-Current (Dc) Magnetron Sputtering Process,” Tampere University of technology Master of Science Thesis, no. October, (2015).

[90] M. Aiempanakit, “Reactive High Power Impulse Magnetron Sputtering of Metal Oxides”, Linköping Studies in Science and Technology thesis No.1519. (2013).

[91] J. T. Gudmundsson, “Physics and technology of magnetron sputtering discharges,” Plasma Sources Sci. Technol., Vol. 29, No. 11, (2020),

[92] E. Walford, “Inorganic Chemicals,” Vol. 8, No. 245. P.P.192, (1896),

[93] D. Nunes, A. Pimentel, A. Gonçalves, S. Pereira, R. Branquinho, P. Barquinha, E. Fortunato, and R. Martins, “Metal oxide nanostructures for sensor applications,” Semiconductor . Sci. Technology ., Vol. 34, No. 4, P.P. 1–178, (2019).

[94] Chow EK, Ho D: Cancer nanomedicine: from drug delivery to imaging. Science translational medicine , Vol.5, No.(216),(2013).

[95] Fang J, Nakamura H, Maeda H: The EPR effect: Unique features of tumor blood vessels for drug delivery, factors involved, and limitations and augmentation of the effect. Adv Drug Deliv Rev,Vol. 63, No.(3), P.P136-151. (2011).

[96] Kamaly N, Xiao Z, Valencia PM, Radovic-Moreno AF, Farokhzad OC. Targeted polymeric therapeutic nanoparticles: design, development and clinical translation. Chem Soc Rev,Vol.41, P.P 2971-3010,(2012)

[97] Farokhzad OC, Langer R.,”Impact of nanotechnology on drug delivery”. ACS Nano, Vol. 27, No.3, P.P.16-20, (2009).

[98] Kircher, M. F., de la Zerda, A., Jokerst, J. V., Zavaleta, C. L., Kempen, P. J., Mittra, E., … Gambhir, S. S. “A brain tumor molecular imaging strategy using a new triple-modality MRI-photoacoustic-Raman nanoparticle”, Nature Medicine, Vol. 18, No.(5), P.P 829–834, (2012).

[99] Nam, J.-M. ,”Nanoparticle-Based Bio-Bar Codes for the Ultrasensitive Detection of Proteins.” Science Scope, Vol.301, No.(5641), P.P. 1884–1886, (2003).

[100] Fan R, Heath JR , Integrated barcode chips for rapid, multiplexed analysis of proteins in microliter quantities of blood,” Nat Biotechnol.,Vol.26, P.P.1373, (2008).

[101] Duan, X., Chan, C., Guo, N., Han, W., Weichselbaum, R. R., & Lin, W. “Photodynamic Therapy Mediated by Nontoxic Core–Shell Nanoparticles Synergizes with Immune Checkpoint Blockade To Elicit Antitumor Immunity and Antimetastatic Effect on Breast Cancer.” Journal of the American Chemical Society, Vol.138, No.(51), (2016).

[102] He, C., Duan, X., Guo, N., Chan, C., Poon, C., Weichselbaum, R. R., & Lin, W. Core-shell nanoscale coordination polymers combine chemotherapy and photodynamic therapy to potentiate checkpoint blockade cancer immunotherapy. Nature Communications, Vol.7, P.P 12499, (2016).

[103] Park, S., Wong, D. J., Ooi, C. C., Kurtz, D. M., Vermesh, O., Aalipour, A., … Gambhir, S. S.” Molecular profiling of single circulating tumor cells from lung cancer patients”, Proceedings of the National Academy of Sciences, Vol. 113, No.(52), (2016).

[104] Lin, M., Chen, J.-F., Lu, Y.-T., Zhang, Y., Song, J., Hou, S. Tseng, H.-R. “Nanostructure Embedded Microchips for Detection, Isolation, and Characterization of Circulating Tumor Cells” Accounts of Chemical Research, Vol.47, No.(10), P.P 2941–2950, (2014).

[105] Jiang, R., Lu, Y.-T., Ho, H., Li, B., Chen, J.-F., Lin, M., … Posadas, E. M. “A comparison of isolated circulating tumor cells and tissue biopsies using whole-genome sequencing in prostate cancer”. Oncotarget, Vol.6, No.(42),(2015).

[106] Ritu Gupta and Huan Xie,” Nanoparticles in Daily Life: Applications, Toxicity and Regulations”, J Environ Pathol Toxicol Oncol, Vol. 37, P.P 209–230, (2018).

[107] Shuhendler, A. J., Ye, D., Brewer, K. D., Bazalova-Carter, M., Lee, K.-H., Kempen, P Rao, J. “Molecular Magnetic Resonance Imaging of Tumor Response to Therapy”, Scientific Reports,Vol. 5, No.(1). (2015).

[108] Kaur, Gurvinder, and Jannette M Dufour. “Cell lines: Valuable tools or useless artifacts.” Spermatogenesis ,Vol. 2,No.1, (2012).

[109] Yao, Tatsuma, and Yuta Asayama. “Animal-cell culture media: History, characteristics, and current issues.” Reproductive medicine and biology, Vol. 16, No.2 , P.P. 99-117,(2017).

[110] Hudu, Shuaibu Abdullahi et al. “Cell Culture, Technology: Enhancing the Culture of Diagnosing Human Diseases.” Journal of clinical and diagnostic research ,Vol. 10, No.3, (2016).

[111] Verma, Anju. “Animal tissue culture principles and applications.” Animal Biotechnology , P.P 269–293, (2020).

[112] Kaur, G., & Dufour, J. M. “Cell lines”. Spermatogenesis, Vol.2, No.(1), P.P. 1–5. (2012).

[113] Fasciano, A. C., Mecsas, J., & Isberg, R. R. “New Age Strategies To Reconstruct Mucosal Tissue Colonization and Growth in Cell Culture Systems”, Microbiology Spectrum, Vol. 7, No.(2)P.P. 10, (2019).

[114] Weigelt B, Ghajar CM, Bissell MJ. “The need for complex 3D culture models to unravel novel pathways and identify accurate biomarkers in breast cancer”, Advance Drug Deliver Review. P.P 69–70. (2014).

[115] Breslin, S, & O’Driscoll, L. Three-dimensional cell culture: the missing link in drug discovery. Drug Discovery Today, Vol. 18 No.(5-6), P.P 240–249. (2013).

[116] Griffith LG, Swartz MA. “Capturing complex 3D tissue physiology in vitro.” Nat Rev Mol Cell Biol, Vol.7, P.P.211–224, 2006.

[117] Chen L, Xiao Z, Meng Y, Zhao Y, Han J, Su G, Chen B, Dai J. The enhancement of cancer stem cell properties of MCF-7 cells in 3D collagen scaffolds for modeling of cancer and anti-cancer drugs. Biomaterials. Vol. 33, P.P. 1437–1444,(2012).

[118] Fong EL, Lamhamedi-Cherradi SE, Burdett E, Ramamoorthy V, Lazar AJ, Kasper FK, Farach-Carson MC, Vishwamitra D, Demicco EG, Menegaz BA,”Modeling Ewing sarcoma tumors in vitro with 3D scaffolds .“ Proc Natl Acad ,Vol. 110, Nol. 6500–6505. (2013).

[119] Wastfeet, M., Fadeel, B., & Henter, J.-I. “A journey of hope: lessons learned from studies on rare diseases and orphan drugs , Journal of Internal Medicine, Vol. 260, (1), (2006).

[120] Hutmacher DW. “Biomaterials offer cancer research the third dimension” Nat Mater. ;Vol.9, P.P.90–93,(2010).

[121]. Jemal A, Bray F, Center MM, Ferlay J, Ward E, Forman D., "Global cancer statistics", CA Cancer J Clin.,Vol. 61, No.(2),P.P.69-90, (2011).

[122] Peter Ashjian and Amir Elbarbary, "Noninvasive in Situ Evaluation of Osteogenic Differentiation by Time-Resolved Laser-Induced Fluorescence Spectroscopy", Original Articles, Vol. 10, No. 3-4, ,(2004).

[123] Ohe, Y., "Treatment-related death from chemotherapy and thoracic radiotherapy for advanced cancer", Panminerva Med., journal pone, Vol.44, No.(3), P.P 205- 212, (2002).

[124] Das A. and Ferbel T., "Introduction to Nuclear and Particle Physics", World Scientific Publishing Co., (2003).

[125] Khan F.M., "The Physics of radiation Physics", third edition, Lippincptt Williams and Wilking, (2003).

[126] Powsner R. and Powsner E., "Essential Nuclear Medicine Physics", second edition, Blackwell Publishing , (2006).

[127] M.A. Hassouba and N. Dawood, “Study the Effect of Magnetic Field on the Electrical Characteristics of the Glow Discharge”, third edition, Lippincptt Williams and Wilking ,Vol.2, No.(4), P.P. 123-131 (2011).

[128] Mohammed K. Khalaf, Influence of Discharge Pressure on the Plasma Parameter in a Planar DC-Sputtering Discharge of Argon, Int. J. of Recent Research. Review, P.P.13-16, (2013).

[129] E. A. Abdullah, “Synthesis and Spectroscopic Study of Doped TiO_2 Nanostructures Using Sputtering System for Photocatalytic Applications,” Thesis Submitted to the Council of College of Science, University of Baghdad ,2019.

[130] Zhijiang, C., Ping, X., Cong, Z., Tingting, Z., Jie, G., & Kongyin, Z. Preparation and characterization of a bi-layered nano-filtration membrane from a chitosan hydrogel and bacterial cellulose nanofiber for dye removal. Cellulose, Vol.25, No.(9), 5123–5137, (2018).

[131] P. Scherrer, "Göttinger Nachrichten Gesell" Göttingen, Vol. 2, P.P. 98, (1978).

[132] Johan van Meerloo [1], Gertjan J L Kaspers, Jacqueline Cloos" Cell sensitivity assays: the MTT assay", Vol. 731,(2011).

[133] Kao, K. C., & Hockham, G. A. “Dielectric-fibre surface waveguides for optical frequencies”. Proceedings of the Institution of Electrical Engineers, Vol. 113 No,(7), P.P 1151–1158.(2012).

[134] Mohammed K. Khalaf, Influence of Discharge Pressure on the Plasma Parameter in a Planar DC-Sputtering Discharge of Argon, Int. J. of Recent Research Review., P.P. 13-16 (2013).

[135] Giessibl, F. J “Advances in atomic force microscopy.” Reviews of Modern Physics, Vol.75 , No.(3),P.P. 949–983. (2003).

[136] Leamy, H. J. “Charge collection scanning electron microscopy.” Journal of Applied Physics, Vol. 53, No.(6), (1982).

[137] ämpfe, B., Luczak, F., & Michel, B. “Energy Dispersive X-Ray Diffraction” Particle & Particle Systems Characterization, Vol. 22, No.(6), P.P 391–396. (2005).

[138] Brown, J. Q., Vishwanath, K., Palmer, G. M., & Ramanujam, N. Advances in quantitative UV–visible spectroscopy for clinical and pre-clinical application in cancer.” Current Opinion in Biotechnology”,Vol. 20, No.(1), P.P.119–131. (2009).

[139] rrondo, J. L. R., Muga, A., Castresana, J., & Goñi, F. M. Quantitative studies of the structure of proteins in solution by fourier-transform infrared spectroscopy. Progress in Biophysics and Molecular Biology, Vol. 59, No.(1), P.P .23–56. (1993).

[140] Rigby, C. C., & Franks, L. M. A Human Tissue Culture Cell Line from a Transitional Cell Tumour of the Urinary Bladder: Growth, Chromosome Pattern and Ultrastructure. British Journal of Cancer, Vol.24, No.(4), P.P 746–754. (1970).

[141] Kumano, M., Miyake, H., Kurahashi, T., Yamanaka, K., & Fujisawa, M. Enhanced progression of human prostate cancer PC3 cells induced by the microenvironment of the seminal vesicle. British Journal of Cancer, Vol.98, No.(2), P.P.356–362 ,(2008).

[142] Kimoto, S., Dick, W. D., Hunt, B., Szymanski, W. W., McMurry, P. H., Roberts, D. L., & Pui, D. Y. H. “Characterization of nanosized silica size standards.” Aerosol Science and Technology, Vol. 51, No.(8), P.P. 936–945. (2017).

[143] Oloche Owoicho, Charles Ochieng’ Olwal and Osbourne Quaye, " Potential of laser-induced fluorescence-light detection and ranging for future stand-off virus surveillance", (2021).